2019

SPATIAL AND TEMPORAL DISTRIBUTION OF HYDROTHERMAL MINERALS AND SOURCES OF HYDROTHERMAL FLUIDS INFERRED FROM LIGHT STABLE ISOTOPES, KEWEENAW PENINSULA NATIVE COPPER DISTRICT, MICHIGAN

Thomas Bodden

SPATIAL AND TEMPORAL DISTRIBUTION OF HYDROTHERMAL MINERALS AND SOURCES OF HYDROTHERMAL FLUIDS INFERRED FROM LIGHT STABLE ISOTOPES, KEWEENAW PENINSULA NATIVE COPPER DISTRICT, MICHIGAN

By

Thomas J. Bodden

A THESIS

Submitted in partial fulfillment of the requirements for the degree of

MASTER OF SCIENCE

In Geology

MICHIGAN TECHNOLOGICAL UNIVERSITY

2019

This thesis has been approved in partial fulfillment of the requirements for the Degree of MASTER OF SCIENCE in Geology.

Department of Geological and Mining Engineering and Sciences

Thesis Co-Advisor:	*Dr. Theodore J. Bornhorst*
Thesis Co-Advisor:	*Dr. Chad Deering*
Committee Member:	*Dr. Florence Bégué*
Department Chair:	*Dr. John S. Gierke*

Table of Contents

List of figures v

List of tables vii

Acknowledgements viii

Abstract ix

1 Chapter 1: Spatial Distribution of Hydrothermal/Metamorphogenic Minerals in the Keweenaw Peninsula, Michigan 1

1.1 Introduction 1

1.2 Previous Works 1

1.3 Geologic Setting 2

1.3.1 Native Copper Deposits 4

1.3.2 Minerals of the Keweenaw Peninsula 5

1.3.3 Genetic Model 6

1.3.4 Metamorphic Mineral Zones/Temperatures 7

1.4 Methods 9

1.5 Results 10

1.6 Discussion 12

1.7 Conclusion 14

1.7.1 Future Work 14

2 Inferences on the origin of native copper deposits of the Keweenaw Peninsula, Michigan using light stable isotopes 15

2.1 Introduction 15

2.2 Previous Works 16

2.3 Geologic Setting 16

2.3.1 Native Copper Deposits 18

2.3.2 Mineral Paragenesis and Temperature of Precipitation 18

2.3.3 Genetic Model 21

2.4 Methods 22

2.4.1 Compilation 22

2.4.2 Data Collected for This Study 23

2.4.3 Mineral-Fluid Fractionation 24

2.5 Calcite Oxygen and Carbon Isotopic Compositions 25

2.5.1 Temperature and Analytical Errors 25

2.5.2 Bulk Mineral Isotope Data 26

2.5.3 Comparison of Bulk versus In-situ Stable Isotope data 28
2.5.4 All Calcite Data 30
2.6 Discussion 32
2.6.1 Anomalous Bulk Calcite Isotopic Analyses 32
2.6.2 Published Calcite Data when Stage Assignment is Difficult 32
2.6.3 Main-Stage and Late-Stage Overlap 35
2.6.4 Comparison of Calcite to other minerals 36
2.6.5 Interpretation of Oxygen Isotopic Composition of Main-Stage Fluids 37
2.6.6 Interpretation of Isotopic Composition of Late-Stage Fluids 39
2.6.7 Carbon Stable Isotopes 40
2.6.8 Hydrogen Stable Isotopes 41
2.7 Conclusion 44
2.7.1 Future Work 45
3 Reference List 46
4 Appendix I: Mineral Assemblages 50
4.1 XRD: 58
5 Appendix II: Bulk Raw Stable Isotope Data 64
5.1 Legend for Table 64
6 Appendix III: SIMS Raw Stable Isotope Data 71
6.1 Spot Analysis Cathodoluminescence Images: 71
6.2 Legend for Table 75
7 Appendix IV: Assigned Paragenetic Stage and Calculated Stable Isotope Data 79
7.1 Legend for Table 79

List of figures

Chapter 1:

Figure 1.1: Geologic index map of the Keweenaw Peninsula 3

Figure 1.2: Mineral Paragenesis of hydrothermal/metamorphogenic minerals in the Keweenaw Peninsula native copper district. 6

Figure 1.3: Main-stage hydrothermal/metamorphic mineral assemblages 9

Figure 1.4: Main-stage mineral assemblages mapped for each location 11

Figure 1.5: Spatial distribution of mineral assemblages of main-stage hydrothermal/metamorphogenic minerals of the Keweenaw Peninsula. 12

Figure 1.6: Temperature zonation of the Keweenaw Peninsula. 13

Chapter 2:

Figure 2.1: Geologic index map of the Keweenaw Peninsula 17

Figure 2.2: Mineral Paragenesis of hydrothermal/metamorphogenic minerals in the Keweenaw Peninsula native copper district 19

Figure 2.3: Selected calculated d18OH2O and D13CCO2 showing analytical and temperature errors as described in the text. 26

Figure 2.4: Bulk calcite analyses plotted by paragenetic stage. 27

Figure 2.5: Bulk calcite $\delta^{18}O$ H_2O and $\delta^{13}C$ CO_2 subdivided by paragenetic stage. 27

Figure 2.6: Cathodoluminescence image of the three samples analyzed for this study using the SIMS method.. 28

Figure 2.7: Comparison of main-stage bulk isotopic analyses and the spot analyses by SIMS. 29

Figure 2.8: Comparison of late-stage data of bulk analysis and SIMS techniques. 30

Figure 2.9: Comparison of main- and late-stage stable isotope calcite combined bulk and spot data. 31

Figure 2.10: Plots of the $\delta^{18}O_{H2O}$ and $\delta^{13}C_{CO2}$ values separately and stacked on top of each other based on stage. 31

Figure 2.11: Anomaly analyses that were excluded from the general data. 32

Figure 2.12: Native copper district calcites compared to the outside the district amygdule calcites 33

Figure 2.13: Native copper district calcites compared to the Lakeshore vein calcites 35

Figure 2.14: Overlap of main- and late-stage analyses data points. 36

Figure 2.15: Comparison of calcite $\delta^{18}O$ H_2O data to quartz and clinochlore/chlorite main-and late-stage data. 37

Figure 2.16: All main-stage $\delta^{18}O_{H2O}$ data compared to fluid sources. 39

Figure 2.17: All late-stage $\delta^{18}O_{H2O}$ data compared to fluid sources.. 40

Figure 2.18: δD_{H2O} values plotted based on minerals and stage 41

Figure 2.19: δD_{H2O} and $\delta^{18}O_{H2O}$ main-stage analyses plotted as ranges 43

Figure 2.20: δD_{H2O} and $\delta^{18}O_{H2O}$ late-stage analyses plotted as ranges 44

Appendices:

Figure I-1: Sample locations are displayed on this map……52

Figure I-2a-r: XRD data results for the newly collected outcrop samples……..58

Figure III.1: Cathodoluminescence image of the three samples analyzed for this study using the SIMS method……71

Figure III.2: Cathodoluminescence image of WAS-752……..72

Figure III.3: Spot Analysis Cathodoluminescence image of TB-293……...73

Figure III.4: Spot Analysis Cathodoluminescence image of WAS-121……...74

List of tables

Table I-1: Collected Mineral Descriptions……52

Table I-2: Compiled Mineral Descriptions (Stoiber and Davidson)……...…..55

Table I-3: Quadrangle Map Mineral Descriptions……57

Table II: Bulk Raw Stable Isotope Data……...67

Table III: SIMS Raw Stable Isotope Data……77

Table IV: Assigned Paragenetic Stage and Calculated Stable Isotope Data……...…..84

Acknowledgements

I would like to thank my principal advisor Dr. Theodore J. Bornhorst for his guidance through each stage of this thesis. He was always willing to provide insight and ask thoughtful questions which pointed me in the right direction. In addition, he thoroughly and carefully reviewed the multiple thesis drafts. The A.E. Seaman Mineral Museum provided samples for this study from the museum's Keweenaw Research Suite and some funding for this project.

My co-advisor Dr. Chad Deering for providing valuable input and feedback during my thesis research. His critical review of my thesis improved the final product. Dr. Florence Bégué at the Institute of Earth Sciences University of Lausanne Switzerland, prepared the samples, completed the analyses themselves, and did the analytical corrections for the SIMS analyses presented in this thesis. I sincerely appreciate the time she spent on completing the analyses for without them this study would not have been possible. I thank her for being a member of my thesis committee and review of my thesis. I thank Dr. Edward Laitila, Materials Science and Engineering, for helping me prepare and collect the XRD data that was used to supplement my hand sample descriptions. Robert Barron, GMES Department Lab Coordinator, for provide some samples for my research and taught me how to safely use the sample preparation laboratory.

The Institute on Lake Superior Geology (ILSG) for providing me an ILSG Student Research Award in 2018. Through Eisenbrey Travel Award from ILSG and support from the A. E. Seaman Mineral Museum I was able to present part of my thesis results at the 2019 ISLG meeting in Terrace Bay which resulted in valuable feedback.

My special thanks to my parents, Todd and Mary Alice Bodden, and my brother, Mathew Bodden, for believing in me, giving me the opportunity to obtain a good education, and keeping me focused on completing my M.S. degree. Their support and my experiences on the family farm that I grew up on, made my pursuit of higher education go from a dream to reality.

Abstract

Hydrothermal native copper deposits are hosted by Mesoproterozoic Midcontinent Rift-filling volcanic and sedimentary rocks in Michigan's Keweenaw Peninsula. The genesis of the native copper deposits has been a point of interest since their discovery. Native copper and associated mineral assemblages vary temporally and spatially. A refined mineral paragenesis is presented and used as the basis to spatially compare mineral assemblages as it is essential that spatial comparison involve only minerals that are temporally/genetically, related to each other. The main-stage minerals associated with precipitation of native copper are spatially zoned. The higher-grade zones correspond to the area of native copper deposits and cross-cut stratigraphy. Late-stage minerals are superimposed on main-stage minerals and are not spatially zoned. The mineral assemblages can be equated to temperature of precipitation through previously published experimental metamorphic petrology, mineral chemistry, and stable isotope pairs.

Synthesis of previously published and new light stable isotopic data on hydrothermal minerals are used to draw inferences about the sources of the hydrothermal fluids. The equated temperatures of precipitation with isotopic fractionation equations are used to calculate the isotopic composition of the hydrothermal fluids. The oxygen isotopic composition of main-stage hydrothermal fluids based on isotopic composition of calcite, quartz, and chlorite, when combined with limited hydrogen isotope data for chlorite, epidote, and pumpellyite infer that the fluids were generated by metamorphogenic processes. These copper-bearing hydrothermal/metamorphogenic fluids rose from the deep source zone and mixed with meteoric waters in the zone of precipitation of native copper and associated minerals. Prior to mixing, the relatively shallow meteoric waters may have evolved in the rift-filling clastic sedimentary rocks overlying rift-filling basalts. Main-stage calcite can be distinguished from late-stage calcite by oxygen and carbon isotopes suggesting a different source of the late-stage hydrothermal fluids. The late-stage hydrothermal fluids are primarily meteoric waters although the meteoric waters may also have evolved in the rift-filling sedimentary rocks. Mixing of late-stage fluids with metamorphogenic fluids cannot be precluded. This study confirms the long-held hypothesis that the native copper precipitating hydrothermal fluids were generated by burial metamorphism. The hypothesis that fluid mixing was a mechanism promoting precipitation of native copper is supported by this study. In contrast, post-native copper late-stage fluids are dominantly meteoric water.

1 Chapter 1: Spatial Distribution of Hydrothermal/Metamorphogenic Minerals in the Keweenaw Peninsula, Michigan

1.1 Introduction

The native copper district of the Keweenaw Peninsula is the largest accumulation of native copper on Earth. It has been a topic of geologic investigation since Douglass Houghton's 1841 report which led to the beginning of modern mining of native copper in 1845. The origin of these unique mineral deposits is still a topic of particular interest. The focus of this research is to improve our understanding of the spatial distribution of hydrothermal/metamorphogenic minerals and their temperature of formation. These minerals were precipitated before, during, and after the precipitation of native copper.

The spatial variation of hydrothermal/metamorphogenic minerals of the Keweenaw Peninsula have been described in the framework of burial metamorphism (e.g., Jolly and Smith, 1971). It is well known that the assemblage of minerals can be used to bracket the formation temperature of metamorphic facies (Feenstra and Franz, 2015). While formation temperature has been previously inferred for mineral assemblages in the Keweenaw Peninsula (Jolly and Smith, 1971; Jolly, 1974; Livnat, 1983; and Püschner, 2001), the spatial distribution is not well defined. Stoiber and Davidson (1959) produced a strike parallel cross section showing the distribution of some minerals in the native copper district. The objective of this study is to expand on the work of Stoiber and Davidson (1959) by producing a map of the spatial variation in mineral assemblages of rift-filling rocks of the Keweenaw Peninsula and corresponding formation temperatures.

1.2 Previous Works

While early workers described the minerals associated with precipitation of native copper, it was Butler and Burbank (1929) in the definitive U. S. Geological Survey Professional Paper who provided the first integrated summary of the mineral assemblages of the Keweenaw Peninsula. They described the mineral paragenesis on a district-wide basis, although they noted that there are local deviations. Subsequent studies (e.g., Stoiber and Davidson, 1959; White 1968; and many more) invariably refer to their proposed model for mineral paragenesis and it is still valid today.

Stoiber and Davidson (1959) were the first to describe the regional pattern of mineral zoning within the Portage Lake Volcanics (PLV). They distinguished the main zones as being denoted by the minerals prehnite, epidote and quartz. This zonation was based on mineral distribution in stratigraphic sections of drill cores as well as between and within mines throughout the Keweenaw Peninsula. Jolly and Smith (1971) subdivided the mineral assemblages of the PLV in a single cross-section of stepped drill cores into three main low-grade burial metamorphic zones of decreasing grade: epidote zone, pumpellyite

zone, and laumontite zone. Subsequently, Livnat (1983) expanded on both Stoiber and Davidson (1959) and Jolly and Smith (1971) by providing additional information on spatial zonation of the minerals and mineral compositions by electron microprobe. Based on experimental data for metamorphic minerals, stable isotopes, and fluid inclusions, Livnat (1983) proposed formation temperatures. Livnat (1983) also showed that mineral zonation was not strictly stratigraphically controlled as proposed by Stoiber and Davidson (1959) and Jolly and Smith (1971). Livnat (1983) showed that isograds dip more shallowly than the lava flows which is consistent with mineral precipitation during structural tilting. Püschner (2001) refined Butler and Burbank's (1929) mineral paragenetic sequence and added additional mineral composition, stable isotope, and fluid inclusion data. He also applied the chlorite geothermometer to estimate the formation temperatures.

This study relies heavily on all of these, and other, previous studies which describe mineral assemblages at particular locations in the Keweenaw Peninsula. These previous works also provide the foundation to estimate the formation temperature of the mineral assemblages. The aim of the results presented here is to provide a spatial mineral zonation map of the entire Keweenaw Peninsula, not just within the exposed PLV. Previous studies did not fully consider the mineral paragenesis when evaluating spatial mineral zonation. Minerals must be precipitated during more or less the same event and be genetically related to one another to be useful in mapping mineral zonation. In this study, the impact of paragenesis on spatial mineral zonation will be considered.

1.3 Geologic Setting

The native copper mines produced about 5 billion kg of refined copper (Weege and Pollack, 1971) mostly from a 45 km long area from South Range to Copper Falls/Delaware (Figure 1.1). The native copper deposits of the Keweenaw Peninsula are hosted by Mesoproterozoic basalt lava flows and interflow conglomerates that fill the western Lake Superior segment of the Midcontinent Rift (Bornhorst and Lankton 2009). The Midcontinent Rift system extends over 2000km from Kansas to Lake Superior (Figure 1.1) and was formed around 1100Ma accompanied by extensional thinning of the Precambrian Superior block (Cannon et.al 1989).

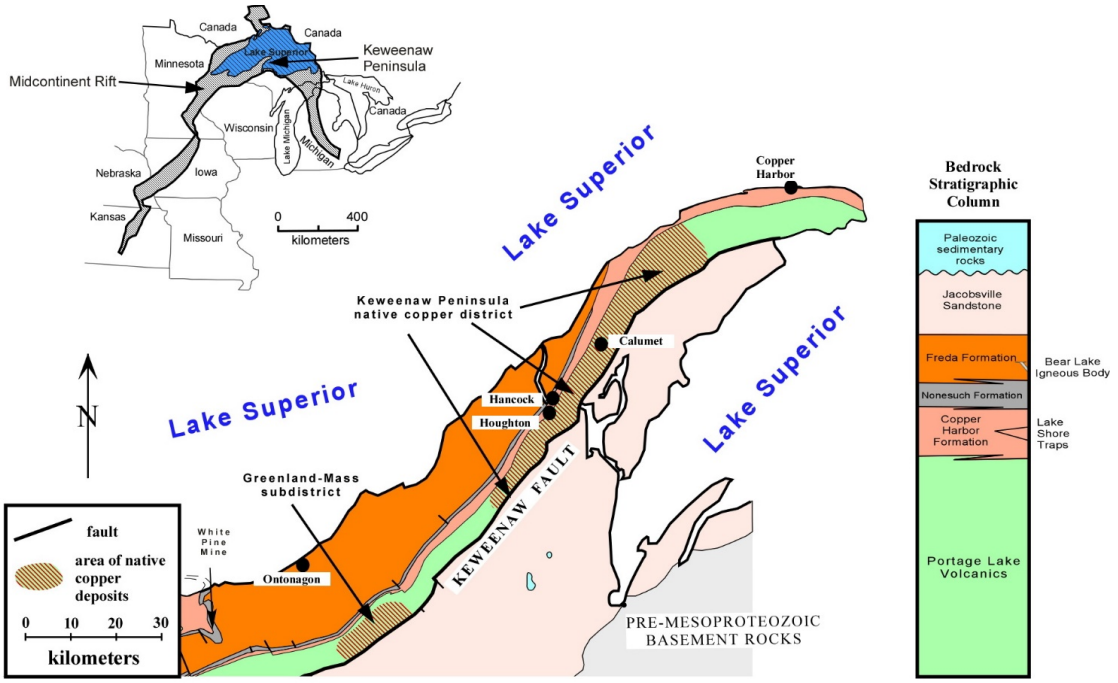

Figure 1.1: Geologic index map of the Keweenaw Peninsula showing bedrock geology. Inset shows trend of the Midcontintent Rift. Bedrock Stratigraphic column is also presented here, modified from Bornhorst and Williams (2013).

The bedrock geology of the Keweenaw Peninsula consists of Mesoproterozoic volcanic and clastic sedimentary rocks overlain by Paleozoic limestone (Figure 1.1). Economic and near economic native copper-dominated deposits are hosted by the PLV. The other Mesoproterozoic rock units of the Keweenaw Peninsula host at least small amounts of native copper (White, 1968; Bornhorst, 1997). The exposed PLV is composed of about 200 subaerial basalt flows and scattered interlayered conglomerate with lesser sandstone (Butler and Burbank, 1929; White, 1968; Merk and Jirsa, 1982). The subaerial basalt lava flows consist of a massive interior capped by an amygdaloidal and/or brecciated flow top. Lava flows are typically around 10 to 20m thick (White, 1960). The basal part of some lava flows consists of sparsely amygdaloidal basalt. Above this basal zone is massive basalt that lacks porosity; except for cross-cutting fractures. Massive basalt grades upward into increasingly amygdaloidal basalt with low to moderate porosity. Amygdaloidal basalt grades upward into basalt with even more amygdules corresponding to higher porosity with the top being smooth and ropy or alternatively, amygdaloidal basalt grades into brecciated flow top with breccia blocks being amygdaloidal basalt. Brecciated flow tops typically have higher porosity than amygdaloidal flow tops.

The interflow clastic sedimentary rocks within the PLV can range from a few cm up to 40 m thick consisting of conglomerate with lesser amounts of interbedded sandstone and sometimes siltstone and shale (White, 1968). The conglomerate is well-lithified, consisting of pebble to boulder sized clasts, which are sub-rounded to angular in texture.

The clasts are dominantly felsic, though variation from mafic to felsic compositions do exist. White (1968) interpreted the interflow sedimentary beds as alluvial fan deposits.

The PLV is overlain by the Copper Harbor Formation, composed of red-colored conglomerate with pebbles and boulders of rhyolite and lesser amounts of basalt (Figure 1.1). Within the Copper Harbor Formation is the Lake Shore Traps, a succession of interbedded basaltic lava flows. The Lake Shore traps are compositionally different and more variable than the PLV, with Fe-rich olivine tholeiites at the base to tholeiitic andesites near the top (Paces and Bornhorst, 1985).

The Nonesuch Formation overlies and interfingers with the Copper Harbor Formation (Figure 1.1). It is composed of gray to black siltstone and shale. The Nonesuch Formation has a transitional contact with the overlying red-colored sandstone and siltstone of the Freda Formation. There is an intrusive igneous rock that cross-cuts the Freda Formation at Bear Lake (Figure 1.1). The Bear Lake igneous body is dark grey to red in color, intermediate in composition, and has micro-phenocrysts of K-feldspar, biotite, hornblende, quartz, apatite, and iron oxides. It is altered and has veinlets of calcite, quartz, and heulandite (Kulakov et. al. 2018).

The Jacobsville Sandstone is in fault contact with the PLV (Figure 1.1). It is made up of red to white, coarse-to-fine grained quartz and feldspar sandstone with lesser amounts of shale, siltstone and conglomerate. It has no known igneous deposits within the formation (Kalliokoski, 1982).

1.3.1 Native Copper Deposits

The most significant native copper found in the Keweenaw Peninsula is hosted by, and within, the tops of the lava flows and interflow conglomerates. These native copper deposits are typically characterized by an association with calcite, quartz, epidote, prehnite and pumpellyite; although not all are always present. Those occurrences of native copper deposits from which there has been a production of 1 million lbs of copper or more are concentrated in two separate areas: 1) the main district from South Range to Copper Falls, and 2) the Greenland-Mass sub-district (Figure 1.1). About 58.5% of the deposits are hosted by brecciated and amygdaloidal flow tops, 39.5% by interflow conglomerate and sandstone layers, and 2% by cross-cutting veins (Bornhorst and Lankton, 2009).

The porosity and permeability of the flow tops and interflow conglomerates facilitates the movement of hydrothermal/metamorphogenic fluids until the open space is filled with precipitated minerals (Jolly and Smith, 1971; Bornhorst, 1997; Püschner, 2001). Bornhorst (1997) proposed that faults and fractures formed during late rift compression integrated the pathways for hydrothermal/metamorphogenic fluids leading to the formation of the native copper deposits.

1.3.2 Minerals of the Keweenaw Peninsula

There are over 100 minerals found in the Keweenaw Peninsula albeit many of them are rare, volumetrically insignificant, and of limited value to understanding the genesis of the deposits. Butler and Burbank (1929) were the first to provide a comprehensive summary of the minerals within the native copper district and their temporal relationship (paragenesis) with each other. They subdivided the minerals into those formed during a "rock-forming period," "ore period," and "weathering period." Their "rock-forming period" includes minerals precipitated during crystallization of the basaltic magmas as well as minerals formed during early surface and shallow burial processes (very low-grade metamorphic alteration) such as the minerals chlorite and hematite. Butler and Burbank's (1929) "ore period" includes the metallic minerals native copper and copper sulfides and associated non-metallic minerals. The last temporal subdivision of Butler and Burbank (1929) is a period of weathering or supergene alteration resulting from downward percolation of groundwater including minerals such as cuprite, tenorite, malachite, chrysocolla, and azurite. The igneous and weathering minerals are not discussed further here as this study focuses on the hydrothermal/metamorphogenic minerals.

The post-magmatic crystallization minerals grouped as "rock-forming period" by Butler and Burbank (1929) have been termed "early-stage" in this study. The "ore-forming period" of Butler and Burbank (1929) has been subdivided into two stages of hydrothermal-metamorphogenic mineral formation: main-stage, and late-stage. This subdivision is critical to developing a more complete understanding of the spatial distribution of hydrothermal/ metamorphogenic minerals.

During the pre-ore stage the minerals chlorite, hematite, and serpentine were noted by Butler and Burbank (1929). However, more recently agate, a low-temperature mineral forming in the 50-100°C range (Fallick et al, 1985 and Harris, 1989) has been discovered as occurring in amygdules cross-cut by native copper. Thus, agate is interpreted as part of the pre-ore stage (Figure 1.2). By far the main ore mineral of the district is native copper. The precipitation of native copper generally temporally overlaps with all of the minerals assigned here to the main-stage as they are interpreted to have formed during the same hydrothermal/metamorphogenic event (Figure 1.2).

The native copper deposits are cut by veins and fractures with the minerals filling them being late in the paragenetic sequence (Butler and Burbank, 1929); these minerals are grouped here as late-stage. This suite of minerals includes copper sulfides. Bornhorst and Suchoski (1995) have shown that even a very small amount of sulfur in the hydrothermal/metamorphogenic fluids would likely lead to precipitation of copper sulfide minerals rather than native copper. Therefore, the occurrence of copper sulfide minerals may be from a genetically unique fluid that was involved during the latter part of the hydrothermal/metamorphorgnic event. The suite of late-stage minerals is indicative of temperatures of formation significantly less than the main-stage minerals (Püschner, 2001). The minerals phyllosilicate/chlorite, hematite, and calcite are also notable for

occurring in the early, main and late-stages, hence, their paragenesis may not be able to be interpreted with certainty in individual specimens.

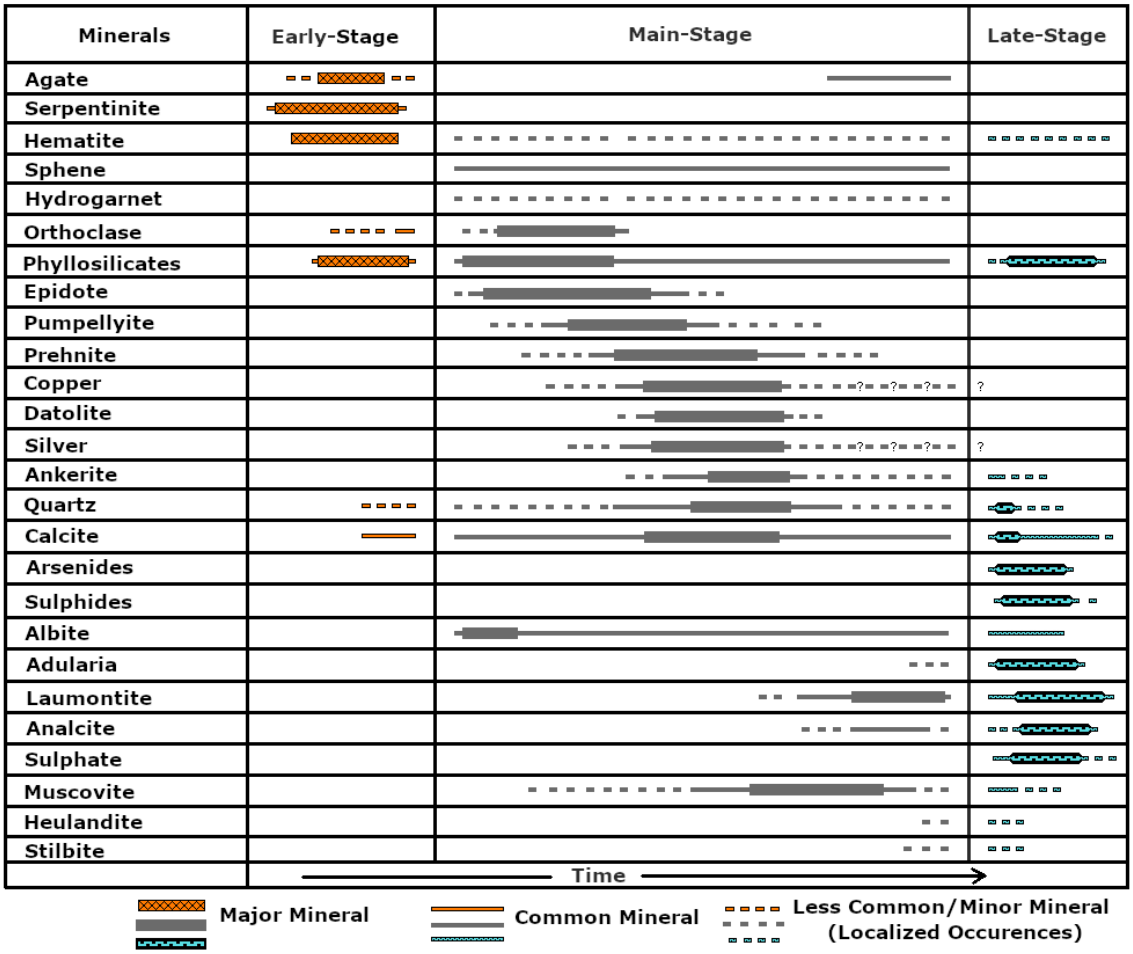

Figure 1.2: Mineral Paragenesis of hydrothermal/metamorphogenic minerals in the Keweenaw Peninsula native copper district and within the surrounding vicinity, modified from Butler and Burbank (1929), Jolly and Smith (1971) Livant (1983), Püschner (2001).

1.3.3 Genetic Model

The genesis of native copper and associated minerals has been recently summarized by Bornhorst and Mathur (2017, 2018). The most likely source of most of the copper is from leaching of the rift-filling basaltic rocks at depth beneath the native copper deposits by metamorphogenic hydrothermal fluids (White, 1967; Bornhorst and Mathur, 2017). Copper-bearing main-stage ore fluids were likely derived from rift-filling basalts at temperatures of around 300-400°C. During ascent from the source zone to the zone of precipitation the fluids cooled. Precipitation of native copper and associated minerals is hypothesized to be the result of cooling of the fluids, reaction of the fluids with host rocks, and mixing with reduced meteoric waters (Bornhorst and Mathur 2017and 2018).

1.3.4 Metamorphic Mineral Zones/Temperatures

The hydrothermal minerals of the Keweenaw Peninsula have been interpreted as a result of low temperature burial metamorphism and, therefore, assigned to metamorphic zones by Butler and Burbank (1929), Stoiber and Davidson (1959), Jolly and Smith (1971), Livnat (1983), Püschner (2001) among others. Jolly and Smith (1971) subdivided the hydrothermal minerals into three zones : 1) ***epidote zone***: characterized by chlorite, albite, sphene, hydrogarnet calcite, muscovite, prehnite, pumpellyite, quartz, and epidote; 2) ***pumpellyite zone***: characterized by chlorite, albite, sphene, hydrogarnet, calcite, muscovite and traces of laumontite, prehnite, pumpellyite, quartz and epidote; and 3) ***a laumontite zone***: characterized by chlorite, albite, sphene, hydrogarnet, calcite, muscovite, analcime, laumontite, prehnite and traces of pumpellyite and quartz. These zones consist of a paragenetic sequence of minerals that formed during the main-stage (Figure 1.2). The main-stage is cross-cut throughout the native copper district by readily discernable veins and veinlets of late-stage minerals (Figure 1.2). The assemblage of late-stage minerals is the same everywhere throughout the PLV and, therefore, this suite of minerals is superimposed on the spatially variable distribution of main-stage minerals. Since the late-stage mineral assemblage is similar to the laumontite zone, it is difficult to distinguish between main-stage and late-stage minerals in the areas of the laumontite zone.

Schimdt (1997) studied the metamorphogenic minerals in the Keweenawan North Shore Volcanics of Minnesota which is stratigraphically beneath the PLV. It can be reasonably assumed that the North Shore metamorphogenic minerals formed at about the same time as the main-stage minerals of the Keweenaw Peninsula. Schmidt subdivided the minerals into distinct metamorphic zones (from highest to lowest grade): 1) ***epidote zone***: characterized by actinolite (not found in the Keweenaw Peninsula), epidote, pumpellyite, prehnite, chlorite, and garnet; 2) ***pumpellyite zone***: characterized by epidote, pumpellyite, prehnite traces of laumontite, chlorite, potential garnet and corrensite; 3) ***laumontite zone***: characterized by laumontite, chlorite, calcite, phyllosilicates (corrensite), epistilbite, and quartz; 4) ***heulandite-stilbite zone***: characterized by laumontite, calcite, phyllosilicates (smectite), heulandite, stilbite, scolecite, mordenite, and epistilbite; 5) ***thomsonite-scolecite-smectite zone***: characterized by smectite, thomsonite, calcite, heulandite, scolecite and quartz. Phyllosilicates are noted as having a discontinuous transition from chlorite to corrensite to smectite with decreasing temperature.

For each of these zones a temperature of the precipitation was inferred by Schmidt (1997) on the basis of the dominant type of phyllosilicate mineral. The temperature of formation for the mineral zones (Figure 1.3) used in the North Shore of Minnesota and in the Keweenaw Peninsula geology are summarized below.

Schmidt (1997) interprets the epidote zone of the North Shore to have formed at greater than 275°C, whereas for a similar assemblage Livnat (1983) proposed a formation temperature of 280-320°C +/- 10°C in the Keweenaw Peninsula. Püschner (2001) also inferred temperatures that can be applied based on chlorite geothermometry, the epidote

zone in the Keweenaw Peninsula would be around 275°C. Based on these independent estimates, the formation temperature of the epidote zone is assumed to be 275°C +/- 25°C. Schmidt (1997) interpreted the pumpellyite zone to have formed at around 220-260°C whereas, Livnat (1983) proposed temperatures of 210-260°C +/- 10°C. Püschner (2001) interpreted the pumpellyite zone to be around 175-200°C. The formation temperature of the pumpellyite zone is assumed to be 200-225°C +/- 25°C. Schmidt (1997) interprets the laumontite zone to have formed at 150°C +/- 25°C. Similarly, Livnat (1983) proposed formation temperatures associated with the laumontite zone to be 150°C +/-10°C. Püschner (2001) interpreted the laumontite zone to be around 125-150°C. The formation temperature of the laumontite zone is 150°C +/- 25°C.The heulandite-stilbite zone for the North Shore, as described by Schmidt (1997), has not been noted as occurring in the Keweenaw Peninsula previously. However, there are areas that match the North Shore mineral assemblage for this zone. Schmidt (1997) interpreted the heulandite-stilbite zone to have formed at temperatures <150°C. This also aligns with Püschner's (2001) late-stage temperature of 125-150°C.

The late-stage mineral assemblage within the native copper district can be readily identified (Figure 1.2) and shares a very similar mineral assemblage to the cooler temperatures of the laumontite and heulandite-stilbite zones. The temperature of formation from Püschner (2001) for the laumontite zone is the same as that for the late-stage, thus the late-stage temperature of formation is similar to the temperature proposed for the laumontite and heulandite-stilbite zones; <150°C.

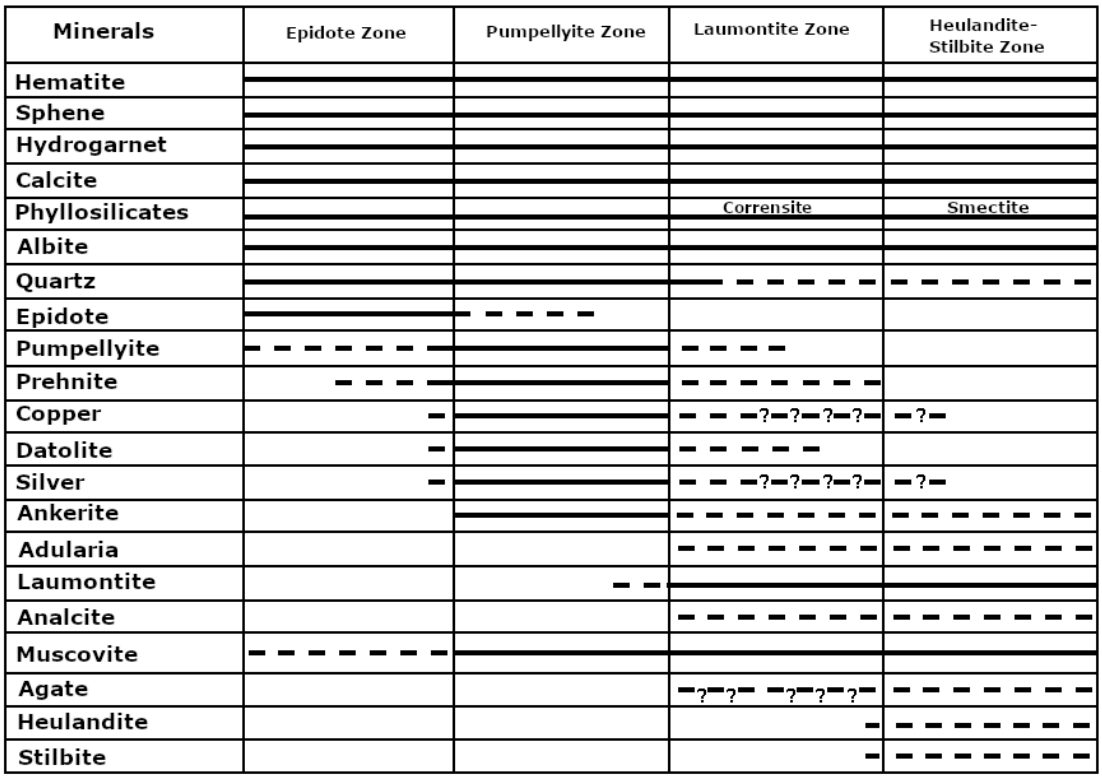

Figure 1.3: Main-stage hydrothermal/metamorphic mineral assemblages can be broken up into zones in the Keweenaw Peninsula. Paragenesis and previous zone work compared from Butler and Burbank (1929); Jolly and Smith (1971); Livnat (1983); Schmidt (1997). Since the heulandite-stilbite zone is only described from two areas of the Keweenaw Peninsula, the occurrence of minerals in this zone, such as native copper, are not well defined.

1.4 Methods

The focus of the research presented in this section was to determine the spatial distribution of hydrothermal mineral assemblages within the rocks of the native copper district of the Keweenaw Peninsula and nearby. Data from previous studies were compiled including: Butler and Burbank (1929), Stoiber and Davidson (1959), Jolly and Smith (1972), Livnat (1983), Bornhorst and Woodruff (1997), and Püschner (2001). In addition to data from published papers, descriptions on published U.S. Geological Survey geologic quadrangle maps and some unpublished data from Stoiber and Davidson (1959) were included in the compilation. The geologic quadrangle maps referenced in this study include Bruneau Creek (Wright and Cornwall, 1954), Mohawk (Davidson et. Al, 1955), Phoenix (Cornwall, 1954), Eagle Harbor (Cornwall, 1954), Ahmeek (Cornwall and Swanson, 1953), Delaware (Cornwall, 1954), Fort Wilkins (Cornwall, 1955), Lake Medora (1955), and Manitou Island (Cornwall and White, 1955).

To complement this compiled data, new samples were collected from mine piles and outcrops to fill in missing areas, especially areas that didn't have good representations or descriptions perhaps neglected due to lack of copper deposits. The collection of new samples was limited to areas of volcanic rocks which avoids the issue of secondary

minerals that may be associated with diagenesis/cementation. Some samples were also collected to confirm the minerals present at certain locations. Minerals in the newly collected samples were identified using hand sample techniques and later supplemented using x-ray diffraction.

X-ray Diffraction was used to identify minerals in outcrop samples. Mineralogically representative samples were selected and about 1 gram of rock was powdered to the range of 100-200 mesh grain size using a mortar and pestle. The powders were analyzed on a Scintag XDS2000 powder X-ray diffractometer, configured with a graphite monochromoter, with the settings of around 20kV and 20mA at the Michigan Technological University. The standard measurement range was between 2° and 70° Theta with a scan speed of 1° 2-Theta/min. The system is set up to a workstation running Scintag DMSNT software for display and identification of characteristic X-ray peaks. An additional program called "Materials Data Jade" was used for partial automated identification of some peaks.

1.5 Results

The compiled mineral assemblage data were color coded according to main-stage hydrothermal/metamorphogenic zones (Figure 1.4) on a basic geologic map. Colors were assigned to the data points of the map to indicate the mineral zones denoting mineral abundances. These colors were later used to determine zone distribution. Colors were assigned based on mineral abundance and presence compared to the metamorphic zones as given in Figure 1.4. Locations that are dominated by epidote are assigned the epidote zone. When a location has pumpellyite and prehnite present it is likely the pumpellyite zone. When there is little to no epidote or prehnite present, it is most likely in the laumontite zone. The spatial distribution of main-stage minerals associated with precipitation of native copper of the Keweenaw Peninsula can be subdivided into four metamorphogenic zones (Figure 1.4). These zones are consistent with those used for the North Shore Volcanics of Minnesota by Schmidt (1997).

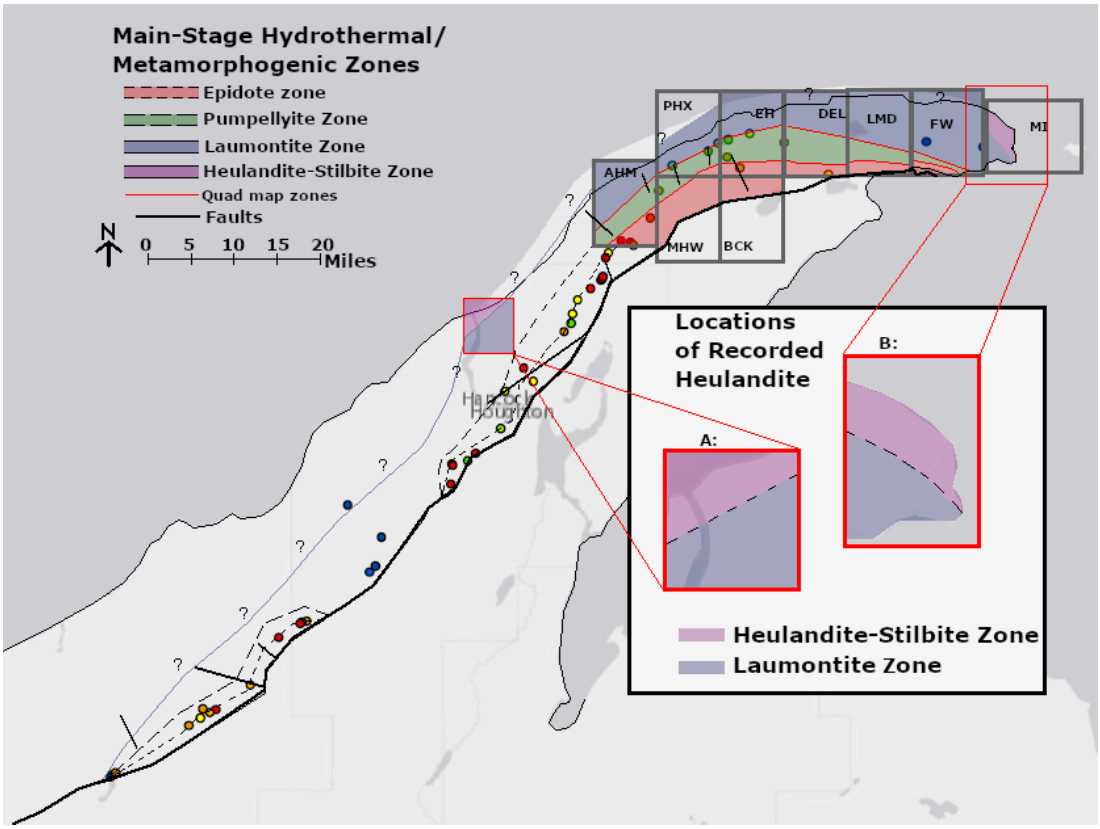

Figure 1.4: Main-stage mineral assemblages mapped for each location, dots represent minerals present at a sample location.Data are from Stoiber and Davidson (1959) as well as the newly collected samples (see Appendix I map for source of data). Quadrangle map data is represented as the rectangles, the zones in them are assigned using the descriptions. Red dots = dominant mineral is epidote, orange dots = epidote and prehnite present in roughly equal parts, green dots = pumpellyite and minor traces of epidote, yellow dots = traces of prehnite and potential laumontite, blue dots = no notable zone minerals denoted other than calcite and quartz and potential laumontite. Inset shows locations of recorded heulandite from Kulakov (2018) and Manitou Island Quadrangle map.

Schmidt's (1997) zones for the North Shore Volcanics included zones of lower grade than the laumontite zone with the next lowest grade being the heulandite-stilbite zone. Heulandite has been identified in two locations in the Keweenaw Peninsula (Figure 1.4). Within the Bear Lake igneous body (Figure 1.4.A), veinlets of calcite, quartz and heulandite had been noted by Kulakov et. al. (2018). Near the tip of the Keweenaw Peninsula (Figure 1.4.B), the back of the USGS Manitou Island map described heulandite as being present as well. While the heulandite-stilbite zone is only documented in these two areas, it is likely to exist elsewhere, especially within the Freda Formation and, hence, the full extent of distribution is uncertain.

Generalized visual trends in the spatial variation of minerals are summarized here. Epidote decreases in abundance further away from the core of the native copper district. Prehnite and pumpellyite are present in varying amounts being more dominant at mines like Seneca mine, near the middle of the native copper district. Chlorite is present in practically all localities, some vesicles and amygdules are fully filled by chlorite. Calcite is present at all if not most areas as well. In some locations there is just a trace of calcite,

while in other places calcite is abundant. Amygdules can be completely filled with calcite. Quartz is present at most of the localities, but in lesser abundance further from the core of the main native copper district. Potassium feldspar is present in varying amounts and is more concentrated in some places. Copper is present in all if not most of the mines and can be found throughout the native copper district as well as in veins and faults outside the district. Silver is less commonly found than native copper, but when found it is typically in association with native copper. Laumontite becomes more abundant further from the core of the native copper district. Datolite is not always present as it is localized in some places. Agate is rarely present within the native copper district.

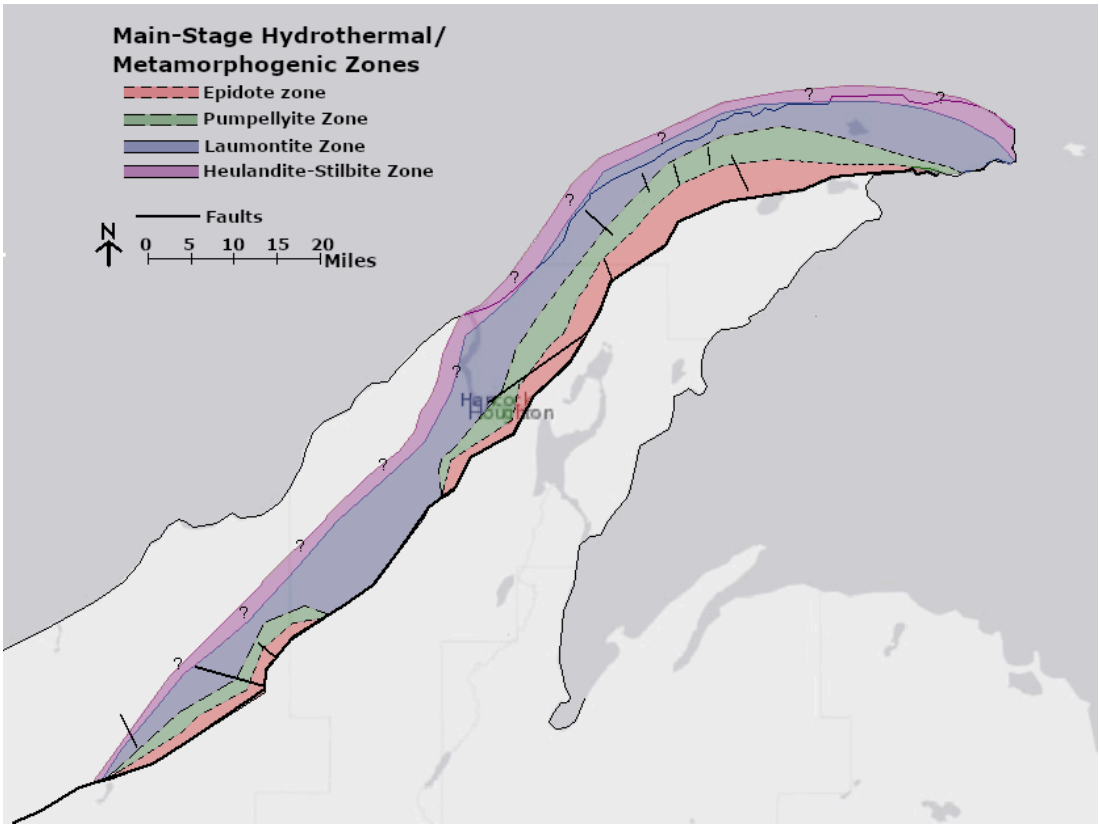

Figure 1.5: Spatial distribution of mineral assemblages of main-stage hydrothermal/metamorphogenic minerals of the Keweenaw Peninsula by zone as defined in Figure 1.4. Map interpretation based on data as discussed in the text.

1.6 Discussion

Stoiber and Davidson (1959) provided the first attempt to determine the spatial distribution of main-stage hydrothermal/metamorphogenic minerals in the Keweenaw Peninsula. Jolly and Smith (1971) applied the concept of metamorphic mineral zones to a single stratigraphic column. Both Stoiber and Davidson (1959) and Jolly and Smith (1971) presented their discussion of mineral assemblages in a stratigraphic framework which implied a connection between mineral zonation and stratigraphic location. However, Livnat (1983) disagreed with this interpretation of mineral zonation being strictly connected with stratigraphy as he demonstrated the zones dip more shallowly than

stratigraphy. The results of this study demonstrate that mineral zones clearly cross-cut stratigraphy and that the higher-grade zones are coincident with the occurrence of the principal area of native copper deposits within the Keweenaw Peninsula (Figure 1.1 and 1.5). While within the native copper district, the mineral zones are subparallel to stratigraphy, to the northeast towards Keweenaw Point the zones clearly cross-cut stratigraphy as well as to the southwest of Houghton. Further to the southwest in the Greenland-Mass subdistrict, the mineral zones are again coincident with the higher-grade zones.

The main-stage hydrothermal/metamorphogenic mineral zones can be approximately equated to the temperature of the fluids that precipitated the minerals as illustrated in Figure 1.6. The native copper deposits, especially the larger economic deposits are associated with the thermal high. The thermal high demonstrates that the native copper deposits are not an outcome of simple burial metamorphism, but due to concentrated hydrothermal/metamorphogenic processes resulting in a thermal high.

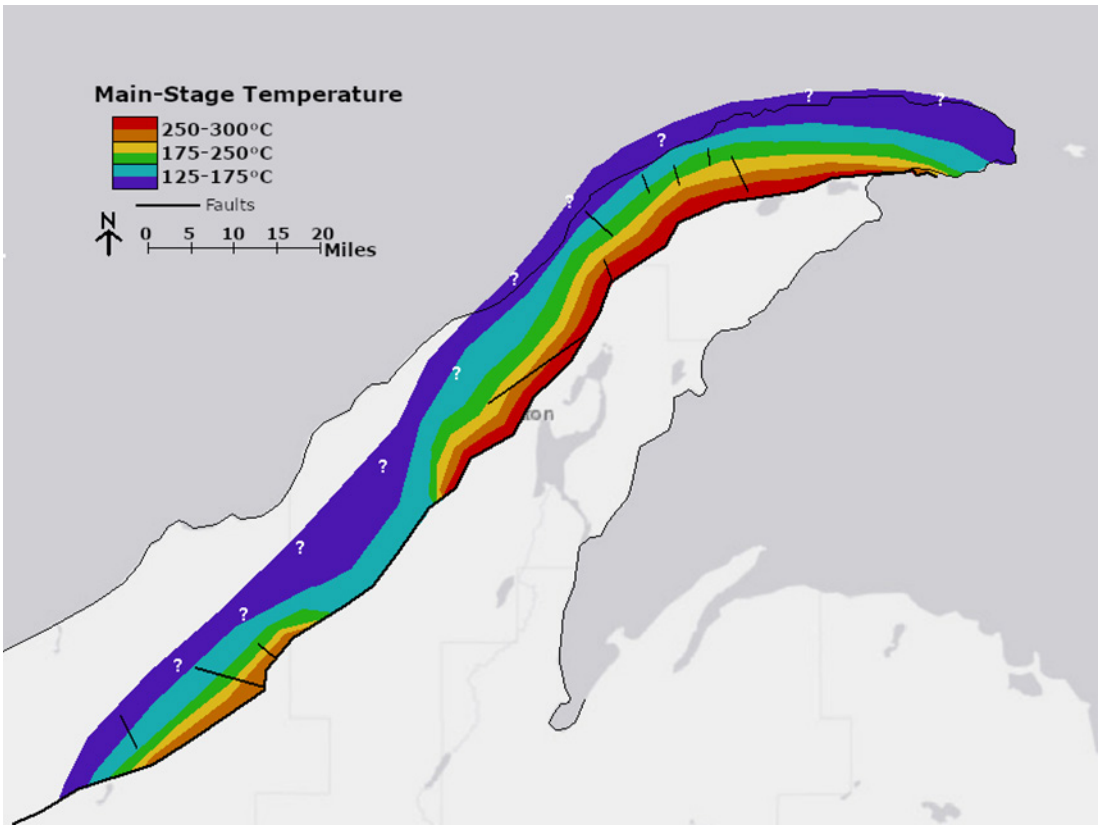

Figure 1.6: Temperature zonation of the Keweenaw Peninsula based on mineral zonation shown in Figure 1.5 and corresponding temperature of formation discussed in the text.

Within the area of the epidote and pumpellyite zones (Figure 1.5), the main-stage minerals are readily distinguished from the late-stage minerals (Figure 1.2). Outside these areas, recognition of the late-stage mineral assemblage is difficult - except when copper sulfide minerals are present -because the predicted main-stage hydrothermal/

metamorphogenic mineral assemblage would be more or less the same as the late-stage mineral assemblage (Figure 1.2 and 1.3). While there does not appear to be any zoning of late-stage minerals within the two higher main-stage hydrothermal/ metamorphogenic mineral zones the abundance of late-stage minerals is far from uniform. Late-stage minerals are more abundant along faults and fractures and notably more abundant near the Keweenaw fault in structurally disturbed PLV. This suggests that the late-stage minerals are more localized than those associated with the main-stage. By this rationale, in areas outside of the epidote and pumpellyite mineral zones the general occurrence of lower grade minerals such as those in the laumontite and heulandite-stilbite zones (Figure 1.3) are assumed to be paragenetically main-stage minerals rather than late-stage

1.7 Conclusion

In this study we focused on determining the spatial distribution of hydrothermal/ metamorphogenic minerals in the Keweenaw Peninsula. Only minerals temporally/ genetically related to each other can be mapped together. Thus, the paragenesis for the district was carefully refined based on previously published information. The main-stage hydrothermal/metamorphogenic mineral assemblage can be readily subdivided into zones based on Schmidt (1997) to describe metamorphogenic mineral zonation in basalts of the Keweenawan North Shore Volcanics in Minnesota: i.e. epidote, pumpellyite, laumontite and heulandite-stilbite zones. These zones are comparable to Jolly and Smith (1971), although the presence of the heulandite-stilbite zone in the Keweenaw Peninsula has not been previously recognized. The main-stage mineral zones of the Keweenaw Peninsula have a regular spatial distribution, but cross-cut stratigraphy. The mineral zonation is a result of spatial variation in the temperature of mineral formation. The spatial pattern represents two thermal highs in the Keweenaw Peninsula that are coincident with the more significant native copper deposits. The thermal high demonstrates that the native copper deposits are a result of more than just simple burial metamorphic processes but rather concentrated hydrothermal fluid flow leading to localized thermal highs. Thus, hydrothermal/metamorphogenic fluids are responsible for the native copper deposits, whereas outside of the native copper district burial metamorphogenic processes may have been dominant.

1.7.1 Future Work

Spatial mapping of mineral zonation in Keweenawan aged rocks of the entire western Upper Peninsula of Michigan (beyond the Keeweenaw Peninsula) would continue to improve our understanding of the Keweenawan hydrothermal/metamorphogenic event. Within the Keweenaw Peninsula and elsewhere additional data is especially needed to better map the heulandite-stilbite and lower zones of Schmidt (1997).

2 Inferences on the origin of native copper deposits of the Keweenaw Peninsula, Michigan using light stable isotopes

2.1 Introduction

Hydrothermal/metamorphogenic native copper deposits of the Keweenaw Peninsula produced 11 billion lbs. of refined copper from the opening of the first profitable mine in 1845 to closing of the last mine in 1968. The Keweenaw Peninsula is home to the largest copper district wherein 99% of the copper occurs as the mineral species native copper. The origin of the native copper deposits has been in question since their discovery. The deposits were described by geologists while the mines were open as being hosted by volcanic and sedimentary rocks (Butler and Burbank, 1929; and Stoiber and Davidson, 1959) that fill the Midcontinent Rift (Bornhorst, 1997). They hypothesized about the origin of the deposits testing models that invoke transportation by copper-bearing waters that descended to produce the deposits, to ascending fluids that derived the copper from an igneous source. With limited modern experimental data on the stability of minerals and a lack of analytical tools such as microprobe mineral analysis, light stable isotopes, chlorite geothermometry and an ever-growing list of tools and techniques, it was difficult to accurately determine these origins. After the mines closed more recent studies have used such modern data to provide more constraints on the origin of the deposits; e.g. recent studies targeting variations in copper isotopes (Bornhorst and Mathur, 2017, 2018). For about 50 years light stable isotopes (oxygen, carbon, and hydrogen) have played an important role in understanding the origin of fluids involved in the formation of hydrothermal mineral deposits. Livnat (1983) proposed the fluids depositing native copper of the Keweenaw Peninsula were modified seawater. Subsequently Bornhorst and Woodruff (1997), combined a small subset of Livnat's (1983) data on oxygen and carbon isotopic composition of calcite restricted to one deposit with new data to propose mixing of two fluids during the time of precipitation. The latest study by Püschner (2001) proposed mixing of metamorphic and meteoric waters. The hypothesis of fluid mixing is based on stable isotope variability.

The purpose of this study is to better understand the origin of the stable isotope variability. Secondary ion mass spectrometry (SIMS) was utilized to obtain data with a high spatial resolution that can resolve differences within individual mineral zones that could be compared to previously published bulk-mineral stable isotope data. An important part of this study is to analyze and interpret the data using the context of our refined mineral paragenesis to separate data into those more likely to be genetically related to one another. Since the mineral calcite occurs in all of the paragenetic stages and is geographically widespread, this study has focused on the oxygen and carbon isotope composition of calcite. Data from other minerals (quartz, chlorite, clinochlore, pumpellyite, epidote) are also used for comparison and provide more depth to the conclusions drawn from the calcite data.

2.2 Previous Works

The native copper deposits of the Keweenaw Peninsula have been geologically described and studied for almost 175 years since Douglass Houghton's 1841 report sparked the first mining rush in North America in search of riches mining copper in the Keweenaw Peninsula. Butler and Burbank (1929) summarized geology studies in a U. S. Geological Survey Professional Paper. Subsequent notable studies are those of Stoiber and Davidson (1959), White (1968), Jolly (1974), Livnat (1983), Püschner (2001) and Bornhorst and Mathur (2017).

Livnat (1983) was the first to undertake light stable isotope studies in the Keweenaw Peninsula. He presented results for light stable isotope studies to establish the source(s) and history of the fluids. Livnat (1983) collected a variety of samples from all over the Keweenaw Peninsula to analyze for stable isotopes, roughly 120 amygdular and vein-carbonates were collected for analysis of $\delta^{18}O$ and $\delta^{13}C$. Additionally, in his study he acquired about 100 hydrogen isotopic analyses, $\delta^{18}O$ data on silicates and oxides, and 18 sulfur analyses from sulfides and sulfates. The minerals that were analyzed included quartz, calcite, and chlorites as the major minerals as well as fewer numbers of prehnite, pumpellyite, epidote, k-spar, muscovite, hematite, and ankerite.

Bornhorst and Woodruff (1997) approached the origin of the native copper district by proposing that fluid-mixing of two or more fluids precipitated the copper. To test their hypothesis, they used a suite of 41 calcite samples from mine rock piles. The samples came from a 12 km stretch along strike of the Kearsarge deposit with the intent of minimizing temperature variation as compared to using samples from spatially diverse deposits. They analyzed calcite for $\delta^{18}O$ and $\delta^{13}C$ stable isotope data and then the ranges were compared and interpreted.

Püschner (2001) focused on the metamorphism of the Portage Lake Volcanics. He collected roughly 112 sets of stable isotope data from three drill hole profiles from Ahmeek, Eagle Harbor, and Copper Harbor. The minerals calcite, clinochlore, quartz, epidote and corrensite were analyzed for $\delta^{18}O$ and $\delta^{13}C$ data when applicable. Püschner (2001) collected this stable isotope data to "get a better understanding about the nature of the alteration fluids". While doing so, he compared the ranges of $\delta^{18}O$ values to known fluid values in attempts to better understand the source of the fluids.

Each study provided a different insight on the sources of the fluids involved in the precipitation of native copper. These $\delta^{18}O$ and $\delta^{13}C$ stable isotope data, determined from bulk samples, were compiled for comparison to the high spatial resolution, SIMS data, of this study.

2.3 Geologic Setting

The native copper mines produced about 5 billion kg of refined copper (Weege and Pollack, 1971) mostly from a 45 km long area from South Range to Copper

Falls/Delaware (Figure 2.1). The native copper deposits of the Keweenaw Peninsula are hosted by Mesoproterozoic basalt lava flows and interflow conglomerates that fill the western Lake Superior segment of the Midcontinent Rift (Bornhorst and Lankton 2009). The Midcontinent Rift system extends over 2000km from Kansas to Lake Superior (Figure 2.1) and was formed around 1100Ma accompanied by extensional thinning of the Precambrian Superior block (Cannon et. Al. 1989)

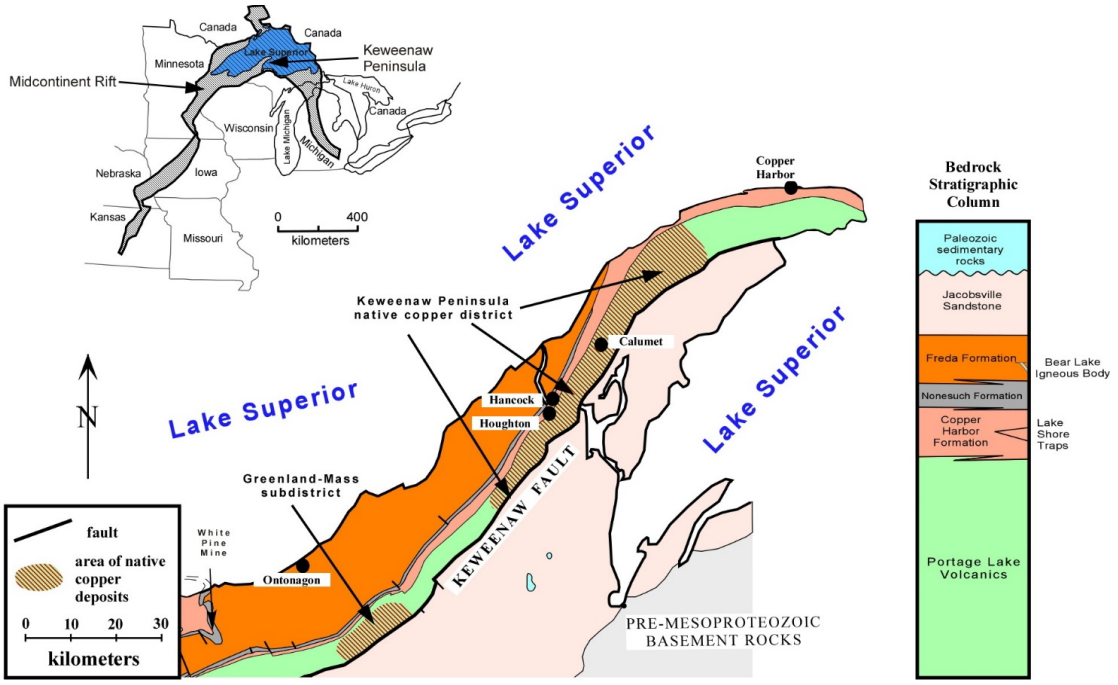

Figure 2.1: Geologic index map of the Keweenaw Peninsula showing bedrock geology and stratigraphic column. Inset shows trend of the Midcontinent Rift. Modified from Bornhorst and Williams (2013).

The bedrock geology of the Keweenaw Peninsula consists of Mesoproterozoic volcanic and clastic sedimentary rocks overlain by Paleozoic limestone (Figure 2.1). Economic and near economic native copper-dominated deposits are hosted by the PLV. The other Mesoproterozoic rock units of the Keweenaw Peninsula host at least small amounts of native copper (White, 1968; Bornhorst, 1997). The exposed PLV is composed of about 200 subaerial basalt flows and scattered interlayered conglomerate with lesser sandstone (Butler and Burbank, 1929; White, 1968; Merk and Jirsa, 1982). The subaerial basalt lava flows consist of a massive interior capped by an amygdaloidal and/or brecciated flow top. Lava flows are typically around 10 to 20m thick (White, 1968). The basal part of some lava flows consists of sparsely amygdaloidal basalt. Above this basal zone is massive basalt that relatively lacks porosity except for cross-cutting fractures. Massive basalt grades upward into increasingly amygdaloidal basalt with low to moderate porosity. Amygdaloidal basalt grades upward into basalt with even more amygdules corresponding to higher porosity with the top being smooth and ropy or alternatively, amygdaloidal basalt grades into brecciated flow top with breccia blocks being amygdaloidal basalt. Brecciated flow top typically has higher porosity than amygdaloidal flow tops.

The interflow clastic sedimentary rocks within the PLV can range from a few cm up to 40 m thick consisting of conglomerate with lesser amounts of interbedded sandstone and sometime siltstone and shale (White, 1968). The conglomerate is well-lithified, consisting of pebble- to boulder-sized clasts, which are sub-rounded to angular in texture. The clasts are dominantly felsic, though variation does exist. White (1968) interprets the interflow sedimentary beds as alluvial fan deposits. The PLV is overlain by the Copper Harbor Formation, composed of red-colored conglomerate with pebbles and boulders of rhyolite and lesser amounts of basalt (Figure 2.1). Within the Copper Harbor Formation is the Lake Shore Traps, a succession of interbedded basaltic lava flows. The Nonesuch Formation overlies and interfingers with the Copper Harbor Formation (Figure 2.1). It is composed of gray to black siltstone and shale. At the White Pine Mine, the base of the Nonesuch hosts significant copper deposits. The White Pine Mines is outside the scope of this study. The Nonesuch Formation is overlain by and transitional into red-colored sandstone and siltstone of the Freda Formation. The Jacobsville Sandstone is in fault contact with the PLV (Figure 2.1). It is made up of red to white, coarse-to-fine grained quartz and feldspar sandstone with lesser amounts of shale, siltstone and conglomerate. It has no known igneous rocks within the formation (Kalliokoski, 1982).

2.3.1 Native Copper Deposits

The known significant native copper in the Keweenaw Peninsula is hosted within the tops of the lava flows and interflow conglomerates. These native copper deposits are typically characterized by having native copper associated with calcite, quartz, epidote, prehnite and pumpellyite, although not all need to be present. Those occurrences of native copper deposits from which there has been a production of 1 million lbs. of copper or more are concentrated in two separate areas, the main district from South Range to Copper Falls and the Greenland-Mass sub-district (Figure 2.1). About 58.5% of the deposits are hosted by brecciated and amygdaloidal flow tops, 39.5% by interflow conglomerate and sandstone layers, and 2% by cross-cutting veins (Bornhorst and Lankton, 2009).

The porosity and permeability of the flow tops and interflow conglomerates facilitates the movement of hydrothermal/metamorphogenic fluids until the open space is filled with precipitated minerals (Jolly and Smith, 1971; Bornhorst, 1997; Püschner, 2001). Bornhorst (1997) proposed that faults and fractures formed during late rift compression integrated the pathways for hydrothermal/metamorphogenic fluids leading to the formation of the native copper deposits.

2.3.2 Mineral Paragenesis and Temperature of Precipitation

An overall mineral paragenesis for the Keweenaw Peninsula native copper district was first well established by Butler and Burbank (1929). There are local variations such that the overall paragenesis does not exactly match paragenesis for a particular mine or locality. In addition, Butler and Burbank (1929) focused on the area of native copper

mines. Outside of that area, such as at the tip of the peninsula or along the lakeshore of Lake Superior, there are minerals not incorporated into their paragenetic diagram. Chapter 1 of this study discusses and presents a refined mineral paragenesis applicable for all of the rift-filling rocks of the Keweenaw Peninsula (Figure 2.2).

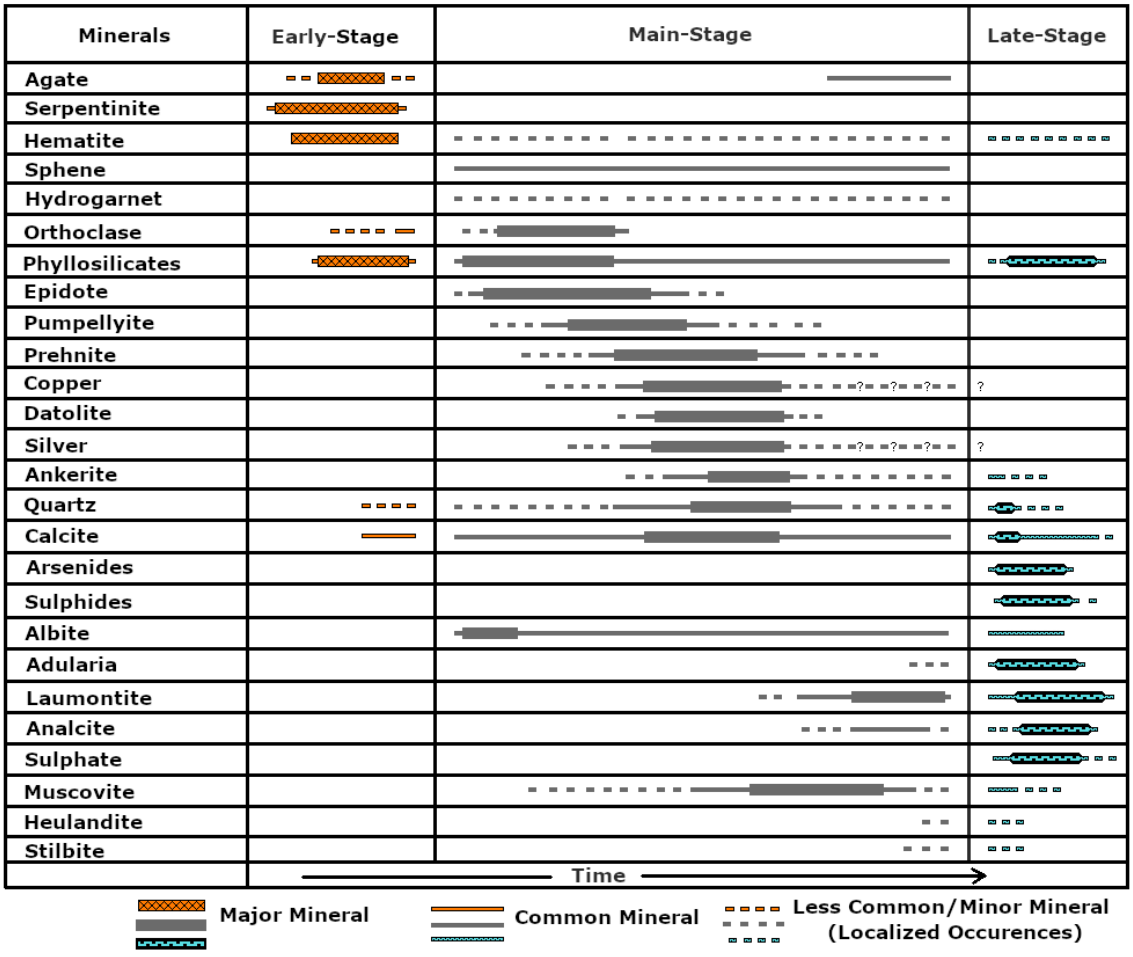

Figure 2.2: Mineral Paragenesis of hydrothermal/metamorphogenic minerals in the Keweenaw Peninsula native copper district and within the surrounding vicinity, modified from Butler and Burbank (1929), Jolly and Smith (1971) Livant (1983), Püschner (2001). See Chapter 1 for more details on minerals of the Keweenaw Peninsula.

The paragenetic diagram is subdivided into stages. A stage represents a suite of minerals temporally precipitated at the same time and believed to be genetically related to one another. There may or may not be a time break between stages. The early-stage represents a suite of minerals believed to be precipitated during burial metamorphism prior to the influx of hydrothermal/metamorphogenic fluids. It may well be that there is not a break between early-stage burial metamorphism and the beginning of main-stage hydrothermal/metamorphogenic alteration; with the beginning characterized by a combination of specific minerals and the intensity of alteration as a result of increased fluid flow. The main-stage represents the hydrothermal/metamorphogenic event that resulted in precipitation of native copper. A suite of paragenetically late-stage minerals

was recognized by Butler and Burbank (1929) overprinting earlier native copper associated minerals and filling fractures that cut across the native copper deposits. There may not be a significant temporal break between the main- and late-stages, but the break is proposed to be genetically significant; this hypothesis will be tested by the results presented in this chapter.

Interpretation of light stable isotope data relies on the temperature dependent fractionation between the fluid and precipitating minerals assuming everything is in equilibrium. Thus, establishing the temperature of precipitation is an important component of interpretation of light stable isotope data. The temperature of precipitation of the main-stage and late-stage minerals in the Keweenaw Peninsula has been discussed and estimated in Chapter 1 of this thesis. The general temperature of main-stage fluids varies spatially; however, locally along pathways of high fluid flow, such as veins, the temperature may be higher. The late-stage mineral assemblage is not spatially zoned, but similar everywhere in the Keweenaw Peninsula. Hence, it follows that the temperature of late-stage precipitation is generally the same everywhere.

A well-established mineral paragenesis is an important aspect of this study. The interpretation of the stable isotope data relies on using data from only minerals that are temporally/genetically related to each other. It is easy to group the stable isotope data from minerals that are exclusively or nearly exclusively precipitated in only one stage, such as epidote. For the mineral calcite, which is the focus of this study, it is more difficult to determine the stage of precipitation as it occurred during more than one stage. Without the context of a suite of minerals it is sometimes not possible to determine the paragenesis. In addition to establishing the mineral paragenesis, the location of main-stage minerals provides a better estimate of the temperature of precipitation other than the average of the main-stage.

Livnat (1983) did not rely on paragenesis for his interpretation of the stable isotope data. However, Püschner (2001) did incorporate paragenesis into his interpretation of the stable isotope data. Püschner (2001) subdivided the hydrothermal/metamorphogenic mineral paragenesis into three stages: Stage 1 (pre-native copper), Stage 2 (syn-native copper), and Stage 3 (post-native copper). Püschner's (2001) stage 1 and 2 overlap locally and on the basis of Butler and Burbank's (1929) interpretation of paragenesis would be part of the main-stage. Chapter 1 interprets Püschner's (2001) Stage 1 and 2 as main-stage and part of the continuous evolving episode of mineral precipitation related to native copper. Stage 3 of Püschner (2001) is equivalent to late-stage used here (Figure 2.2). Püschner (2001) interpreted this as a distinct stage as it is interpreted here.

2.3.3 Genetic Model

The district-wide model of genesis of native copper and associated minerals has been recently summarized by Bornhorst and Mathur (2017, 2018). The most likely source of most of the copper is leaching from rift-filling basaltic rocks at depth beneath the native copper deposits by fluids at temperatures of around 300-400°C (White, 1968; Bornhorst and Mathur, 2017). These copper-bearing main-stage ore fluids evolved and cooled during ascent from the source zone to the zone of precipitation into the main-stage ore fluids. Precipitation of native copper and associated minerals is hypothesized to be the result of cooling of the fluids, reaction of the fluids with host rocks, and mixing with reduced meteoric waters (Bornhorst and Mathur 2017and 2018).

The origin of the fluids is a key component in the genetic model of the native copper deposits. White (1968) concluded that the fluids were metamorphic in origin and were not related to cooling of a magma body. Jolly and Smith (1971) invoked burial metamorphic fluids for the precipitation of native copper and associated minerals. In a follow-up study, Jolly (1974) addressed the composition of the metamorphic fluids based on thermodynamic calculations. He demonstrated that copper was transported in the metamorphic ore-forming fluids as Cu^{+} as a chloride complex in a brine and used hydrothermal/metamorphogenic environments as an analog. Livnat (1983) proposed the metamorphic fluid was a Ca-Na brine. On the basis of oxygen and hydrogen isotopes, he concluded that shortly after emplacement there was low temperature exchange between the rocks and meteoric surface waters. Prior to burial, seawater that infiltrated into the rocks extensively exchanged with rocks at elevated temperature during dehydration. According to Livnat (1983) the hydrothermal ore fluid has an oxygen isotope composition of about 6 +/- 1.5‰ and a hydrogen isotope composition of about 0 +/-10‰ and it was the result of a mixture of several fluids that evolved through reaction with surrounding rocks. Bornhorst and Woodruff (1997) noted a high degree of variation in Livnat's (1983) oxygen and carbon isotopic data that could have been the result of the use of incorrect temperatures for the mineral-fluid fractionation calculations. Thus, they sampled calcite from a single deposit which was presumably precipitated at a reasonably constant temperature thus, minimizing temperature as a possible explanation of the variation. Their new data combined with Livnat's continued to show large variability. Thus, they suggested that mixing of two or more hydrothermal/metamorphogenic fluids occurred during precipitation of native copper and could have been a cause of precipitation. Püschner (2001) using oxygen and hydrogen isotopes proposed fluid mixing between a metamorphic derived fluid and meteoric water but did not require involvement of seawater as proposed by Livnat (1983). Livnat (1983) proposed meteoric water involvement prior to burial and Bornhorst and Woodruff (1997) proposed involvement during precipitation. Püschner (2001) was not definitive about the timing of fluid mixing.

On the basis of 25°C eH-pH diagrams, Brown (2006) proposed meteoric surface water penetrated to the depths of the source zone and while doing so reacted with rocks evolving into an oxidized saline brine. At depth this fluid mixed with metamorphogenic

fluid and acquired sufficient copper to be an ore-forming fluid when it ascended into the zone of precipitation. He called the ore-fluid a "hybrid evolved meteoric-metamorphogenic ore-forming hydrothermal brine" (Brown 2006). On the basis of copper isotopes as well as other arguments, Bornhorst and Mathur (2017, 2018) have argued that this model is unlikely.

Using various approaches and lines of reasoning, it is generally agreed that metamorphic processes, metamorphogenic, is a key component of producing the main-stage ore-forming fluids. Mixing of metamorphogenic fluids and meteoric waters is likely with the timing being during main-stage precipitation. Most previous authors don't consider the origin of the late-stage fluids. A box in an oxygen-hydrogen plot of Livnat (1983) shows the late-stage fluids being near the meteoric water line but he does not comment in the text on these fluids.

2.4 Methods

2.4.1 Compilation

Previous oxygen, carbon, and hydrogen stable isotope data from Livnat (1983), Bornhorst and Woodruff (1997), and Püschner (2001) was compiled to interpret patterns with the complete set of available data (Appendix II). These large number of data have a much wider spatial distribution than the data collected for this study. The oxygen and carbon data for calcite, the focus of this study, includes 111 analyses for oxygen and carbon in calcite collected by Livnat (1983), 41 analyses collected by Bornhorst and Woodruff (1997), and 32 analyses collected by Püschner (2001) for total of 184 sets of compiled bulk analyses of stable isotope data for calcite. An additional 109 analyses of oxygen and hydrogen isotopes were compiled from Livnat (1983) and Püschner (2001) determined from clinochlore, chlorite, and quartz; these were used for comparison with the calcite data.

All previous stable isotope data were collected via a bulk analysis method. For calcite, typically a small amount of sample is recovered from the sample and powdered. The powder is dissolved in acid (for $\delta^{13}C$ it is likely anhydrous phosphoric acid) and the resulting CO_2 gas is analyzed for oxygen and carbon isotopes by a mass spectrometer. Precision for calcite analyses is about +/- 0.2‰. Livnat (1983) analyzed his samples at the U.S. Geological Survey Isotope Geology Laboratory in Denver. Livnat's (1983) oxygen isotopes on silicates and oxides were analyzed using extraction methods after Clayton and Mayeda (1963). Püschner (2001) listed that his stable isotope analyses were done at the stable isotope lab of the Geological Department at the Indiana University of Bloomington.

When possible each analysis was assigned to one of the paragenetic stages: early-stage, main-stage, or late-stage. Multiple criteria are used to assign an analysis to a particular paragenetic stage. The primary criteria are the description of the minerals in the sample.

If the minerals are uniquely associated with a particular stage (Figure 2.1) then the analysis is assigned to that stage. For example, if copper and epidote are present the analysis is assigned to the main-stage as compared to the presence of late-stage sulfide minerals. The location was used in cases when the associated minerals were poorly described. For example, analyses from Livnat (1983) collected from Baltic or Shear veins is likely a late-stage due to the nature of these veins crosscutting the main-stage minerals. Areas within the native copper district would be assigned to the main-stage unless the description listed that the analysis came from veins or fissures that crosscut the main-stage or had unique late-stage minerals such as laumontite. Outside of the native copper district, the stages are similarly assigned, if only calcite is listed for minerals in a sample it is difficult to assign, typically leading it to being assigned as uncertain, otherwise if prehnite, pumpellyite or another notable main-stage mineral is listed outside the district it is assigned as main-stage. Main-stage and late-stage outside the district in many locations are mineralogically very similar, in this case, if the samples are noted to be from veins that crosscut other rocks they as assigned as late-stage otherwise they are assigned as main-stage.

It was not always possible to assign a stage to some of the analyses with confidence and these are listed as uncertain. Some but not all of the uncertain samples are presented separately; only analyses able to be assigned to a paragenetic stage are used in diagrams unless otherwise noted. Typically, analyses that were assigned as uncertain were from veins and fissures outside of the bounds of the native copper district. Analyses in the uncertain category are those within the district that only have minerals that are found in more than one stage making assignment to a particular stage uncertain. The uncertain category also includes analyses within the district that did not list the associated minerals and stage assignment. However, for those outside of the district where the mineral zone was either laumontite or heulandite-stilbite, the samples were assigned as main-stage. Twenty-three analyses are in the uncertain category (Appendix IV).

2.4.2 Data Collected for This Study

Three samples were selected to be analyzed in detail for this study. The samples were selected from the Quincy and Kearsarge deposits. The Quincy sample was a vug-filling calcite crystal. The Seneca sample was selected because the calcite was part of a cross-cutting vein closely associated with laumontite, and natrolite and thus, late-stage. The Wolverine calcite was associated with prehnite and epidote, making it belong to main-stage. The samples were described and sent to the University of Lausanne (Switzerland) for oxygen and carbon isotope analysis by Secondary Ion Mass Spectrometry (SIMS) at the Swiss SIMS national facility.

Each sample was analyzed by SIMS, an in-situ analytical technique used to analyze the mass ratios of secondary ions with the process of hitting the surface of the calcite with a focused ion beam. The same analytical settings for in-situ analyses by SIMS of carbonate material were used as described by Bégué et al. (2019). In-house calcite and rhodochrosite standards were used to correct for instrumental bias due to matrix effect

and for machine drift during the analytical session. The location of the spots was determined by Florence Bégué, University of Lausanne, based on textural information from cold cathode cathodoluminescence images of the carbonates. The spot size for oxygen isotope measurements was between 12 and 14μm and for carbon isotope measurements about 18μm with a 10μm raster.

2.4.3 Mineral-Fluid Fractionation

The stable isotopic composition of a mineral depends on the stable isotope composition of the hydrothermal/metamorphogenic fluid, the temperature of precipitation, and the fractionation factor. In this system there is a temperature dependent fractionation between the hydrothermal/metamorphogenic fluid and the mineral. The fractionation equation for different minerals has been determined by earlier laboratory experiments. (T is temperature in Kelvin for all equations)

The $\delta^{18}O_{H2O}$ fractionation equation for calcite as discussed by O'Neil et al. (1969) and later corrected in Friedman and O'Neil (1977) is:

$(\delta^{18}O_{H2O}‰) = (\delta^{18}O‰ \text{ of calcite}) - ((2.78*10\text{^}6)/T\text{^}2)) + 2.89$

The $\delta^{13}C_{CO2}$ fractionation equation for calcite as discussed by Sheele and Hoefs (1992) is:

$(\delta^{13}C_{CO2}‰) = (\delta^{13}C‰ \text{ of calcite}) -((3.46*10\text{^}6)/T\text{^}2)) + ((9.58 *10\text{^}3)/T)-2.72$

There is an additional 22 $\delta^{18}O$ values for quartz and 57 $\delta^{18}O$ values for chlorite/clinochlore that this study also incorporates into interpretation. The comparison of the quartz and chlorite stable isotope data aids in confirming the trends that are seen in the calcite.

The $\delta^{18}O_{H2O}$ fractionation equation for quartz as discussed by White (2013) is:

$(\delta^{18}O_{H2O}‰) = (\delta^{18}O‰ \text{ of quartz}) - ((1.63*10\text{^}6)/T\text{^}2)) + 5.44$

The $\delta^{18}O_{H2O}$ fractionation equation for chlorite as discussed by Clayton et al. (1972) is:

$(\delta^{18}O_{H2O}‰) = (\delta^{18}O‰ \text{ of chlorite}) - ((3.38*10\text{^}6)/T\text{^}2)) + 3.4$

Temperature is important in fractionation calculations. There is a spatial variation in temperature of precipitation for main-stage minerals (see Chapter 1). The temperatures used for fractionation calculations is based on the geographic location of the sample with respect to the temperature zone shown in Figure 1.6. The midpoint temperature is used as the temperature of precipitation for any analysis from within that particular zone. The temperature range for the zone represents the range in temperature error for the fractionation calculations. The temperature of precipitation during the late-stage was more or less constant (see Chapter 1). Thus, a single temperature of 125°C +/-25°C can be applied to late-stage fractionation calculations.

The oxygen isotope composition of the fluid can be directly calculated from the raw calcite value. The carbon isotope composition of the fluid, however, depends not only on the temperature of precipitation but also on the proportion of carbon species in the fluid which depend on e.g., oxidation state and pH (Ohmoto, 1972). Livnat (1983) concludes that based on the probable conditions during precipitation of native copper in the Keweenaw Peninsula that $\delta^{13}C$ for CO_2 is approximately equal to $\delta^{13}C_{\Sigma C}$ in the fluid. For carbon isotope composition of calcite, the temperature of precipitation and the fractionation equation described above are used to calculate the $\delta^{13}C_{CO2}$ which therefore represents the carbon isotopic composition of the fluid.

2.5 Calcite Oxygen and Carbon Isotopic Compositions

2.5.1 Temperature and Analytical Errors

Temperature uncertainty and analytical error contribute to the error in the calculated $\delta^{18}O_{H2O}$ and $\delta^{13}C_{CO2}$. The $\delta^{18}O_{H2O}$ and $\delta^{13}C_{CO2}$ is calculated using the midpoint of the temperature range for the temperature zone in which a particular analysis is located (see Appendix IV). The uncertainty of the temperature of precipitation for main-stage analyses is assumed to be the temperature range of the particular temperature zone as discussed in Chapter 1. Several representative isotopic values were used to calculate temperature and analytical errors for main-stage analyses as presented in Figure 2.3.

The late-stage minerals are typically found cross-cutting main-stage minerals in veins and is far less abundant than the main-stage. The fixed temperature range for late-stage is estimated at 125°C +/-25°C, producing errors associated with these temperature uncertainty of about +/- 0.75 ‰ for $\delta^{13}C_{CO2}$ and +/-1.75 ‰ for $\delta^{18}O_{H2O}$ (Figure 2.3).

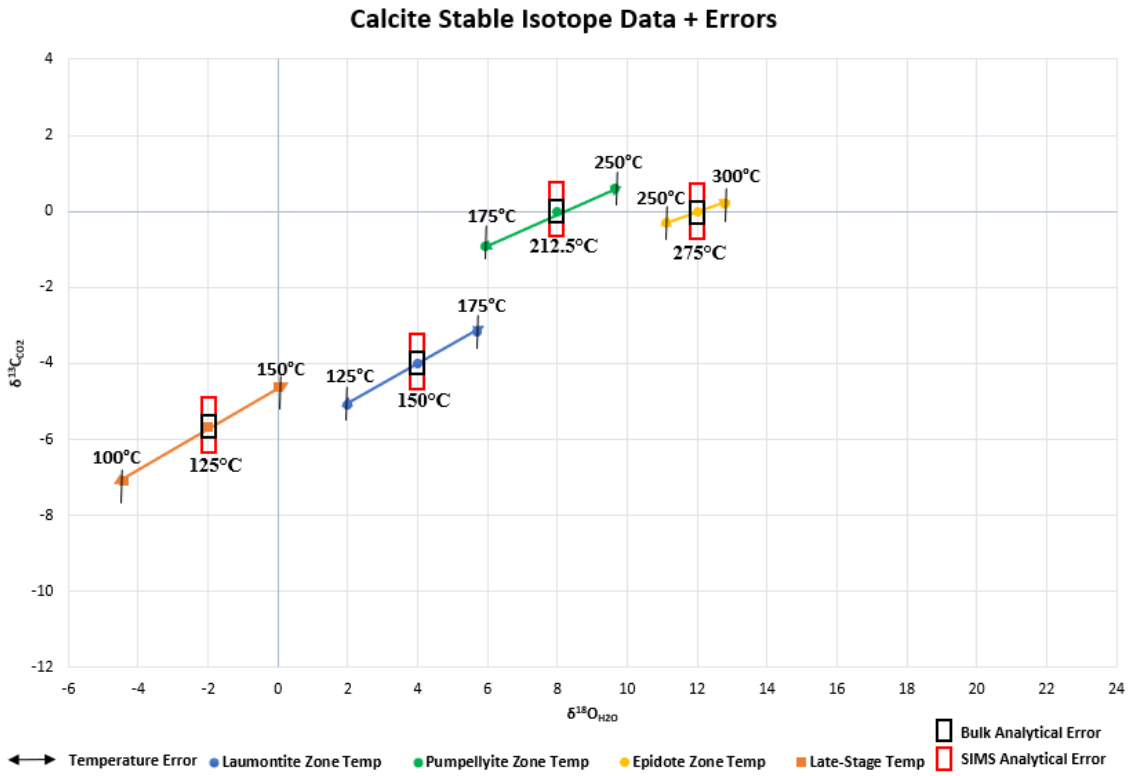

Figure 2.3: Selected calculated d18OH2O and D13CCO2 showing analytical and temperature errors as described in the text.

2.5.2 Bulk Mineral Isotope Data

There are 143 bulk mineral oxygen and carbon isotopic analyses of calcite compiled from published literature used in this study. These bulk analyses of calcite have considerable variation within both the main-stage and late-stage (Figure 2.4). The variation within both main-stage and late-stage calcite exceeds the temperature and analytical errors. The main-stage has a range of $\delta^{18}O_{H2O}$ from +3.10 to + 22.93 ‰ and in $\delta^{13}C_{CO2}$ of -4.76 to +3.54 ‰ whereas late-stage has a range of $\delta^{18}O_{H2O}$ from -4.35 to +8.05‰ and in $\delta^{13}C_{CO2}$ of -10.29 to -0.96‰ (Figures 2.4 and 2.5).

Histograms of $\delta^{18}O_{H2O}$ for both main- and late-stages are visually suggestive of a bimodal distribution slightly skewed towards lower values (Figure 2.5). $\delta^{13}C_{CO2}$ visually appears to be roughly unimodal and perhaps skewed towards higher values.

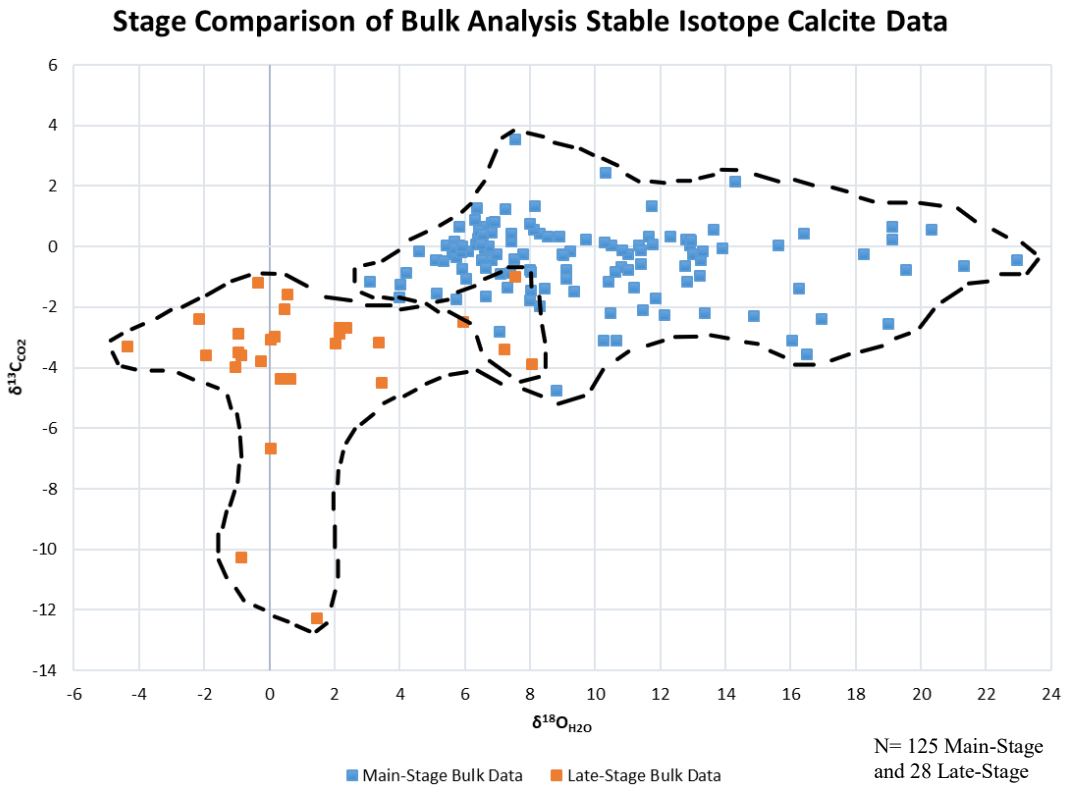

Figure 2.4: Bulk calcite analyses plotted by paragenetic stage. Main-stage uses temperatures from the hydrothermal/ metamorphogenic zones determined in Chapter 1 i.e., epidote zone = 275°C +/-25°C, pumpellyite zone = 212.5°C +/- 37.5°C, and laumontite zone = 150°C +/-25°C and late-stage uses a fixed temperature of 125°C +/-25°C.

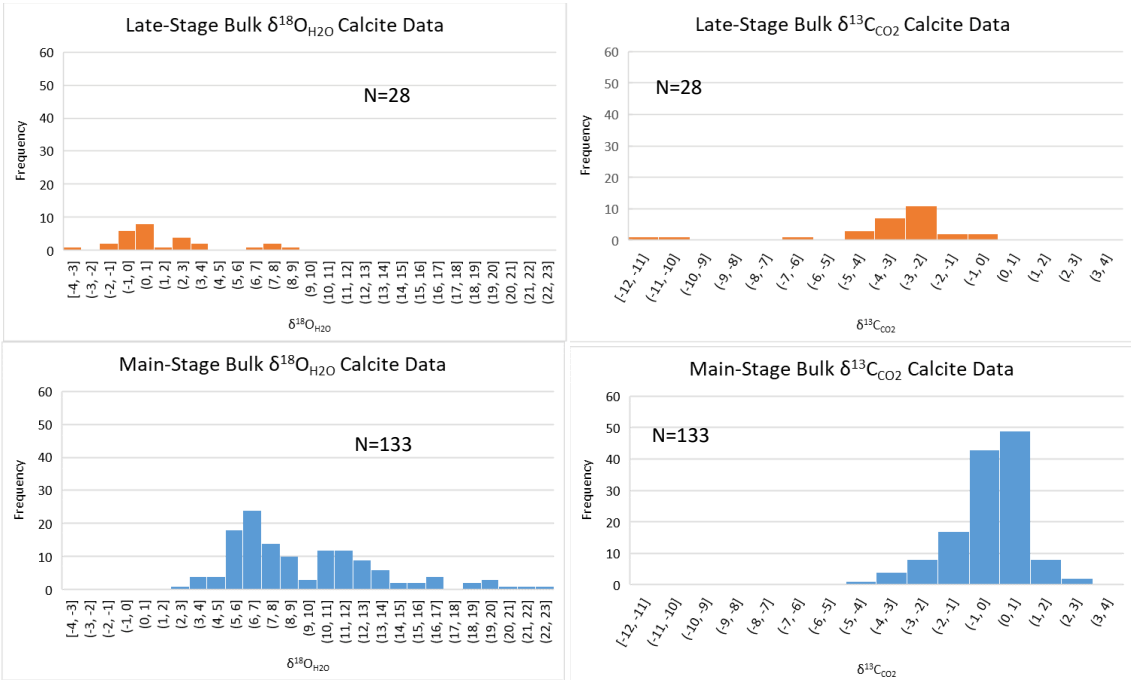

Figure 2.5: Bulk calcite $\delta^{18}O_{H2O}$ and $\delta^{13}C_{CO2}$ subdivided by paragenetic stage.

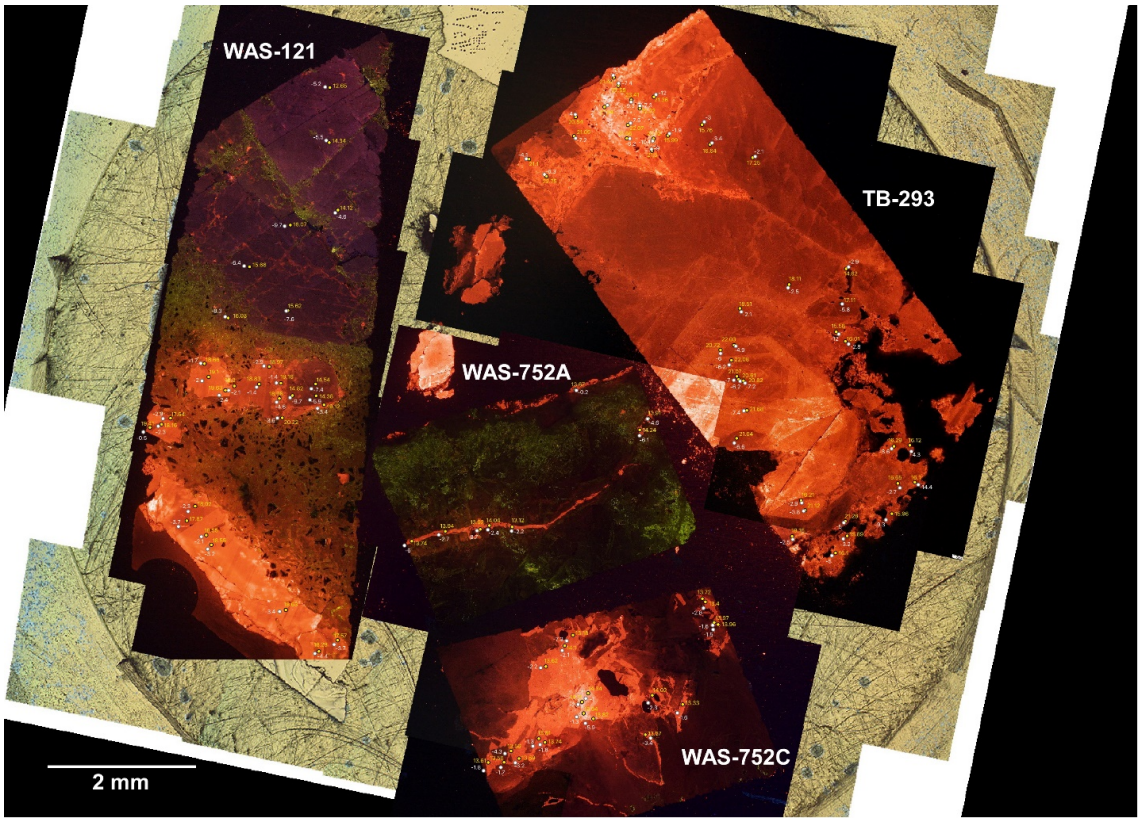

Figure 2.6: Cathodoluminescence image of the three samples analyzed for this study using the SIMS method. Small circles represent spot location for oxygen and carbon isotopic determinations. Details are provided in Appendix III.

2.5.3 Comparison of Bulk versus In-situ Stable Isotope data

All the previously published oxygen and carbon isotopic data for calcite were determined on bulk samples. It is generally assumed that the isotopic composition of the relatively small bulk samples of calcite extracted from specimens is more or less constant. For this study, a sample of main-stage calcite from the Kearsarge deposit (WAS-752), a sample of main-stage calcite from the Quincy Mine (TB-293), and a sample of late-stage calcite from the Kearsarge deposit (WAS-121) were analyzed by SIMS with a spot size of 12 to 14µm for oxygen and 18µm for carbon (Figure 2.6, cathodoluminescence image). The size of each spot analysis is far less than the bulk sample size of either sample. A total of 103 oxygen and carbon isotope pairs were analyzed. The maps of the SIMS data demonstrates significant stable isotope variation greater then the analytical error at a scale of far less than 1 mm (details in Appendix III). The small scale variation is more pronounced in the main-stage calcite.

The variation in oxygen and carbon isotopic composition within an individual grain far exceeds the error of bulk analysis data (Figure 2.3 and 2.7). The larger variation in the spot isotopic analyses suggests that the bulk samples are a weighted average of variation at a scale much smaller than the bulk sample size. The two main-stage spot analyses in

Figure 2.7 shows that there is a higher range in $\delta^{13}C$ than the bulk samples, but the range of $\delta^{18}O$ is less as compared to the bulk data.

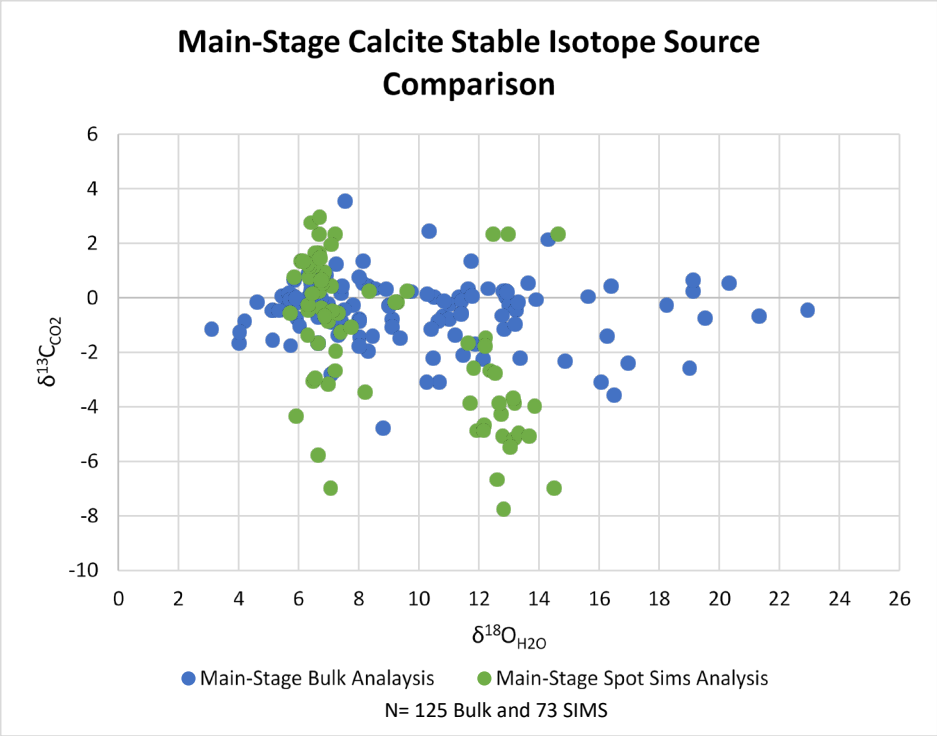

Figure 2.7: Comparison of main-stage bulk isotopic analyses and the spot analyses by SIMS. Temperature for main-stage assigned shown in Appendix IV. Compiled data includes Bornhorst and Woodruff (1997), Livnat (1983) and Püschner (2001).

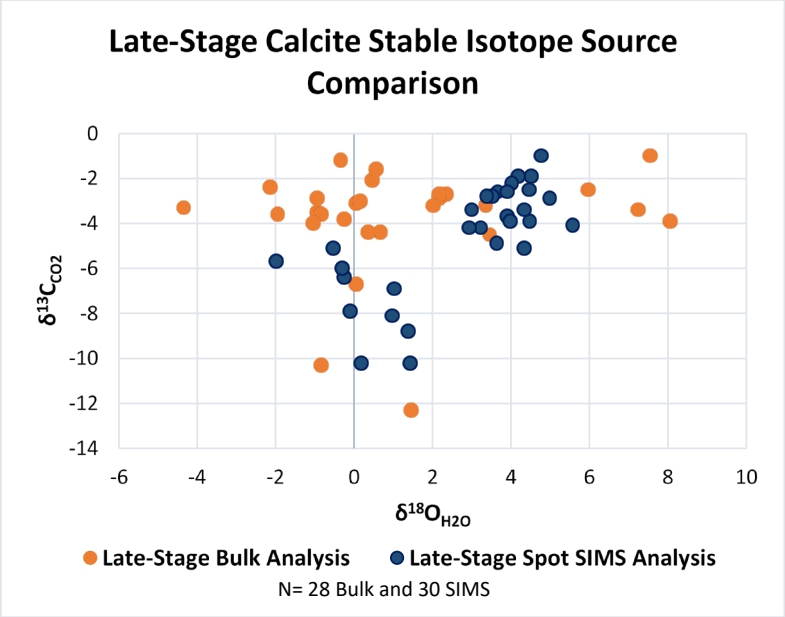

Figure 2.8: Comparison of late-stage data of bulk analysis and SIMS techniques. One SIMS sample has the same amount of variation as the rest of the bulk analyzed data. Temperature for late-stage is 125°C +/-25°C. Compiled data includes Bornhorst and Woodruff (1997) and Livnat (1983).

The one spot analysis sample of late-stage calcite from the Kearsarge deposit has a range of isotopic values that is comparable to the amount of variation found in all of the bulk data from 18 different samples. (Figure 2.8).

2.5.4 All Calcite Data

There are 246 combined bulk and spot analyses of oxygen and carbon from calcite. The oxygen-carbon pattern for the bulk data alone (Figure 2.4) and the combined data (Figure 2.9) is practically the same. The combined variation for the main- and late-stage is the same as it is for the bulk data alone (Figures, 2.5 and 2.10). The combined main-stage values have a range of $\delta^{18}O_{H2O}$ from +3.10 to + 22.93‰ and in $\delta^{13}C_{CO2}$ of -6.86 to +3.54‰ whereas late-stage has a range of $\delta^{18}O_{H2O}$ from -4.35 to +8.05‰ and in $\delta^{13}C_{CO2}$ of -10.285 to -0.985‰ (Figures 2.9 and 2.10).

Generally, the isotopic composition of calcite from the main- and late-stage are distinct from one another (Figure 2.9). The main-stage data are more varied in $\delta^{18}O_{H2O}$ whereas the range of $\delta^{13}C_{CO2}$ is similar. The distrubution of the bulk data alone (Figure 2.5) and the combined bulk and in-situ SIMS data (Figure 2.10) are similar to one another..

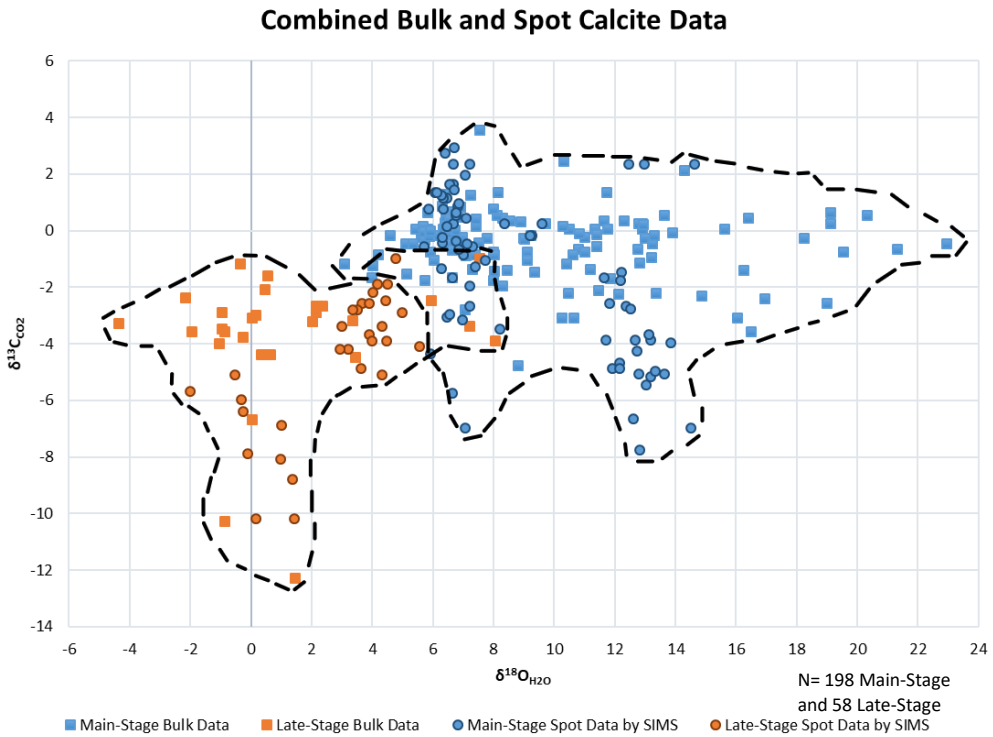

Figure 2.9: Comparison of main- and late-stage stable isotope calcite combined bulk and spot data. Dashed outlined fields denote the approximate $\delta^{13}C$ CO_2 and $\delta^{18}O$ H_2O ranges for main-stage and late-stage. Main-stage uses temperatures from the hydrothermal/ metamorphogenic zones determined in Chapter 1 i.e. epidote zone = 275°C +/- 25°C, pumpellyite zone = 212.5°C +/-37.5°C, and laumontite zone = 150°C +/-25°C and late-stage uses a fixed temperature of 125°C +/-25°C.

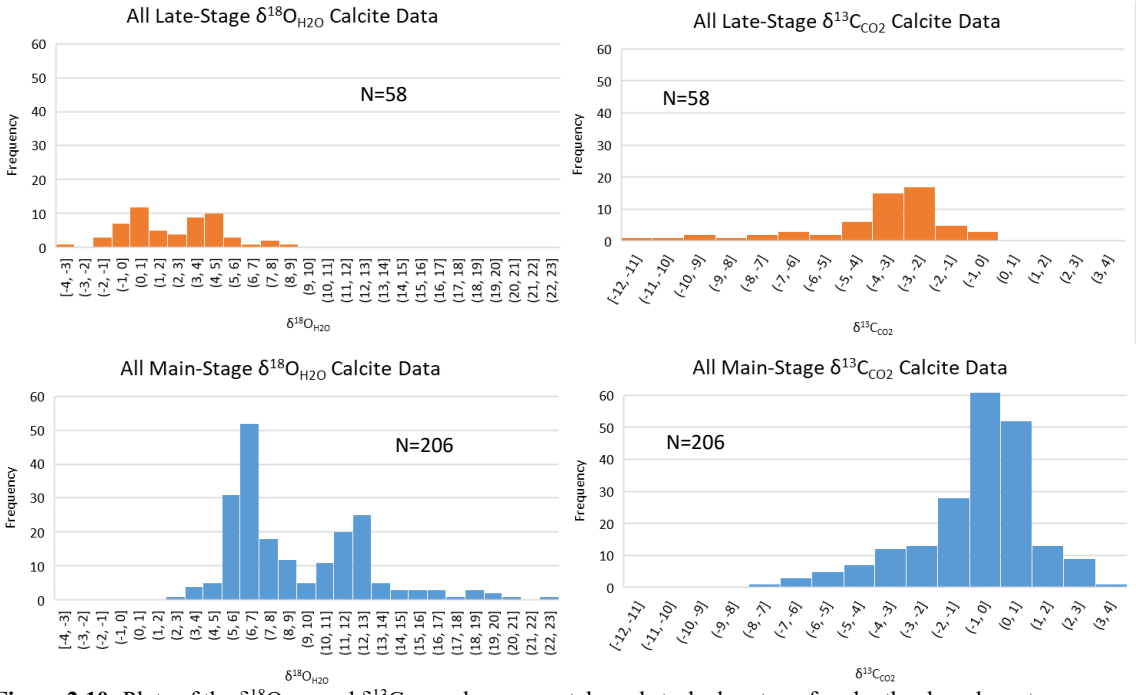

Figure 2.10: Plots of the $\delta^{18}O_{H2O}$ and $\delta^{13}C_{CO2}$ values separately and stacked on top of each other based on stage.

2.6 Discussion

2.6.1 Anomalous Bulk Calcite Isotopic Analyses

There were two bulk calcite isotopic analyses that were assigned to a paragenetic stage but were outliers (Figure 2.11). One of these mineralogically was assigned to the main-stage and the other to the late-stage. The main-stage analysis has a much lighter carbon isotope value than other main-stage bulk calcite analyses. At this time there is no explanation of this outlier and it has been excluded from consideration in this study. The late-stage analysis has a much lighter oxygen isotope value than all other calcite data. However, this value may be real as the oxygen isotopic composition of two quartz samples (see Figure 2.15b) are as negative as this calcite outlier. Thus, this late-stage calcite value is included in Figure 2.15 which is used as a basis to infer fluid source.

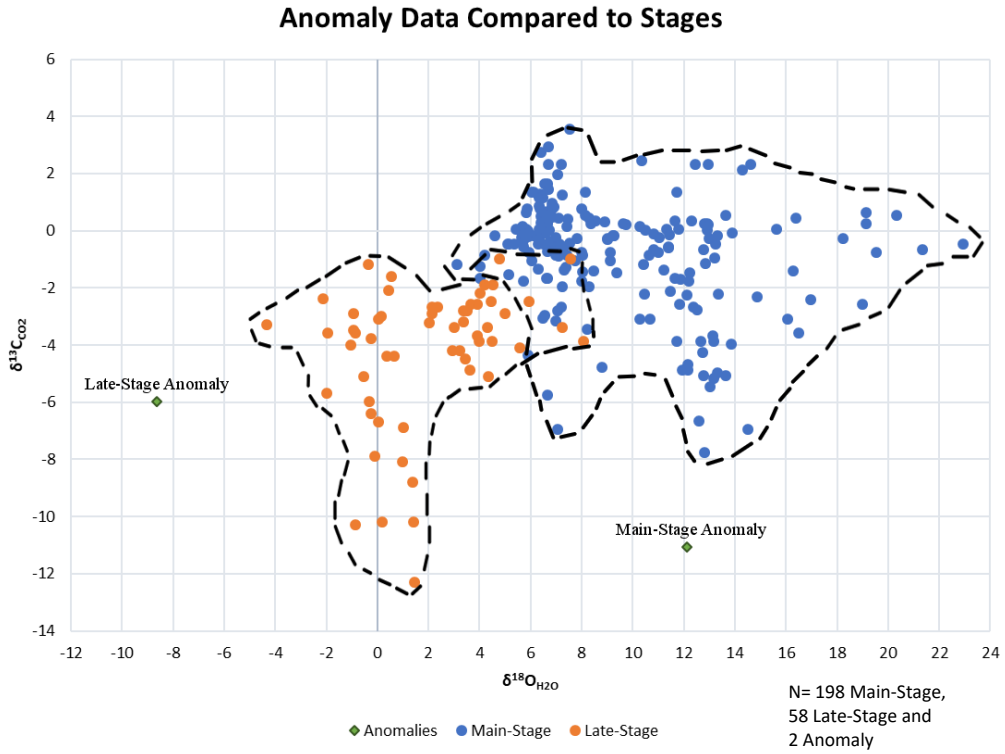

Figure 2.11: Anomaly analyses that were excluded from the general data.

2.6.2 Published Calcite Data when Stage Assignment is Difficult

As discussed in the Methods section, some of the bulk calcite isotopic analyses were not able to be assigned to either main-stage or late-stage with confidence and were not included in the Results section. A few of these analyses were excluded for a common reason which will be discussed here. This could include samples within the copper district where the origin was difficult to determine such as cementing calcite, calcite

hosted in an unusual rock type such as diorite, or samples that are found outside the copper district proper.

The Copper Harbor Conglomerate contains abundant calcite. It is reasonable to assume that at least some of this calcite was likely deposited during burial prior to the influx of hydrothermal/metamorphogenic fluids of the main-stage. The temperature of precipitation is speculative. It is also possible that actual cementing calcite could have been dissolved and reprecipitated during the main-stage. There were multiple samples analyzed by Livnat (1983) labeled as calcite cement in the Copper Harbor conglomerate. Interpretation of the isotopic data of these cements is speculative and not possible at this time.

There are some samples labeled by Livnat (1983) as amygdules that were assigned as uncertain as they were from outside of the native copper district and had minerals listed that could represent either stage. These samples are on the fringe of the native copper district in areas within either the laumontite or heulandite-stilbite mineral zones, where existence of low temperature main-stage hydrothermal/metamorphogenic fluids is reasonable. When applying a main-stage temperature based on the metamorphic zone they were located in, they are reasonably main-stage and are subsequently included in the main-stage (Figure 2.12).

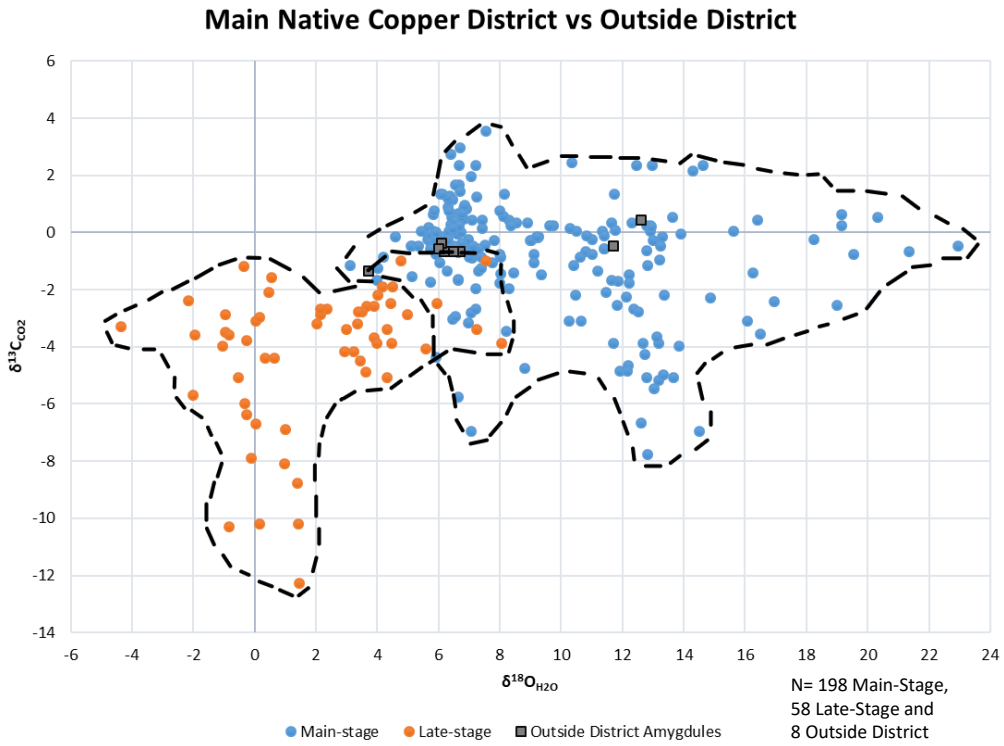

Figure 2.12: Native copper district calcites compared to the outside the district amygdule calcites (Livant, 1983).

There are several analyses that were collected by Livnat (1983) from the Lac La Belle area. These samples are hosted by the Mount Bohemia intrusion and were from veins

associated with minerals such as chalcocite, chalcopyrite, and barite. These samples should have been assigned to the late-stage because of the presence of copper sulfides. However, nearby, Robertson (1975) described deposits with copper sulfides as the principal ore mineral rather than native copper. In addition, there are multiple copper sulfide-rich deposits to the west of Mount Bohemia. Sikkila (1984) proposed the Mount Bohemia stock may be a separate hydrothermal system. Hence, these data are excluded and not discussed further.

Livnat (1983) has provided bulk calcite isotopic analyses from what he terms lakeshore calcite veins. There are multiple calcite veins cross-cutting the Copper Harbor Conglomerate approximately perpendicular to bedding in the east half of the Keweenaw Peninsula. Similar oriented native copper-bearing veins are well known in the Phoenix to Delaware area on the north east part of the native copper district. The lakeshore veins have, in addition to calcite, minerals such as, barite, fluorite, and laumontite. The lakeshore veins are within the main-stage laumontite zone, but the temperature of precipitation would be nearly the same if they were in fact late-stage. Using the laumontite zone temperature for fractionation calculations results in the lakeshore calcite vein analyses that overlap the main- and late-stage fields (Figure 2.13). That all but two of the analyses fall within the main-stage field supports them being part of that field. The two analyses with lighter oxygen could readily be an extension of the main-stage field but this would make the main-stage field less distinct from the late-stage field. The few that fall in or near the late-stage area could be related to late-stage fluids precipitating the calcite instead of main-stage fluids. If main-stage involves mixing of fluids, the light oxygen values of the lakeshore calcite veins could be representative of a meteoric end-member (discussed below).

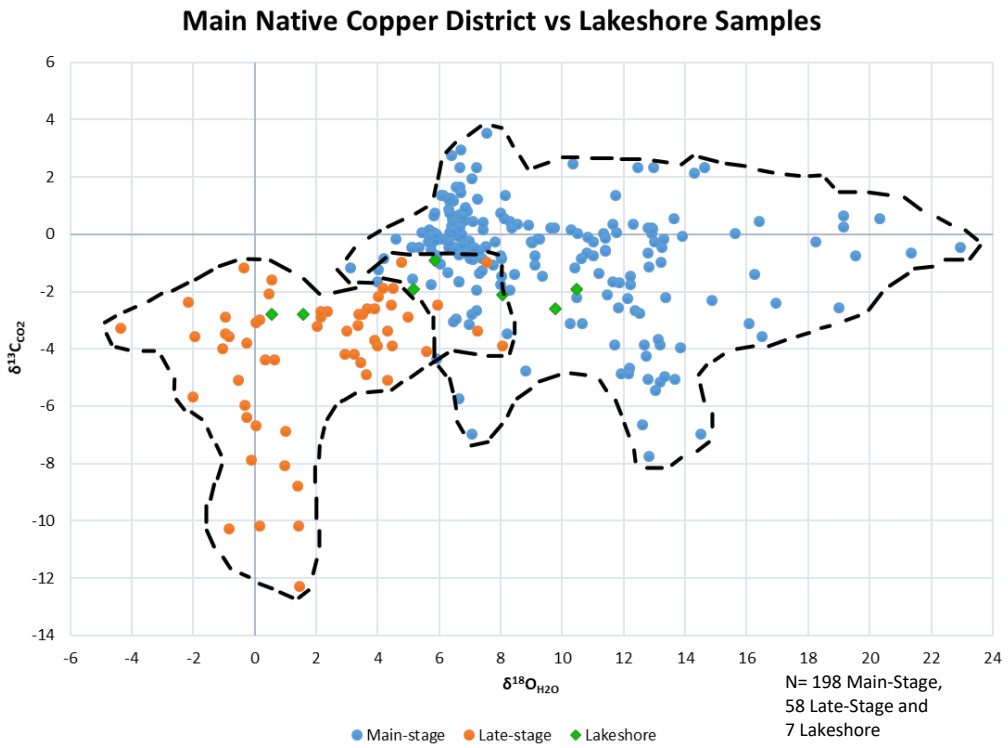

Figure 2.13: Native copper district calcites compared to the Lakeshore vein calcites (Livnat, 1983). The Lakeshore vein calcites were assigned the laumontite zone temperature of 150°C.

2.6.3 Main-Stage and Late-Stage Overlap

Main- and late-stage isotopic compositions of calcite overlap with one another (Figure 2.9). There are five late-stage samples within the main- and late-stage overlap area that will be discussed here (Figure 2.14). A6 (Appendix II) is from the Baltic mine area and was noted by Livnat (1983) to have pink calcite present. The color may be a result of copper inclusions which suggests it is main-stage rather than late-stage. A51 and A52 (Appendix II) are from shear veins, and A124 is from an amygdule near the Phoenix mine area. Livnat (1983) labeled these as being late so they were assigned as late stage. However, there is no real explanation to be found for what Livnat (1983) meant by late. SIMS66 (Appendix III) is one analysis point from the Seneca SIMS analyzed sample. These overlapping late-stage analyses may be due to poor descriptions that resulted in them being mis-assigned. Alternatively, overlap could be due to the origin of the fluids and the uncertainty of the precipitation temperatures.

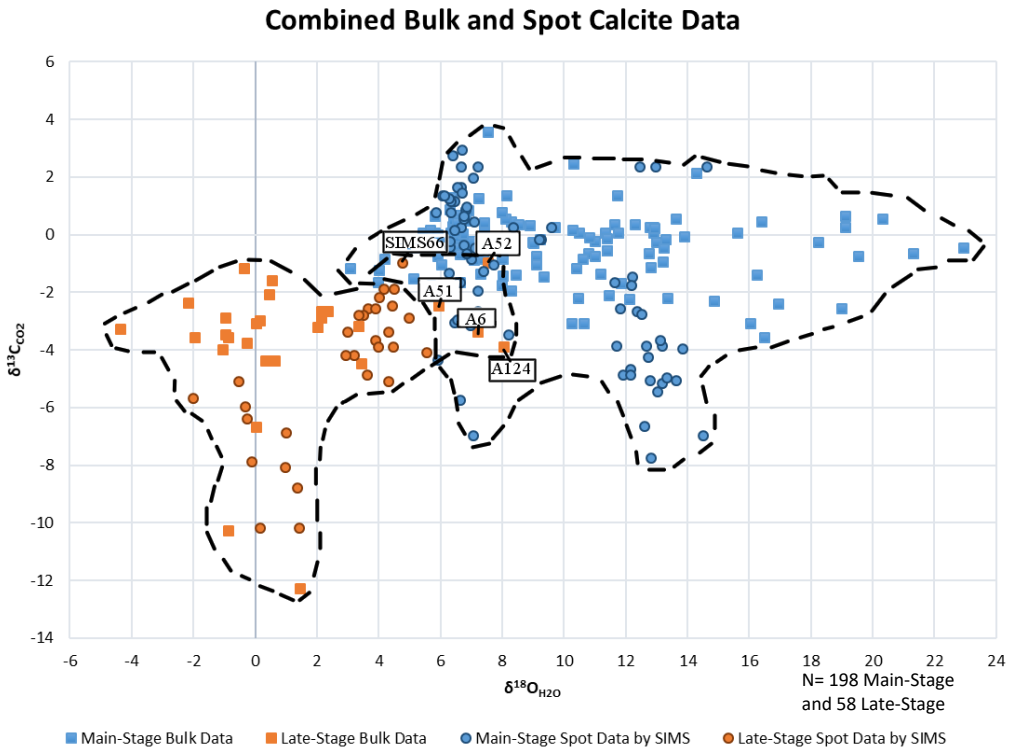

Figure 2.14: Overlap of main- and late-stage analyses data points labeled for reference.

2.6.4 Comparison of Calcite to other minerals

The $\delta^{18}O_{H2O}$ compositions calculated from analyses of calcite are compared here to the $\delta^{18}O_{H2O}$ composition calculated from analyses of other minerals. Main- and late-stage quartz and clinochlore/chlorite were analyzed by Livnat (1983) and Püschner (2001). Clinochlore/chlorite and quartz values overlap with calcite, but both have a few values lower than any found for calcite (Figure 2.15A). Most $\delta^{18}O_{H2O}$ values fall in the range of +3 to +17‰ (Figure 2.15.A).

Late-stage $\delta^{18}O_{H2O}$ values calculated from calcite and quartz and some clinochlore/chlorite analyses overlap with one another. Most $\delta^{18}O_{H2O}$ values fall in the range of -3 to +6‰ (Figure 2.15.B).

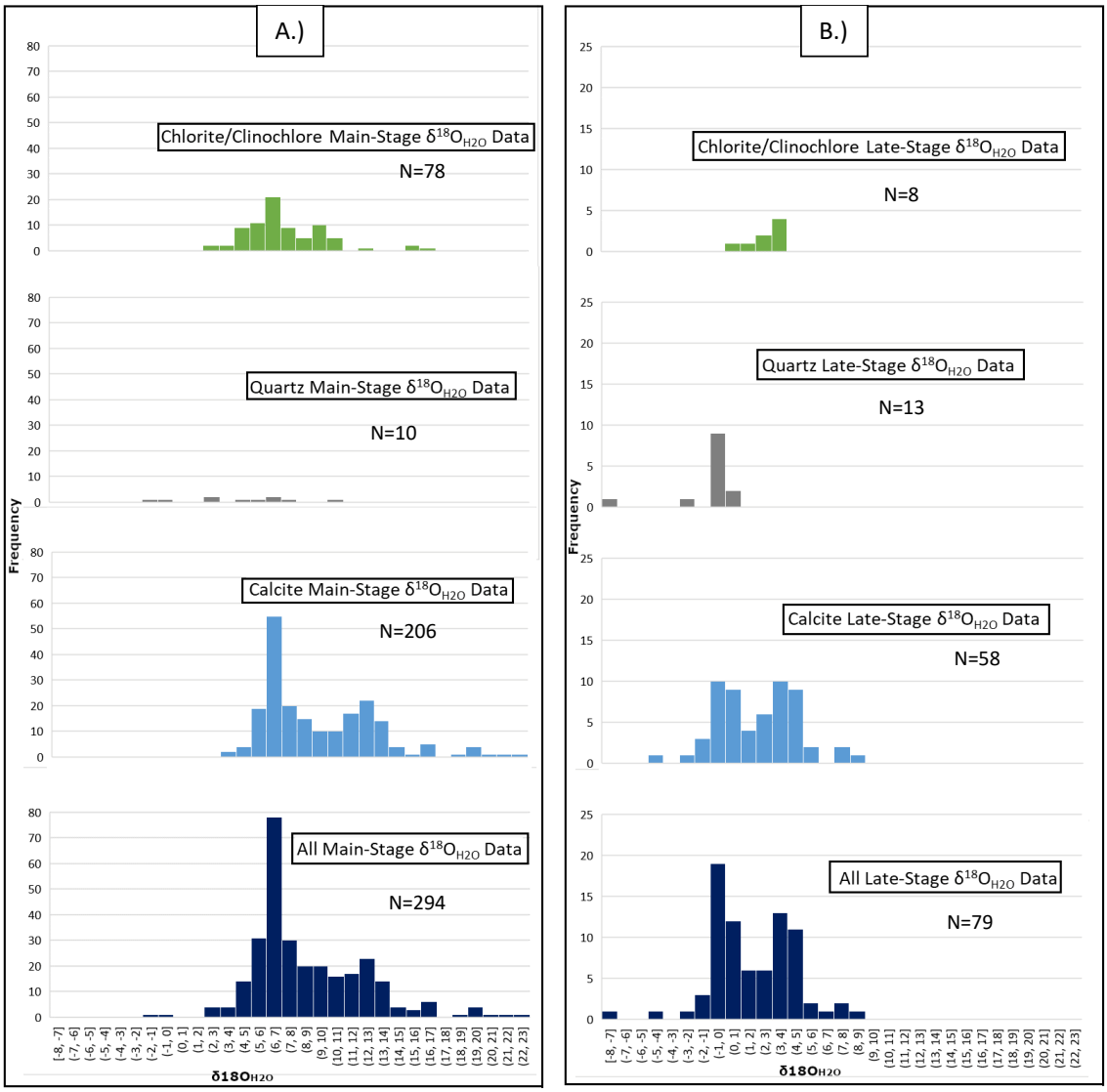

Figure 2.15: Comparison of calcite $\delta^{18}O$ H_2O data to quartz and clinochlore/chlorite main-and late-stage data. Main-stage data calculated using spatial mid-point temperatures from Chapter 1, late-stage data calculated using a fixed temperature of 125°C. Data comes from Livnat (1983) Bornhorst and Woodruff (1997), Püschner (2001), and SIMS data (this study).

2.6.5 Interpretation of Oxygen Isotopic Composition of Main-Stage Fluids

In Figure 2.16, main-stage oxygen isotopic data for calcite is compared to the general ranges for fluid sources (Hoefs, 1973; Rollinson, 1993; Püschner, 2001; Sharp, 2017). Most of the main-stage data lies within the metamorphic fluid source range and on this basis could be interpreted as entirely metamorphogenic in origin.

The variability in main-stage calcite $\delta^{18}O_{H2O}$ cannot be explained solely by temperature and analytical error (see Figure 2.3) as previously concluded by Bornhorst and Woodruff (1997). It is difficult to explain the calcite oxygen isotopic variation by a regional

metamorphogenic only origin. There is considerable variation of calcite oxygen isotopic composition within a single deposit (Kearsarge). To explain this variation only by regional metamorphogenic fluids would require that the regional metamorphogenic processes produce multiple batches of fluid, each with differing oxygen isotopic composition rather than a more consistent composition within a restricted range. The former seems less likely from a deep regional fluid generating process. The in-situ SIMS data demonstrates that isotopic variation occurs on the sub-mm to cm scale within a single continuous mass of calcite. It seems difficult to ascribe small-scale fluid variation to fluids generated by regional metamorphism.

Since the metamorphogenic and meteoric water fields overlap with one another, the variation of the calcite isotopic composition could be explained by mixing of meteoric fluid with metamorphogenic fluid. For calcite alone, the simplest fluid mixing model would be between an oxygen isotopically light meteoric water in the +3 to +6‰ range and a metamorphogenic water in the +15 to +20‰ range. Mixing of the deep derived hydrothermal/metamorphogenic ore-fluids with meteoric water at shallow level during mineral precipitation could readily explain the small-scale calcite isotopic variation. Bornhorst and Woodruff (1997) hypothesized that fluid mixing played a role in native copper precipitation (main-stage) based on a limited data set. Püschner (2001) agreed with the interpretation that metamorphogenic waters from depth mixed with relatively shallow meteoric waters. Significant involvement of seawater as proposed by Livnat (1983) is difficult to reconcile with the oxygen isotope data and, therefore, as concluded by Püschner (2001), seawater is unlikely an important fluid source.

Brown (2006 and 2008) proposed that meteoric surface waters penetrated downward into the fluid source zone wherein they contributed to and mixed with the fluids being generated by regional metamorphogenic processes; termed a hybrid, evolved meteoric and metamorphogenic fluid model by Brown (2006). Conceptually, the mixing of these two fluids at depth should have resulted in an average hybrid fluid, with the average depending on the proportion of meteoric and metamorphogenic waters. The average hybrid fluid would have to be on the isotopically heavy end of metamorphogenic fluid range for it to be able to be mixed with meteoric water to generate the observed isotopic variation. Thus, the composition of this average hybrid fluid would preclude significant involvement of surface meteoric waters penetrating downward into the ore fluid source zone or else the average would be isotopically lighter. Thus, Brown's (2006) hybrid evolved meteoric and metamorphogenic fluid model is not likely.

Involvement of a significant amount of magmatic fluid involves a similarly unlikely model as the evolved meteoric water of Brown (2006). It is possible that above the source area envisioned for the metamorphogenic fluids (Bornhorst and Mathur, 2017) magmatic fluids could mix with metamorphic fluids which further mix with reduced meteoric water in the zone of precipitation, a three-way mix. However, the involvement of magmatic fluids was rejected by White (1968) about 50 years ago primarily based on field evidence that native copper precipitation occurred long after then end of rift magmatism. The widespread distribution of native copper in the rift fits with regional metamorphogenic

fluid rather than magmatic fluids. On the basis of oxygen isotopic data, magmatic waters do not play and important role in the genesis of the native copper deposits.

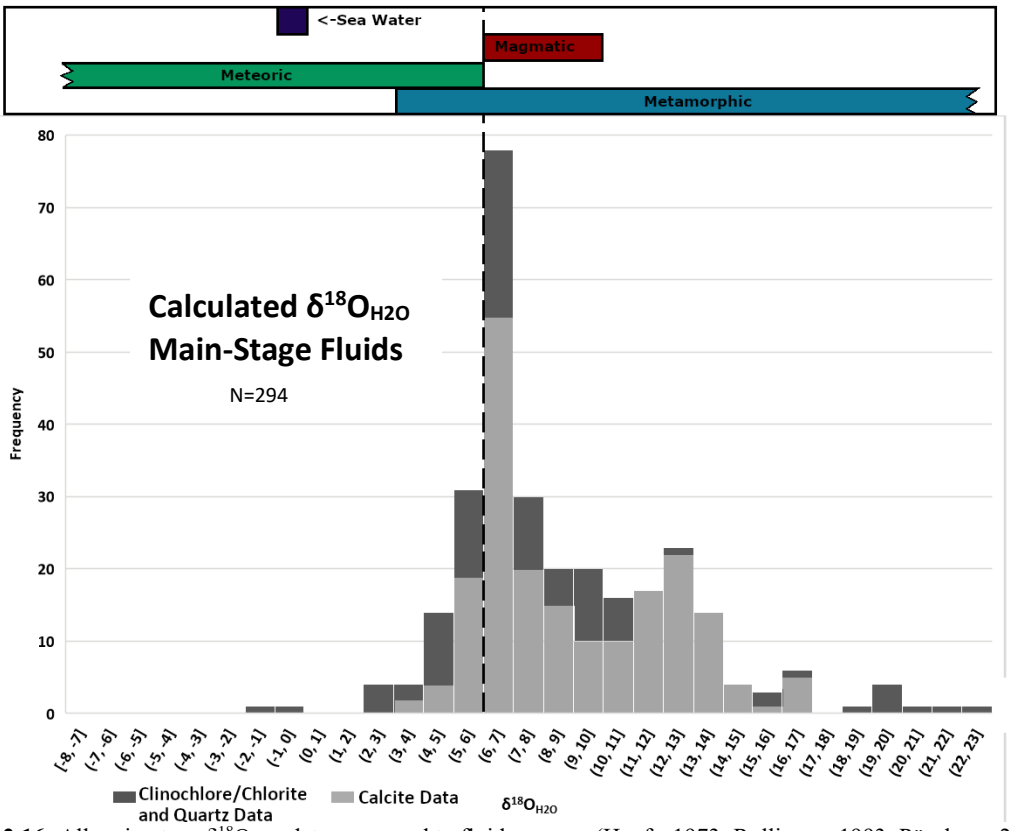

Figure 2.16: All main-stage $\delta^{18}O_{H2O}$ data compared to fluid sources. (Hoefs, 1973; Rollinson, 1993; Püschner, 2001; Sharp, 2017). The vertical dashed line represent the mantle value as indicated in Püschner (2001)..

2.6.6 Interpretation of Isotopic Composition of Late-Stage Fluids

Temperature and analytical error can explain a significant amount of the variability found within late-stage data (Figure 2.3 and 2.11). Most of the late-stage fluid values lie within the meteoric fluid range and on this basis could simply be interpreted as dominated by meteoric water (Figure 2.17). If reported values are considered without error, limited mixing of late-stage fluids with main-stage fluids cannot be precluded since there is an overlap of late-stage with main-stage fluid isotopic compositions (Figure 2.9). However, the mis-assignment of analyses to the late-stage as described for overlapping samples above is another possible explanation instead of fluid mixing. The data are insufficient to draw a conclusion with regards to the involvement of seawater. Given the generally consistent composition of seawater, 0 ‰, involvement of seawater is possible if mixed with meteoric water. With more data it may be possible to infer whether or not more than one fluid was involved in late-stage mineralization. Regardless, late-stage fluids are likely dominantly meteoric waters.

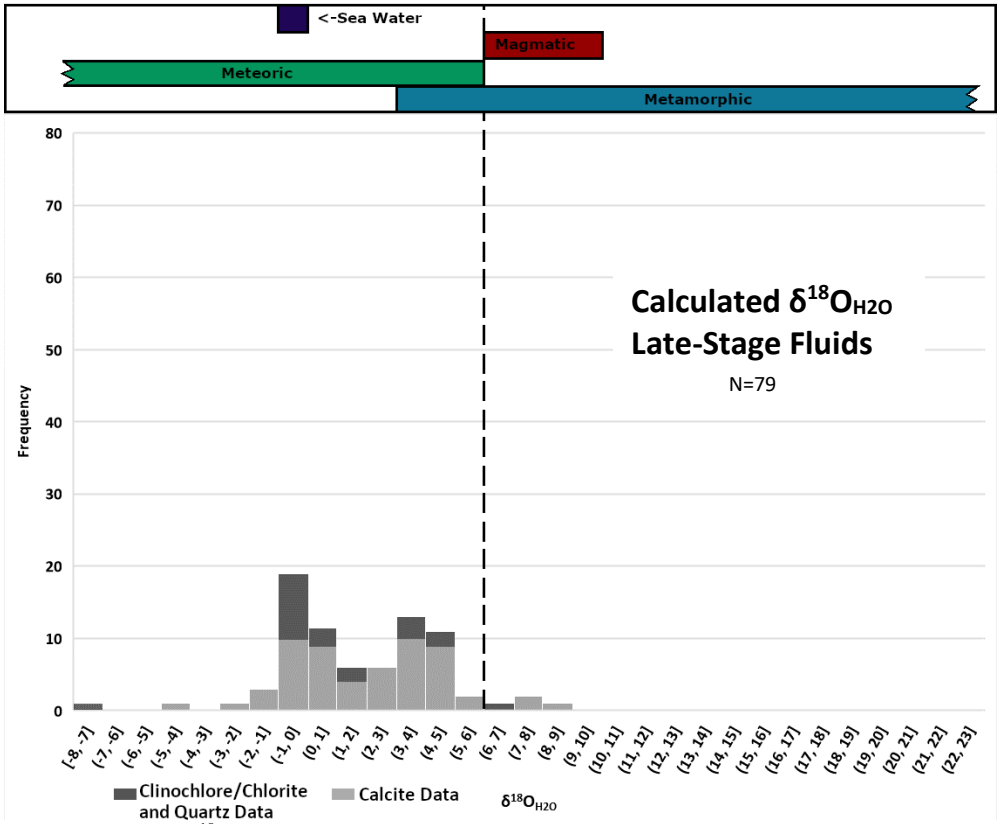

Figure 2.17: All late-stage $\delta^{18}O_{H2O}$ data compared to fluid sources. (Hoefs, 1973; Rollinson, 1993; Püschner, 2001; Sharp, 2017). The dashed line indicates the value of mantle rock.

2.6.7 Carbon Stable Isotopes

Ohmoto (1972) demonstrated that the carbon isotopic composition of calcite is dependent on fugacity of oxygen and carbon dioxide, oxidation, pH, as well as the total amount of carbon in the hydrothermal/metamorphogenic fluids. Ohmoto's (1972) showed that the main-stage carbon isotopic composition of the calcite from this study is approximately the same as the sum carbon in the fluid and CO_2. The values for main-stage carbon isotopic composition of calcite overlaps with ranges for basalts, marbles, ocean water, and fresh water (Sharp, 2017) and is inconclusive with regards to fluid/carbon origin The effect of conditions of precipitation on the isotopic composition of late-stage calcite as compared to that in the fluid is uncertain as conditions during precipitation of late-stage calcite are uncertain. If the $\delta^{13}C_{CO2}$ of late-stage calcite is also approximately the same as total carbon in the fluid then the late stage $\delta^{13}C_{CO2}$ is compatible with a meteoric water origin as freshwater total CO_2 has a range of about -23 to 0‰ (Sharp, 2017).

2.6.8 Hydrogen Stable Isotopes

Livnat (1983) and Püschner (2001) analyzed δD of chlorites, pumpellyite and epidote. These values were compiled and assigned to either the main- or late-stage (Appendix IV). The δD_{H2O} was calculated from the raw δD values of the minerals. For chlorite, fractionation factors of chlorite-H_2O were derived from Graham et al. (1987, op. cit. Figure 3). At temperatures greater than 250°C the fractionation is weakly dependent on temperature. For pumpellyite, Livnat (1983) proposed that δD fractionation can be estimated using the zoisite- H_2O equation. The zoisite- H_2O equation from Graham (1980) was used for pumpellyite. For epidote, the epidote-H_2O equation of Graham (1980) was used to calculate δD_{H2O}. The main- and late-stage δD_{H2O} for each mineral and all minerals is shown in Figure 2.18. The main- and late-stage fluid δD_{H2O} overlap with each another.

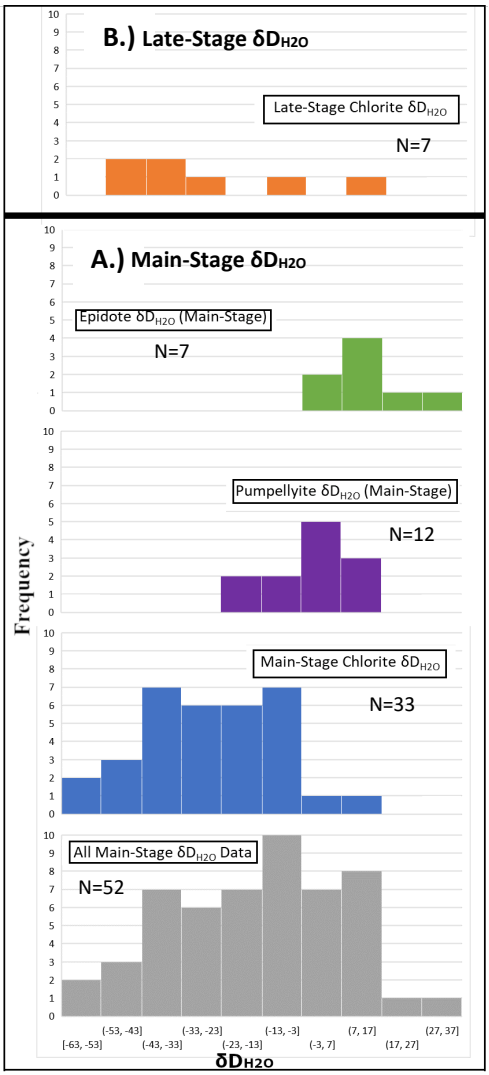

Figure 2.18: δD_{H2O} values plotted based on minerals and stage from Livnat (1983) and Püschner (2001). A.) All main-stage data, B.) the late-stage chlorite data.

The combination of δD_{H2O} and $\delta^{18}O_{H2O}$ data can be used to infer fluid sources perhaps better than by $\delta^{18}O_{H2O}$ alone. Usually, δD_{H2O} and $\delta^{18}O_{H2O}$ for individual samples are plotted. Given the limited number of pairs of data, instead for this study the ranges and percentiles for δD_{H2O} and for $\delta^{18}O_{H2O}$ were used to plot boxes encompassing various proportions of the data (see Figure 2.19 and 2.20). Figure 2.19 shows considerable overlap of the main-stage data with the metamorphic fluid range as well as the main stage field extends to the meteoric water line. The simplest interpretation is that the main-stage δD_{H2O} and $\delta^{18}O_{H2O}$ overall, within deposit, and within sample, variation results from the mixing of metamorphogenic waters and shallow reduced meteoric water. The main-stage data are not consistent with a significant involvement of magmatic water as the hydrogen isotope main-stage data mostly fall outside the magmatic field. For significant involvement of magmatic water, it would need to mix with both oxygen isotopically heavier water, metamorphic in composition, and with isotopically lighter oxygen meteoric water to explain the main-stage data. The uniform composition of seawater, zero δD_{H2O} and zero $\delta^{18}O_{H2O}$, makes it difficult to explain main-stage values both isotopically lighter and heavier than seawater. As was the case for magmatic water, it is possible that the variation could be explained by a three-way mixing of deeply derived metamorphogenic water with shallower meteoric and seawater. Thus, significant main-stage involvement of seawater seems unlikely. Brown's (2006) hybrid evolved meteoric water and metamorphogenic water model is unlikely on the basis of combined δD_{H2O} and $\delta^{18}O_{H2O}$ for the same reasons described above for $\delta^{18}O_{H2O}$ alone.

There are only a few main-stage data that fall approximately on the meteoric water line. Whereas these data would be readily interpreted as meteoric in origin, the meteoric end-member to be mixed with metamorphogenic water may be of a composition between the meteoric water line and the metamorphic water field. Compositions in this area of the diagram have been shown to exist in deep sedimentary basins. They are the result of mixing of meteoric waters with connate or other waters, water-mineral reactions, and fractionation effects (Taylor, 1979). Two examples of deep basin evolved meteoric fluids are shown on Figure 2.19 and 2.20. An evolved meteoric water mixing with metamorphogenic water at a shallow depth could explain both the variation of most of the data as well as within the deposit and within sample variation. It is important to recognize that this is not Brown's (2006) hybrid evolved meteoric water and metamorphogenic water model wherein the evolved meteoric waters enter into and are part of the generation of metamorphogenic ore fluid, but rather as envisioned here the evolved meteoric waters mix in the relatively shallow zone of precipitation with metamorphogenic water.

The Midcontinent Rift is filled with a large thickness of basalt overlain by a large thickness of clastic sedimentary rocks. Conceptually, an evolved meteoric water, that is reduced and sulfur-poor (Bornhorst and Mathur, 2017), could be developed in these overlying sedimentary rocks as demonstrated by Brown (2006). It is possible that a hydrologic flow system could move evolved meteoric fluids derived within the sedimentary rocks of the Midcontinent rift into the relatively shallow zone of precipitation where they mixed with metamorphogenic ore fluids derived at elevated temperature and depth in the very thick section of basalt filling the rift. The shallow

mixing of dominantly meteoric and/or evolved meteoric waters with metamorphogenic water explains the variation in the stable isotopic data.

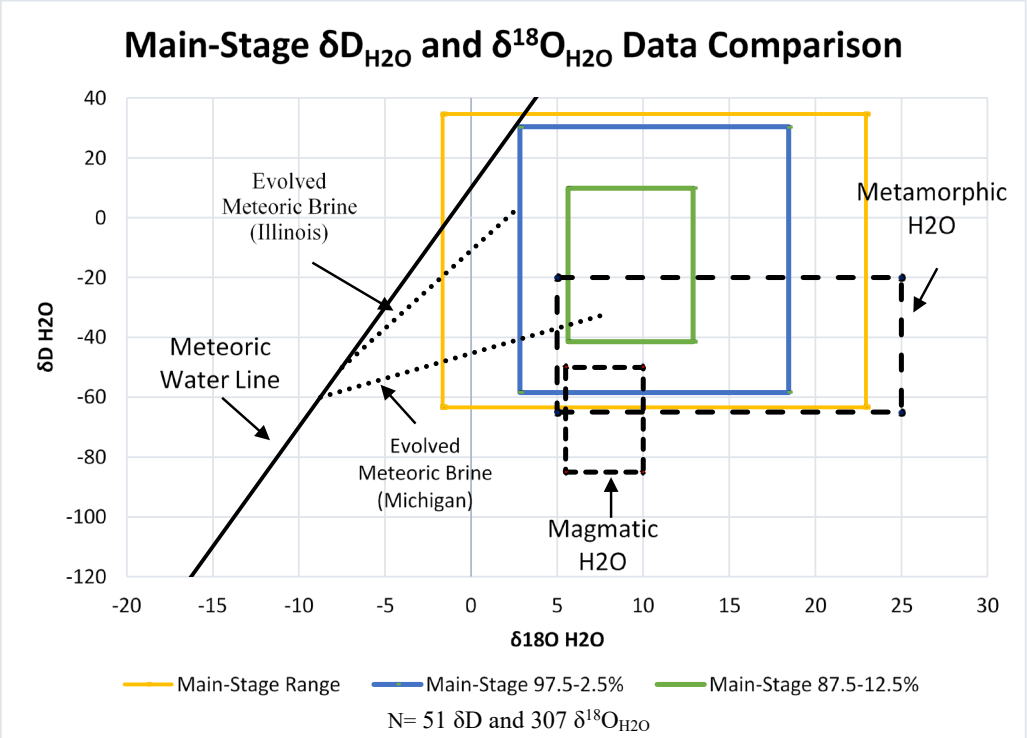

Figure 2.19: δD_{H2O} and $\delta^{18}O_{H2O}$ main-stage analyses plotted as ranges as represented by the boxes. The magmatic and metamorphic ranges, and meteoric water line were from Taylor (1979) and inferred evolved meteoric lines from Clayton et al (1966).

Most of late-stage δD_{H2O} and $\delta^{18}O_{H2O}$ analyses are between the meteoric and metamorphic water fields in either δD_{H2O} or $\delta^{18}O_{H2O}$ (Figure 2.20) with 75% between the meteoric water line and metamorphic water fields. Significant involvement of magmatic water is precluded by the late-stage isotopic data. The late-stage data can be interpreted as either a mix of meteoric and metamorphic waters or as evolved meteoric waters as discussed above. Seawater involvement is possible only if it is part of a mixture with meteoric/evolved meteoric and metamorphic waters. More data are needed to more clearly infer the source or sources of late-stage fluids. Regardless, late-stage fluids are likely dominantly meteoric waters.

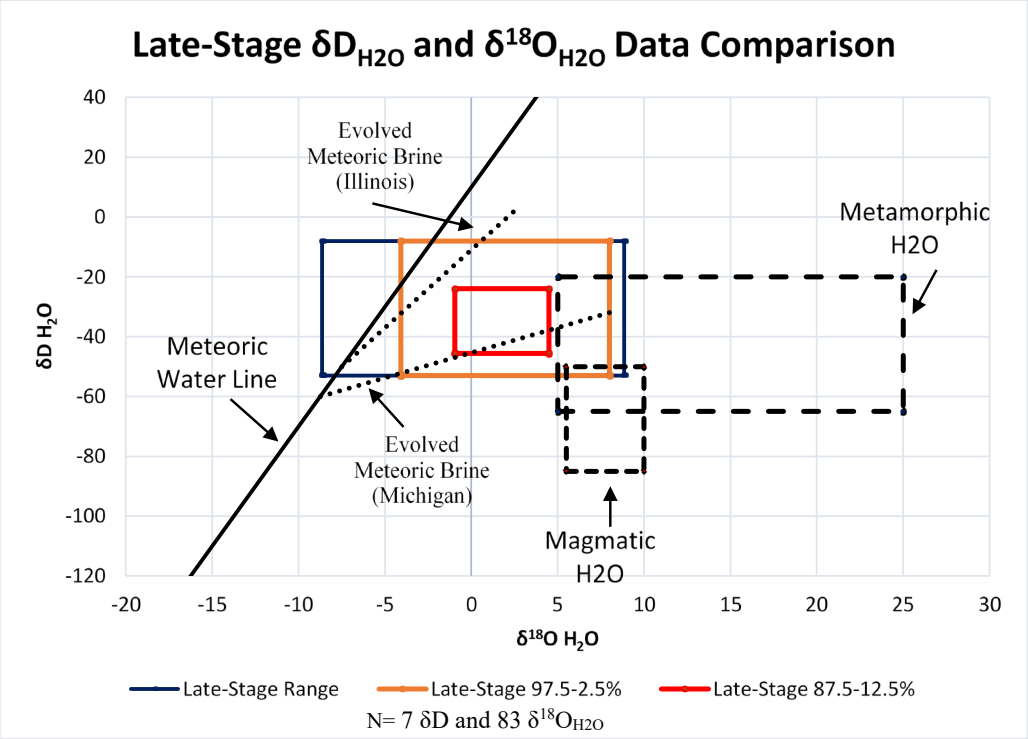

Figure 2.20: δD_{H2O} and $\delta^{18}O_{H2O}$ late-stage analyses plotted as ranges as represented by the boxes. The magmatic and metamorphic ranges, and meteoric water line were from by Taylor (1979).

2.7 Conclusion

This study focused on interpretation of existing bulk oxygen, carbon, and hydrogen stable isotope data from native copper-bearing rocks of the Keweenaw Peninsula of Michigan, supplemented with spot oxygen and carbon analyses by SIMS presented in this study. The data were assigned to either the paragenetic main- or late-stage. Interpretation of δD_{H2O} and $\delta^{18}O_{H2O}$ main-stage data suggests that main-stage fluids are derived from depth during burial metamorphism of rift-filling basalt (metamorphogenic fluids) that mixed with dominantly meteoric water. The meteoric water could have been isotopically evolved as part of a hydrologic system in the rift-filling clastic sedimentary rocks overlying the rift-filling basalt. The fine-scale variation of the new spot analysis data provides evidence that mixing of the hydrothermal/metamorphogenic ore fluids occurred during the time of precipitation; otherwise the deep hydrothermal/metamorphogenic ore fluids would need to have had an unreasonably high amount of temporal isotopic variation. Late-stage fluids can be isotopically distinguished from the main-stage fluids. Interpretation of late-stage δD_{H2O} and $\delta^{18}O_{H2O}$ suggests that the fluids were dominantly meteoric fluids.

2.7.1 Future Work

There is insufficient late-stage isotopic data to draw firm conclusions and thus, additional data would be beneficial. In comparison to oxygen isotopic data, the amount of hydrogen isotopic data is much less for both main- and late-stages. Thus, additional hydrogen isotopic data would also be useful. Additional light stable isotope data on samples with clear paragenesis, could be used to test the hypothesis of Püschner (2001) that the main-stage should be subdivided.

3 Reference List

Bégué, F., Baumgartner, L.P., Bouvier, A.S., Robyr, M., 2019, Reactive fluid infiltration along fractures: Textural observations coupled to in-situe isotopic analyses: Earth and Planetary Science Letters 519, p. 264-273.

Bornhorst, T.J., and Suchoski, J.P., 1995, A physicochemical model for the deposition of native copper and associated minerals in the Keweenaw Peninsula native copper district, Michigan: Proceedings International Field Conference and Symposium, IGCP Project 336, Duluth, MN, p. 19-20.

Bornhorst, T.J., and Woodruff, L.G., 1997, Native Copper Precipitation by Fluid-Mixing, Keweenaw Peninsula, Michigan: Institute on Lake Superior Geology Proceedings, 43rd Annual Meeting, v. 43, part 1, p. 9-10.

Bornhorst, T.J. and Lankton, L.D., 2009, Copper mining: A billion years of geologic and human history: in Schaetzl, R., Darden, J., and Brandt, D., eds, Michigan Geography and Geology, Pearson Custom Publishing, New York, p. 150-173.

Bornhorst, T.J. and Williams, W.C., 2013, The Mesoproterozoic Copperwood Sedimentary Rock Hosted Stratiform Copper Deposit, Upper Peninsula, Michigan: Economic Geology, v. 108, p. 1325-1346.

Bornhorst, T.J. and Mathur, R., 2017-2018, Copper Isotope Constraints on the Genesis of the Keweenaw Peninsula Native Copper District, Michigan, USA: Minerals 2017, v.7, p.185.

Brown, A.C., 2006, Genesis of Native Copper Lodes in the Keweenaw District, Northern Michigan: A Hybrid Evolved Meteoric and Metamophogenic Model: Economic Geology, v. 101, p. 1437-1444.

Brown, A.C., 2008, District-Scale Concentration of Native Copper Lodes from a Tectonically Induced Thermal Plume of Ore Fluids on the Keweenaw Peninsula, Northern Michigan: Economic Geology, v. 103, p. 1691-1694.

Butler, B.S., and Burbank, W.S., 1929, The copper deposits of Michigan: U.S. Geological Survey Professional Paper 144, p.238.

Cannon, W. F., Green, A. G., Hutchinson, D. R., Lee, M.W., Milkereit, B., Behrendt, J.C., Halls, H.C., Green, J.C., Dickas, A.B., Morey, G.B., Sutcliffe, R., and Spencer, C., 1989, The North American mid-continent rift beneath Lake Superior from Glimpse seismic reflection profiling: Tectonics, v. 8, p. 305-332.

Clayton, R.N and Mayeda, T.K., 1963, The use of bromine pentafluoride in the extraction of oxygen from oxides and silicates for isotopic analysis: Geochimica et Cosmochimica Acta, v. 27, p. 45-52.

Clayton, R. N., Friedman, I., Graf, D. L., Mayeda, T. K., Meents, W. F., and Shimp, N. F., 1966, The origin of saline formation waters: 1. Isotopic composition, Journal of Geophysical Research, v.71, p.3869– 3882.

Clayton, R.N, O'Neil, J.R., and Mayeda, T.K., 1972, Oxygen isotope exchange between quartz and water: Journal of Geophysical Research, v. 77, p. 113-135.

Cornwall, H.R. and White, W.S., 1955, Bedrock Geology of the Manitou Island Quadrangle Michigan: Geologic Quadrangle Maps of the United States, United States Geological Survey, Map GQ-73, scale 1:24,000.

Cornwall, H.R, 1954, Bedrock Geology of the Lake Medora Quadrangle Michigan: Geologic Quadrangle Maps of the United States, United States Geological Survey, Map GQ-52, scale 1:24,000.

Cornwall, H.R., 1955, Bedrock Geology of the Fort Wilkins Quadrangle Michigan: Geologic Quadrangle Maps of the United States, United States Geological Survey, Map GQ-74, scale 1:24,000.

Cornwall, H.R., 1954, Bedrock Geology of the Delaware Quadrangle Michigan: Geologic Quadrangle Maps of the United States, United States Geological Survey, Map GQ-51, scale 1:24,000.

Cornwall, H.R. and Wright, J.C., 1954, Bedrock Geology of the Eagle Harbor Quadrangle Michigan: Geological Quadrangle Maps of the United States, United States Geological Survey, Map GQ-36, scale 1:24,000.

Cornwall, H.R., 1954, Bedrock Geology of the Phoenix Quadrangle Michigan: Geological Quadrangle Maps of the United States, United States Geological Survey, Map GQ-34, scale 1:24,000.

Davidson, E.S., Espenshade, G.H., White, W.S., Wright, J.C., 1955, Bedrock Geology of the Mohawk Quadrangle Michigan: Geological Quadrangle Maps of the United States, United States Geological Survey, Map GQ-54, scale 1:24,000.

Fallick, A.E., Jocelyn, J., Donnelly, T., Guy, M., and Behan, C., 1985, Origin of agates in volcanic rocks from Scotland: Nature 313, 672-674.

Feenstra A. And Franz G., 2015, Regional Metamorphism: Encyclopedia of Geology, 2005, Pages 407-413.

Graham, C.M., Sheppard, S.M.F, Heaton, T.H.E, 1980, Experimental hydrogen isotope studies—I. Systematics of hydrogen isotope fractionation in the systems epidote-H_2O, zoisite-H_2O and AlO(OH)-H_2O: Geochimica et Cosmochimica Acta, v.44, Issue 2, p. 353-364.

Graham, C.M, Viglino, J.A., Harmon, R.S., 1987, Experimental study of hydrogen-isotope exchange between aluminous chlorite and water and of hydrogen diffusion in chlorite: American Mineralogist, v.72, p. 566-579.

Harris, C., 1989, Oxygen-isotope zonation of agates from Karoo volcanics of the Skeleton Coast, Namibia: American Mineralogist 74, 476-481.

Hoefs, J., 1973, Stable Isotope Geochemistry: New York, Heidelberg, Berlin, Springer-Verlag, 140 p.

Jolly, W.T. and Smith, R.E., 1972, Degradation and Metamorphic Differentiation of the Keweenawan Tholeiitic Lavas of Northern Michigan: U.S.A. Journal of Petrology, v. 13, Part 2, p. 273-309.

Jolly W.T, 1974, Behavior of Cu, Zn, and Ni During Prehnite-Pumpellyite Rank Metamorphism of the Keweenawan Basalts, Northern Michigan: Economic Geology, V. 69, p. 1118-1125.

Kalliokoski, J., 1982. "7E: Jacobsville Sandstone", Geology and Tectonics of the Lake Superior Basin, Richard J. Wold, William J. Hinze: Geological Society of America, v. 156., p. 147.

Kulakov, E., Bornhorst, T.J., Deering, C., Moore, J.B., 2018, The youngest magmatic activity of the Midcontinent Rift at Bear Lake, Keweenaw Peninsula, Michigan: Institute on Lake Superior Geology Proceedings v. 64, Iron Mountain, Michigan, p. 61-62.

Livnat, A., 1983, Metamorphism and copper mineralization of the Portage Lake Lava Series, northern Michigan: Ph.D. Dissertation, University of Michigan, Ann Arbor, 292p.

Merk, G.P., and Jirsa, M.A., 1982, Provenance and tectonic significance of the Keweenawan interflow sedimentary rocks: Geological Society of America Memoir 156, p. 97105.

O'Neil. J.R., Clayton, R.N., and Mayeda, T.K., 1969, Oxygen isotope fractionation in divalent metal carbonates: Journal of Chemistry and Physics, v. 51, p. 5547-5558.

Ohmoto, H., 1972, Systematics of Sulfur and Carbon Isotopes in Hydrothermal Ore Deposits: Economic Geology, v. 16, no. 5, p. 551-578.

Paces, J.B. and Bornhorst, T.J., 1985, Geology and geochemistry of lava flows within the Copper Harbor Conglomerate, Keweenaw Peninsula, Michigan: Thirty-First Annual Institute on Lake Superior Geology Proceedings, Kenora, Ontario, Canada, p. 71-72.

Püschner, U.R., 2001, Very low-grade metamorphism in the Portage Lake Volcanics on the Keweenaw Peninsula, Michigan, USA: Ph.D. Dissertation, University of Basel, Basel, Switzerland, 82p. and appendices.

Robertson, J.M., 1975, Geology and mineralogy of some copper sulfide deposits near Mount Bohemia, Keweenaw County, Michigan: Economic Geology, v. 70, p. 1202-1224.

Rollinson, H.R., 1993, Using Geochemical Data: Evaluation, Presentation, Interpretation: p.271.

Schmidt, S.T. and Robinson, D., 1997, Metamorphic grade and porosity and permeability controls on mafic phyllosilicate distributions in a regional zeolite to greenschist facies transition of the North Shore Volcanic Group, Minnesota: Geological Society of America Bulletin, p. 683-697.

Sharp, Z.D., 2017, Principles of Stable Isotope Geochemistry, CH 7 & CH 12: Metamorphic Petrology 2nd edition, p. 7-1/7-29 and 12-10/12-36.

Sheele, N. and Hoefs, J., 1992. Carbon isotope fractionation between calcite, graphite and CO2: an experimental study: Contributions to Mineralogy and Petrology, 112: 35-45.

Sikkila, K., 1984, Petrographic and Geochemical Study of the Mount Bohemia Stock, Portage Lake Volcanics, Keweenaw Peninsula, Michigan: Proceedings Institute on Lake Superior Geology, v.30, Program and Abstracts, p. 72.

Stoiber, R.E., and Davidson, E.S., 1959, Amygdule mineral zoning in the Portage Lake Lava Series, Michigan copper district: Economic Geology, v. 54, p. 1250-1277, 1444-1460.

Taylor H. P. jr., 1979, Oxygen and hydrogen isotope relationships in hydrothermal mineral deposits: Geochemistry of Hydrothermal Ore Deposits: New York, Wiley Interscience, p.236-277.

Valley, J.W., 1986, Stable Isotope Geochemistry of Metamorphic Rocks: Reviews in Mineralogy, v. 16, p. 445–489.

Weege, R.J. and Pollock J.P, 1971, The Geology of Two New Mines in the Native Copper District of Michigan: Economic Geology, v.67, p. 622-633.

White, W.S., Cornwall, H.R., and Swanson, R.W., 1953, Bedrock Geology of the Ahmeek Quadrangle Michigan: Geologic Quadrangle Maps of the United States, United States Geological Survey, Map GQ-27, scale 1:24,000.

White, W.S., 1968, The Native-Copper Deposits of Norther Michigan, in Ridge, J.D., ed., Ore Deposits of the United States, 1933-1967 (The Graton Sales volume): American Institute of Mining, Metallurgical and Petroleum, New York, p. 303-325.

Wright, J.C. and Cornwall, H.R., 1954, Bedrock Geology of the Bruneau Creek Quadrangle Michigan: Geological Quadrangle Maps of the United States, United States Geological Survey, Map GQ-35 scale 1:24,000.

4 Appendix I: Mineral Assemblages

Appendix I contains the information used in chapter 1 of this study. This includes the sample location and descriptions displayed in Figure I-1&2, and Tables I1-3. The spatial distribution of mineral assemblages within the Keweenaw Peninsula were determined by compilation of existing published data wherein mineral assemblage for a particular geographic location is described. In addition, samples were collected from outcrops and mine rock piles with minerals identified by hand specimen methods and confirmed by XRD (Figure I-2).

The additional sample collection descriptions are included in Table I-1. Collection of hand samples was limited to volcanic rocks of the Keweenaw Peninsula and was completed primarily over the summer 2018, with a few additional samples collected during the summer 2019. The location of samples in Table I-1 was recorded in UTM coordinates, using a handheld global positioning system (GPS). Upon collection, the samples were labeled and briefly described. Figure I-1 shows the location of samples collected for this study. In Table I-1 and Figure I-1, the map labels MA1-12 were compared to Butler and Burbank's (1929) descriptions.

Minerals and descriptions of the hand samples used in this study are given in Table I-1. Figure I-2a through 2r provides XRD determination of the minerals present in select hand samples. Stoiber gave Professor Bornhorst the original Table used to prepare Figure 1.7 in Stoiber and Davidson (1959). Table I-2 provides a verbal description derived from Stoiber and Davidson's estimates of percentages of minerals. Table I-3 provides a summary of mineral distribution published along with some USGS geologic quadrangle maps.

The mineral assemblages in over 70 different locations from samples collected by this study and Stoiber and Davidson (1959, unpublished) along with mineral distribution from geologic quadrangle maps were grouped into zones as described in the text and geographically compiled in ARC GIS (Table I1-3).

Additional mineral descriptions were referenced and compared to this set of descriptions from Jolly and Smith (1971), Livnat (1983), and Püschner (2001). Jolly and Smith (1971), referenced Stoiber and Davidson (1959) for a lot of their geology reference, any other sample descriptions they had were not included in their published document other than listing minerals present at drill hole locations. Jolly and Smith's (1971) descriptions of mineral assemblages are described in the " Metamorphic Mineral Zones/Temperatures" section of Chapter 1. In addition to the minerals listed for each metamorphic zone, they also provide descriptive terms. The laumontite zone has albite basalts and mentions that chlorite metadomains are rare except in brecciated lavas. The pumpellyite zone has albite basalts and states that pumpellyite metadomains are common in breccias and amygdular parts of flows and along fractures; pumpellyite metadomains are present locally in the upper part of the epidote zone. The epidote zone has albite

basalts and states that epidote metadomains are common in breccias and amygdular parts of flows and along fractures.

Püschner (2001) looked at 3 different drill hole sections from Ahmeek, Eagle Harbor, and Copper Harbor. In them he explained that the Ahmeek profile is dominated in the upper section by prehnite-pumpellyite assemblages to prehnite-epidote assemblages, while in lower sections pumpellyite-epidote was more present. Laumontite was mentioned as being found in crosscutting veins. The Eagle Harbor profile showed prehnite-pumpellyite and pumpellyite-epidote assemblages associated with the epidote. Copper Harbor was listed to have prehnite-pumpellyite and pumpellyite-epidote assemblages near the top, in the lower sections pumpellyite is the dominant mineral, with laumontite being the dominant alteration mineral in the Copper Harbor, superimposed on the pumpellyite-prehnite assemblage. For a more in-depth description refer to Püschner's (2001) Chapter 3 figure 13.

Livnat (1983) included in his Appendix A, a list of 123 locations that were sampled and minerals for each sample were indicated. General trends that could be indicated from looking at sample mineral descriptions table is along the Keweenaw Fault epidote is present, but minerals like pumpellyite and prehnite are scarce. As you travel northwest the presence of pumpellyite and prehnite becomes more prominent, and eventually epidote appears less often. Laumontite appearing in certain locations in faults. Along the northern shore of the peninsula, it appears that little of the secondary mineral assemblages are present, other than some chlorite, potential muscovite and laumontite. This follows the same general pattern of the zones indicated in this study.

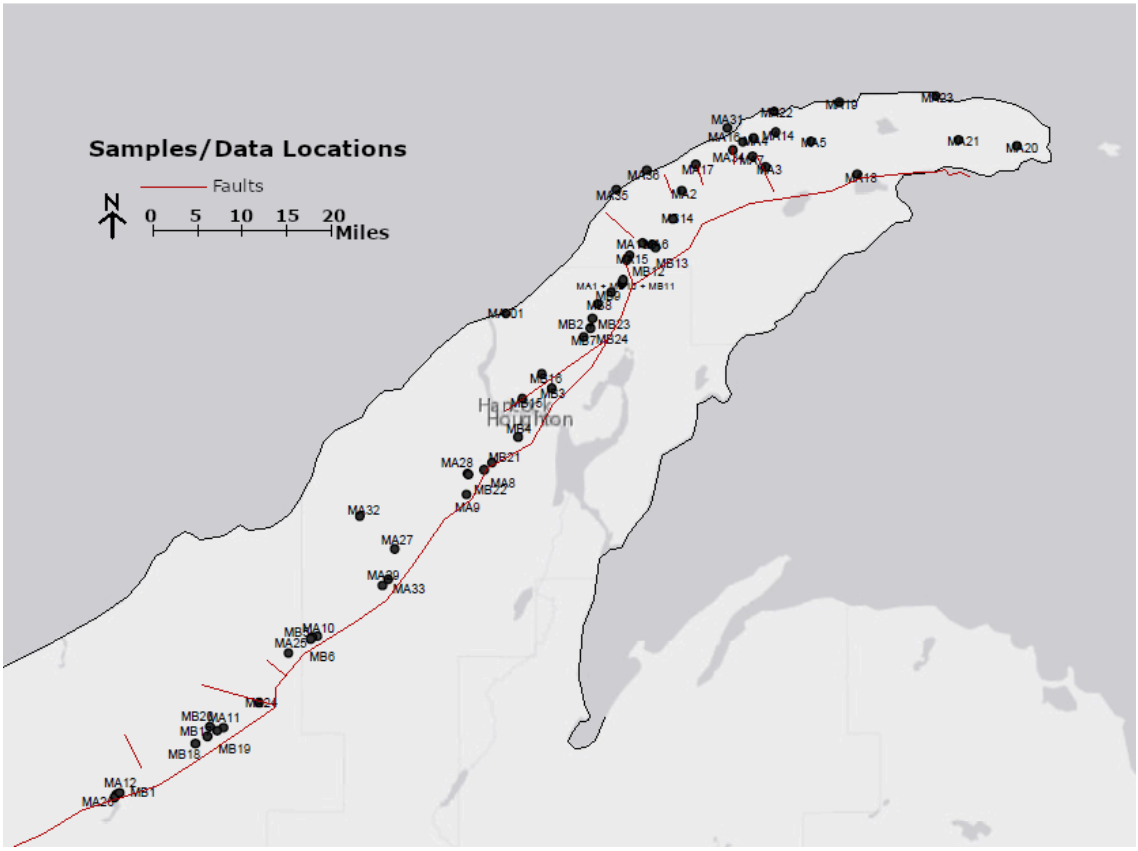

Figure I-1: Sample locations are displayed on this map by the black dots and labels, more detail of the samples found in Table I-1 and I-2.

Table I-1: Collected Mineral Descriptions			
Map Label	**Sample/Location**	**UTM**	**Description/Minerals**
MA1	Wolverine Mine	16T 0393269 5235896	Minerals present are epidote, quartz, calcite, k-spar, prehnite, pumpellyite, copper, potentially malachite, datolite traces, analcime, chlorite.
MA2	Cliff Mine	16T 0400818 5247153	Mineral present are chlorite (coating), laumontite replacing some minerals, quartz, prehnite, pumpellyite, epidote, k-spar, calcite, datolite, albite, copper.
MA3	Central Exploration	16T 0411158 5249925	Minerals present are calcite, chlorite to serpentinite, prehnite, pumpellyite, quartz, laumontite, copper, datolite.
MA4	Petherick Mine	16T 0409727 5253546	Minerals present are calcite, k-spar, chlorite, copper, prehnite, pumpellyite, epidote, datolite, micas.
MA5	Drexel/Delaware Mine	16T 0416815 5252992	Minerals present are calcite, laumontite, quartz, chlorite, datolite, k-spar, prehnite, pumpellyite traces, adularia likely.
MA6	Seneca Mine	16T 0397019 5240668	Minerals present are k-spar, quartz, prehnite, pumpellyite, epidote, chlorite, adularia, copper + oxides, laumontite, potential wavelite.
MA7	Central Mine	16T 0409572 5251238	Minerals present are chlorite, prehnite, quartz, pumpellyite, traces of epidote, copper, variations of plagioclase, calcite.
MA8	Baltic Mine	16T 0375807 5213218	Minerals present are prehnite, copper + oxides, calcite, quartz, k-spar and adularia, chlorite, calcite, pumpellyite.
MA9	Champion Mine	16T 0373573 5210243	Minerals present are quartz, epidote traces, k-spar, adularia, chlorite, calcite, prehnite, pumpellyite.
MA10	Winona Mine	16T 0354723 5193075	Minerals present are quartz, chlorite, adularia, k-spar, calcite, prehnite, copper + oxides, potential traces of epidote.
MA11	Lake Mill/Adventure Mine	16T 0329226 5174054	Minerals present are quartz, chlorite, k-spar, plagioclase, calcite, prehnite, pumpellyite, stilbite potentially, laumontite, potential traces of epidote.
MA12	Victoria Mine	16T 0329226 5174054	Minerals present are chlorite, k-spar, calcite, quartz, plagioclase, copper, prehnite, pumpellyite, traces of epidote.
MA13	OPLV001 (Near Seneca Lake)	16T 0395924 5240868	-This is a Flow Basalt Appears to have some small Calcite crystals. There is some quartz in a sample. There may be Prehnite in this sample as well. K-spar or another mineral that is similar is present too. Very faint green in some areas may be chlorite or epidote? -XRD: quartz, albite, muscovite, clinopyroxene, prehnite, orthoclase, epidote, chlorite.
MA14	OPLV002 (North of Petherick)	16T 0395924 5240868	-There is calcite in these samples. Quartz and maybe datolite. Prehnite may also be present. Chlorite could be faintly on some of the samples too. Some Laumontite or other alteration mineral on some surfaces. -XRD: Prehnite, pumpellyite, albite, quartz, chlorite, calcite, orthoclase

MA15	OPLV003 (Near Ahmeek)	16T 0412515 5254194	-This is mainly a Flow basalt. Difficult to identify minerals but from what I can see there may be calcite, Quartz, a little chlorite, k-spar, and maybe some prehnite present? -XRD: Prehnite, albite, clinochlore, anorthite, quartz, calcite, chlorite.
MA16	OPLV004 (Copper Falls Park)	16T 0394310 5239351	-Quartz present, prehnite present as well. Might have sort of a groundmass of K-spar, quartz and epidote, unsure if epidote or just chlorite. Chlorite present most likely too. (maybe pumpellyite?) -XRD: Albite, chlorite, clinochlore, pumpellyite, prehnite, epidote, calcite, quartz.
MA17	OPLV005 (41/26 intersection)	16T 0408457 5253041	-Basalt flow. Some Quartz, K-spar, and Prehnite. Chlorite likely as a later stage mineral. Very hesitant to state if there is epidote or not. -XRD: Clinochlore, albite, labradorite, microcline, orthoclase, anorthite, calcite.
MA18	OPLV006 (Near Lake La Belle)	16T 0402592 5250369	-Chlorite present as a later stage mineral. Quartz and K-spar throughout. Some Laumontite present either on Quartz or datolite? Prehnite possible, some potential altered epidote. -XRD: Albite, clinochlore, chalcopyrite?, calcite, quartz, pumpellyite, chlorite.
MA19	Esrey Park	16T 0422431 5248885	-Lakeshore Traps -Chlorite present again as a later stage mineral. Some blueish Green alteration on some samples. Might have some agate in a sample or two. Calcite present in some vesicles. Some greenish grains that may be prehnite, unsure. Some areas may have Laumontite. Quartz likely, Potassium Feldspar or hematite (maybe both present as well.
MA20	OPLV007 (On Mandan Road)	16T 0442113 5252119	-What appears to be a sort of fanned textured mineral, such as pumpellyite, unsure if that is what it is though, Hardness around 5. Quartz and Chlorite present. Also some type of plagioclase feldspar. -One sample has an amygdule that appears to be filled with quartz and surrounded by a greenish mineral, most likely chlorite, datolite? -XRD: Anorthite, albite, clinochlore, chlorite, quartz, maybe kaolinite,
MA21	OPLV008 (On Mandan Road)	16T 0434898 525912	-Chlorite present, calcite with alteration to laumontite, quartz likely. -Green mineral in some samples are epidote or prehnite, datolite? -XRD: Microcline, orthoclase, clinochlore, anorthite, augite, kaolinite, unsure if traces of laumontite.
MA22	OPLV009 (Eagle Harbor Marina)	16T 0412392 5256743	-Varying outcrops along the water line. Some obvious basalt with chlorite. -Can identify Adularia, Chlorite and potassium feldspar in sample. -XRD: Albite, anorthite, calcite, quartz.
MA23	OPLV010 (Agate Beach)	16T 0432257 5258323	-Basalt present, there is a green and a black variation of basalt flows, right next to it is the red conglomerate. Can identify Quartz, potassium feldspar, chlorite, and maybe laumontite. -XRD: Clinochlore, oligoclase, albite, anorthite, microcline, quartz.
MA24	OPLV011 (South of Winona)	16T 0347263 5185041	-Another basalt flow, a little bit north of this following highway 26 there is a conglomerate patch, didn't sample from it. Identify chlorite, quartz, k-spar, and maybe traces of epidote. -XRD: Chlorite, albite, epidote, clinochlore, quartz, pumpellyite. (prehnite?)
MA25	OPLV012 (Near Winona)	16T 0351046 5191073	-basalt with veins of k-spar and potentially epidote -Identify K-spar, quartz, either prehnite or epidote, chlorite, and calcite. -XRD: Clinochlore, albite, epidote, oligoclase, quartz.
MA26	OPLV013 (Near Victoria Mine)	16T 0328975 5173744	-Can identify Calcite, chlorite, k-spar, maybe quartz, potential copper traces (greenish blues), maybe laumontite. -XRD: Clinochlore, chlorite, albite, anorthite, microcline, quartz.

MA27	OPLV014 (Between Donken and Toivola)	16T 0364572 5203679	-May be a basalt flow interior -Can identify quartz and k-spar. -XRD: Labradorite, anorthite, albite, augite, quartz.
MA28	OPLV015 (Trimountain area)	16T 0373765 5212816	-Weathered outcrop face, may have traces of copper weathering. -can identify quartz, prehnite, maybe epidote, chlorite. -XRD: quartz, chlorite, clinochlore, albite, potential prehnite.
MA29	OPLV016 (Near Donken)	16T 0362885 5199169	-Likely a basalt flowtop. -There are traces of copper present, along with quartz, and potentially epidote/prehnite, most likely chlorite in terms of weathering present. -XRD: Clinochlore, quartz, anorthite, augite, calcite, diopside, albite, muscovite, unsure if traces of laumontite.
MA30	OPLV017 (Bergland area)	16T 0360957 5162394	-Outcrop face along road, basalt. Appearance is variations of green and black. -Quartz, calcite, chlorite present. -XRD: quartz, albite, hematite, calcite, anorthite, microcline, unsure if traces of laumontite.
MA31	Northern Lakeshore (collected by Bob Barron)	16T 0430534 5260206	-Large copper chunk, has copper and laumontite present for sure. -XRD: Laumontite, copper, prehnite.
MA32	OPLV018 (Near Toivola)	16T 0360296 5207860	Multiple basaltic boulders. Mainly pure basalt, little to no flow top traces, some quartz and minor calcites on some areas.
MA33	OPLV019 (Conglomerate at Donken)	16T 0363650 5199981	Conglomerate, which is reddish hue, some black basalt pebbles, some quartz pebbles, and some rhyolite.
MA34	Arnold Mine	16T 0407213 5252113	Mostly Basaltic rocks, Chlorite replaces and coats samples. Quartz and calcite present throughout. Copper in places, sometime filling cracks other times amygdules. Little to no K-spar.
MA35	Seven Mile Point	16T 0396549 5249755	Minerals noted here are quartz, agate, albite, copper, laumontite, potential prehnite
MA36	Five Mile Point	16T 0392831 5247340	Minerals note here are albite, analcime, calcite, copper, fluorite, potential prehnite, quartz.
MA-01	Bear Lake	16T 0378852 5232627	This location is marked on the map using descriptions of minerals present from Kulakov, Bornhorst, et. al., ILSG abstract from 2018. -They described potassium feldspar, biotite, hornblende quartz, apatite, iron oxides, heulandite, calcite as the main minerals found within the area. (There was also noted heulandite, quartz, and calcite in veinlets.)

Table I-2: Mineral assemblages present at mine poor rocks piles throughout the Keweenaw Peninsula derived from unpublished data of Stoiber and Davidson. The original data had been organized into a table format with the percentage of minerals present at each location. Their original table was converted into a word format to express the general trends of mineral distribution at each location. The locations of the data are primarily from mine sites and mine piles with UTM coordinates based off of the stated locations.

Table I-2: Compiled Mineral Descriptions (Stoiber and Davidson)			
Map Label	**Sample/Location**	**UTM**	**Description/Minerals**
MB1	Victoria	16T 0329582 5174240	Minerals present are epidote, prehnite, red feldspar, quartz, calcite.
MB2	Osceola Centennial	16T 0389544 5231661	Minerals present are little to no epidote, has prehnite, has little to no feldspar, has quartz, and calcite. Traces of Pumpellyite and chlorite.
MB3	Arcadia	16T 0384391 5223172	Minerals present are epidote, prehnite, red feldspar, little quartz, has calcite, some pumpellyite, traces of laumontite.
MB4	Isle Royale	16T 0380087 5217199	Minerals present are little to no epidote, has prehnite, no feldspar, has quartz and pumpellyite.
MB5	Winona	16T 0354008 5192962	Minerals present are epidote, prehnite, no feldspar, has quartz and calcite, no pumpellyite.
MB6	King Philip	16T 0353833 5192781	Minerals present are epidote, prehnite, no feldspar, quartz, little calcite, little pumpellyite.
MB7	La Salle	16T 0388447 5229399	Minerals present are epidote, prehnite, little to no feldspar, quartz, calcite, a little pumpellyite.
MB8	Calumet & Hecla	16T 0390268 5233410	Minerals present are epidote, traces of prehnite, has feldspar, has a little quartz, has calcite, has some pumpellyite. Maybe traces of laumontite.
MB9	Centennial	16T 0391914 5234861	Minerals present are epidote, a little prehnite, some feldspar, quartz, and calcite, also chlorite.
MB10	Wolverine	16T 0393366 5236070	Minerals present are epidote, traces of prehnite, feldspar, quartz a little, calcite.
MB11	North Kearsarge	16T 0393476 5236377	Minerals present are epidote, traces of prehnite, feldspar, quartz, calcite, a little pump.
MB12	Ahmeek	16T 0393939 5238772	Minerals present are epidote, no prehnite, some feldspar, quartz, and calcite.
MB13	Mohawk	16T 0397537 5240289	Minerals present are epidote, some prehnite, feldspar, quartz, calcite, traces of pumpellyite.
MB14	Ojibway	16T 0399696 5243740	Minerals present are epidote, traces of prehnite, feldspar, quartz, calcite, traces of pumpellyite.
MB15	Franklin	16T 0380721 5221922	Minerals present are little epidote, little prehnite, no feldspar, has quartz and calcite and pumpellyite.
MB16	St. Mary's	16T 0383203 5224930	Minerals present are little epidote, prehnite, quartz, calcite, and pumpellyite.
MB17	Flint Steel	16T 0341955 5181686	Minerals present are epidote, prehnite, pink feldspar, quartz, calcite, pumpellyite, and traces of chlorite.
MB18	Old Mass	16T 0339189 5180102	Minerals present are little epidote, no prehnite, has red feldspar, quartz, calcite, traces of pumpellyite, and chlorite.
MB19	Mass	16T 0340707 5181039	Minerals present are epidote, some prehnite, red feldspar, quartz, calcite, pumpellyite, a little chlorite.
MB20	Adventure	16T 0341058 5182191	Minerals present are epidote, no or traces of prehnite, some red feldspar, quartz, calcite, traces of pumpellyite, and traces of chlorite.
MB21	Baltic	16T 0376828 5214065	Minerals present are epidote, little prehnite, red feldspar, quartz, calcite, pumpellyite, chlorite.
MB22	Trimountain	16T 0373866 5212645	Minerals present are epidote, traces to no prehnite, no feldspar, quartz, calcite, little to no pumpellyite, some chlorite.
MB23	Osceola	16T 0389544 5231661	Minerals present are epidote, traces to no prehnite, no feldspar, quartz, calcite, traces of pumpellyite and chlorite.
MB24	Laurium	16T 0389312 5230497	epidote, prehnite, pink feldspar, quartz, calcite, traces of pumpellyite and chlorite, traces of laumontite.

Table I-3: USGS geologic quadrangle maps of the Keweenaw Peninsula included description of the distribution of hydrothermal/metamorphogenic minerals. These descriptions are summarized in this table.

Table I-3: Quadrangle Map Mineral Descriptions		
Map Label	**Sample/Location**	**Description/Minerals**
Quadrangle	Bruneau Creek	-Secondary minerals consist of Calcite, chlorite, epidote, quartz, prehnite and feldspar.
Quadrangle	Mohawk	Basalt and andesite with thin rhyolite conglomerate and sandstone. -Secondary minerals are calcite, quartz, chlorite, pumpellyite, and laumontite. In some places, datolite, thomsonite, native copper, and saponite are present. K-spar also found throughout. -Fissure/Cliff Mine: prehnite, native copper, calcite, and less common is laumontite, silver, epidote, chlorite, quartz.
Quadrangle	Phoenix	-Secondary minerals are Calcite, chlorite, epidote, quartz, prehnite. Some locally abundant minerals are K-spar, pumpellyite, datolite, analcite, laumontite, and native copper. -Cliff mine has calcite, prehnite, epidote, chlorite, quartz, and zeolites present. Cliff Mine: calcite, prehnite, epidote, chlorite, quartz and zeolites. Ashbed flow: calcite, quartz, epidote, pumpellyite, chlorite, analcite, datolite, native copper. -Copper Harbor Conglomerate: calcite, chlorite, laumontite, analcite.
Quadrangle	Eagle Harbor	-Secondary minerals are calcite, chlorite, epidote, quartz, prehnite. Locally abundant minerals are k-spar, pumpellyite, datolite, analcite, laumontite, and native copper. -Fissures below greenstone flow: calcite, chlorite, prehnite, quartz, epidote, pumpellyite, datolite. -Copper Harbor Conglomerate: calcite, laumontite, chlorite, quartz, agates, analcite.
Quadrangle	Ahmeek	-Secondary minerals are calcite, chlorite, epidote, quartz. Locally abundant are prehnite, k-spare, pumpellyite, analcite, laumontite, and native copper. -Copper Harbor Conglomerate: calcite, chlorite, laumontite.
Quadrangle	Delaware	-Secondary minerals are calcite, chlorite, prehnite, quartz, epidote. Locally abundant are k-spar, pumpellyite, datolite, analcite, laumontite, and native copper. -Allouez Conglomerate: calcite, laumontite, chlorite, quartz, agate, analcite. -Delaware and Medora amygdaloid: calcite, prehnite, chlorite, epidote, adularia. -Mt. Bohemia/Lac La Bell: calcite, chlorite, quartz, chalcocite, chalcopyrite.
Quadrangle	Lake Medora	-Secondary minerals are calcite, chlorite, prehnite, quartz, epidote, laumontite, locally abundant are k-spar, pumpellyite, datolite, analcite, thomsonite, and native copper. -Flows adjacent and below Bohemia Conglomerate: calcite, epidote, quartz, chlorite, pumpellyite, feldspar. -Above Bohemia conglomerate to top of PLV: calcite, prehnite, chlorite, laumontite. -Copper Harbor Conglomerate: calcite, laumontite, chlorite, quartz, agates, analcite, feldspar.
Quadrangle	Fort Wilkins	-Secondary minerals are calcite, chlorite, laumontite, prehnite, quartz, thomsonite, epidote, natrolite, orthoclase, adularia, analcine, native copper, pumpellyite, datolite, agate. -Top of PLV to Bohemia Conglomerate: calcite, chlorite, prehnite, laumontite. -Bohemia Conglomerate to west of Fish Cove: calcite, chlorite, quartz, epidote. -East of Fish Cove: Same but epidote scarce. -Keystone Bay area: calcite, chlorite, laumontite, thomsonite, natrolite. -Copper Harbor Conglomerate: calcite, chlorite, laumontite, agate, adularia, analcite.
Quadrangle	Manitou Island	- (All from peninsula mainland and not from on Manitou Island) Secondary minerals are chlorite, laumontite, calcite, quartz, agate, natrolite, analcite, heulandite, adularia, thomsonite, epidote and native copper. -Copper Harbor Conglomerate: chlorite, agate, laumontite, calcite, quartz, analcite, adularia, heulandite.

4.1 XRD:

Figure I-2a

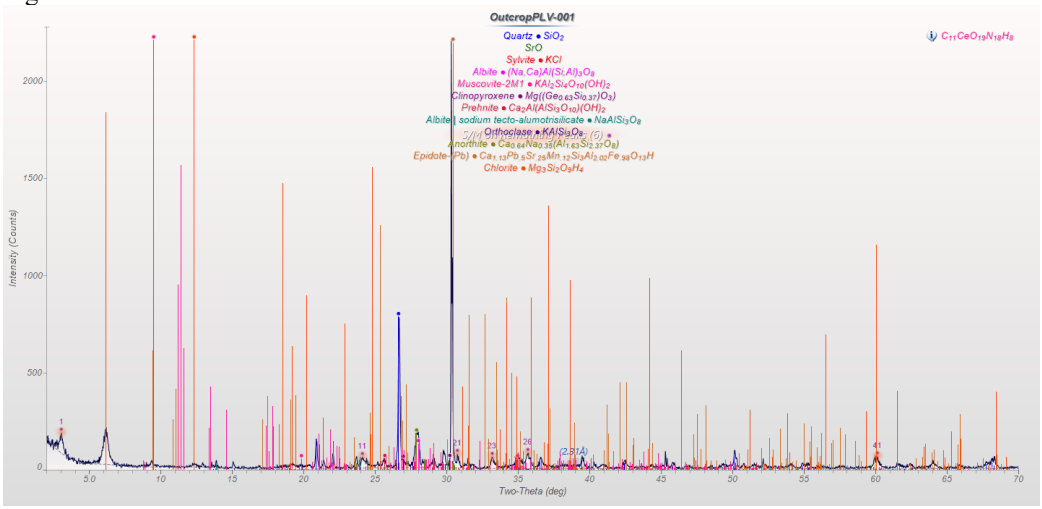

Figure I-2b

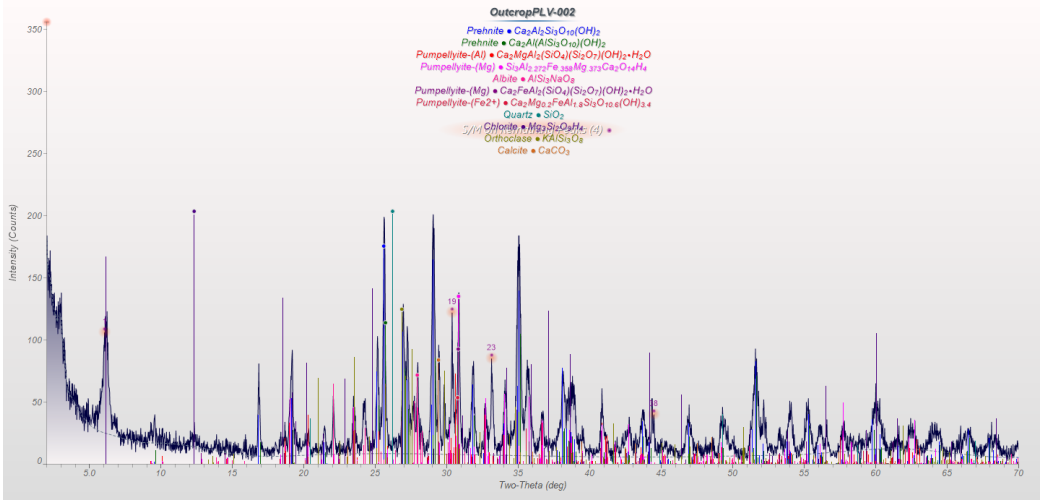

Figure I-2c

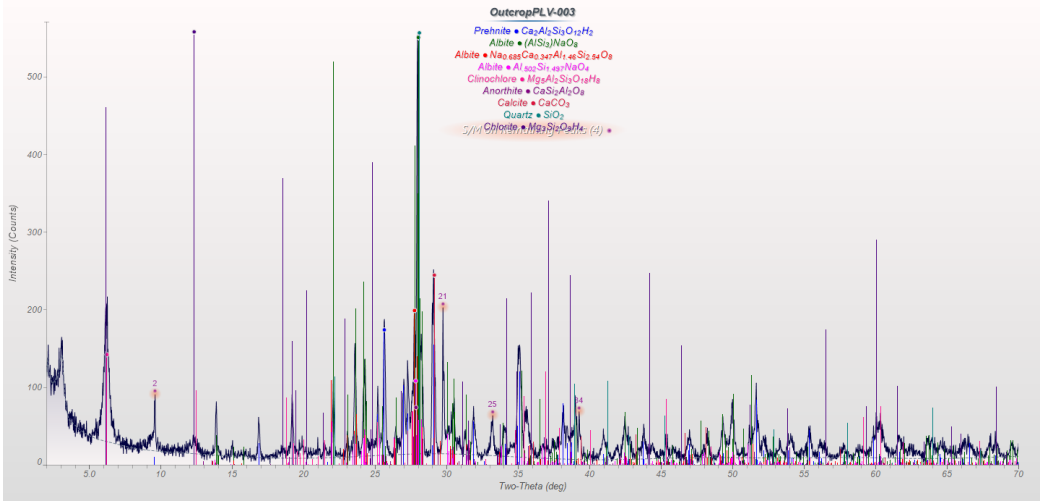

Figure I-2d

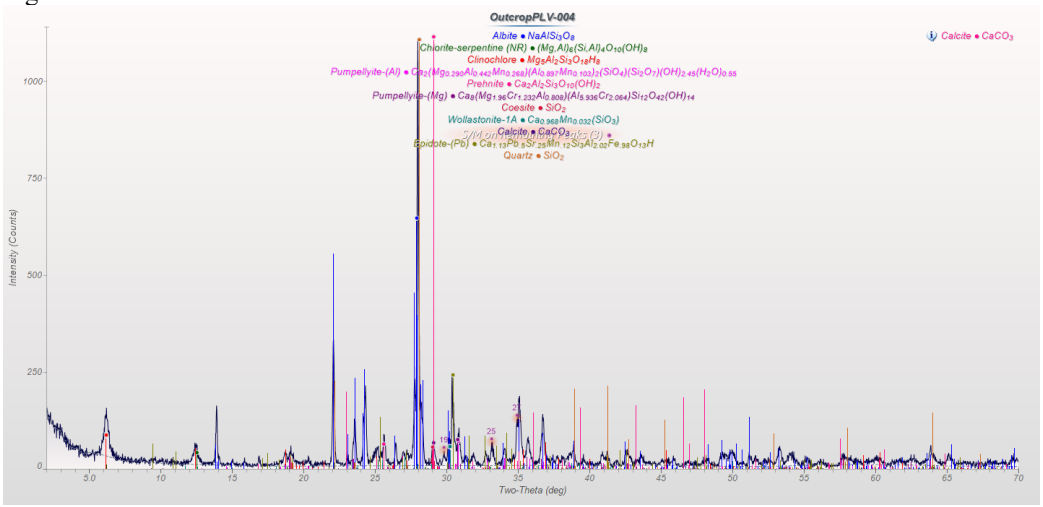

Figure I-2e

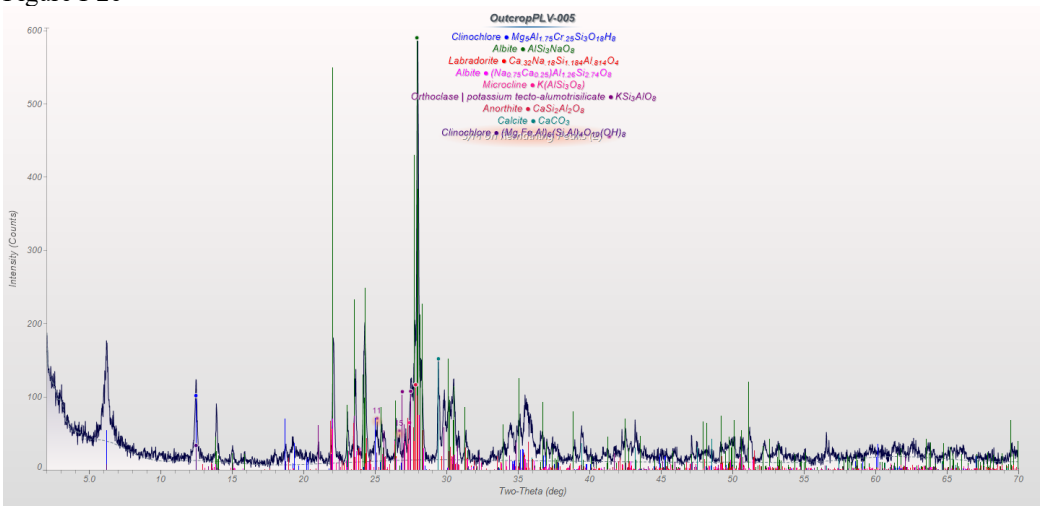

Figure I-2f

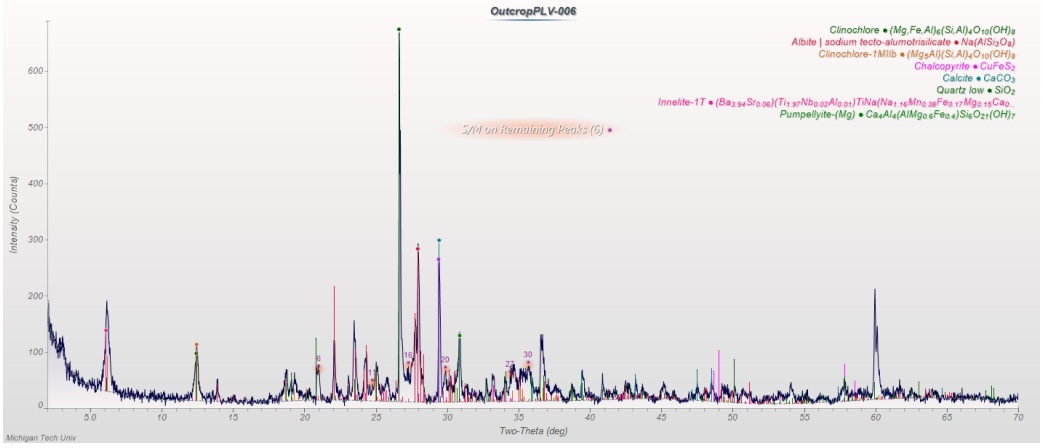

Figure I-2g

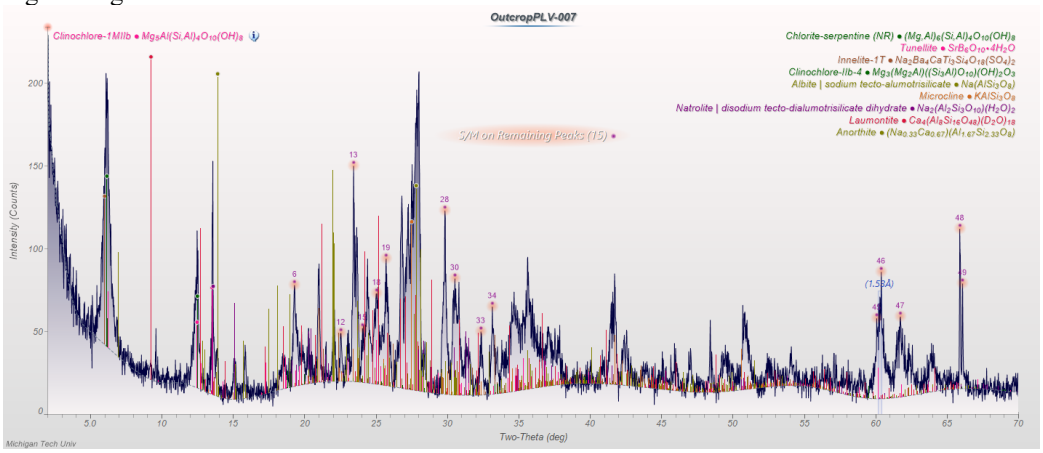

Figure I-2h

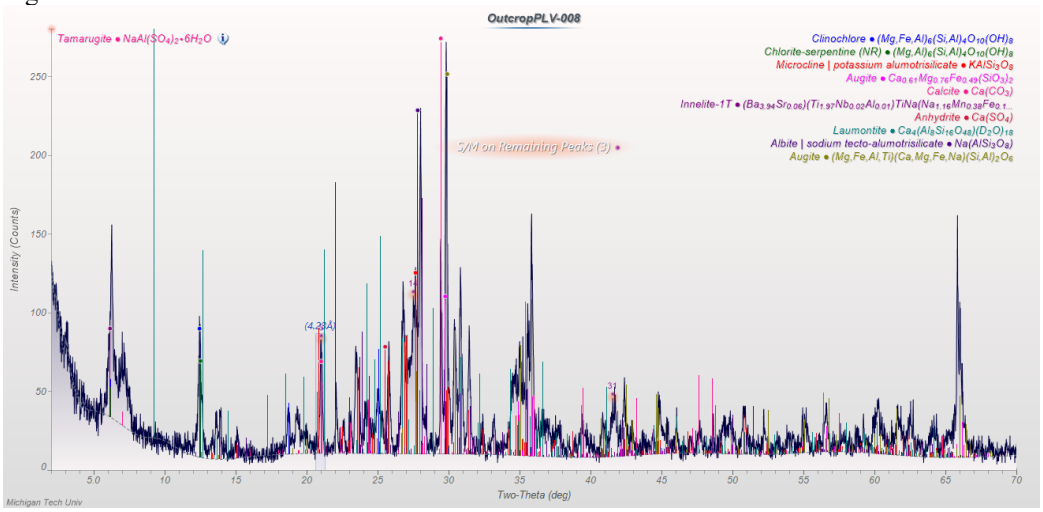

Figure I-2i

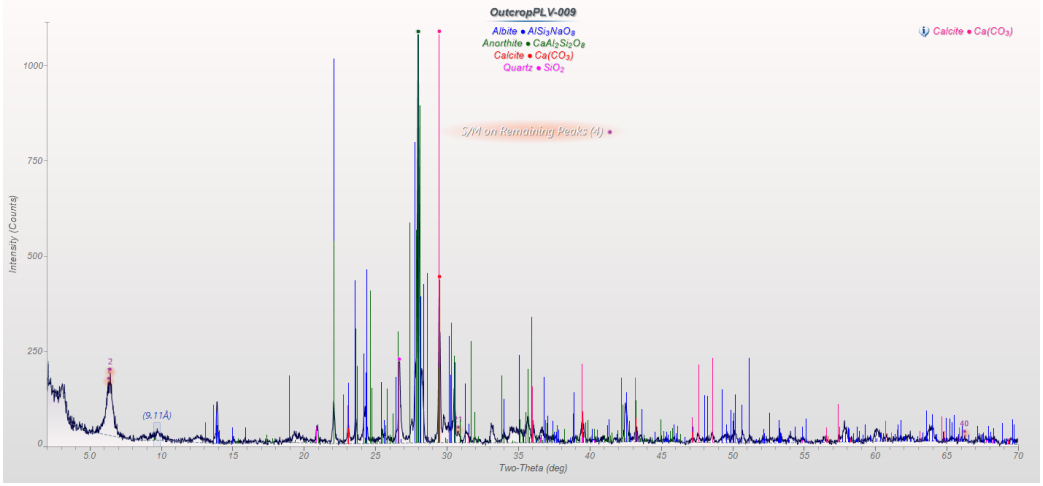

Figure I-2j

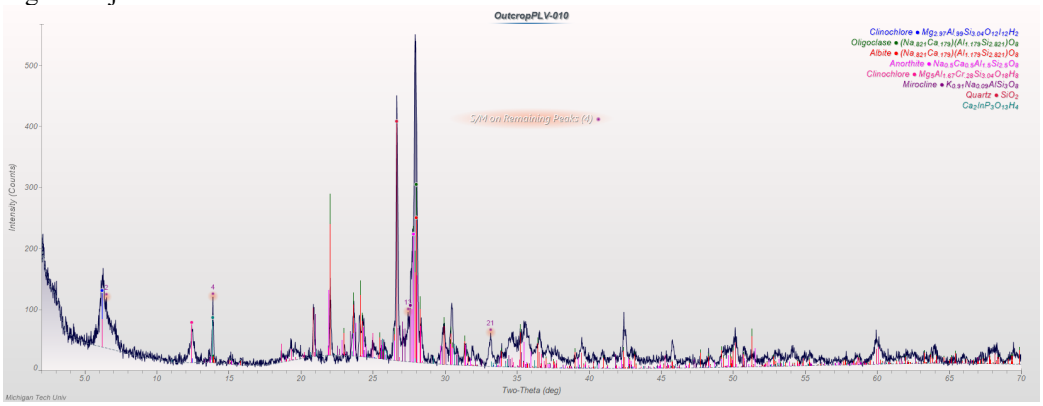

Figure I-2k

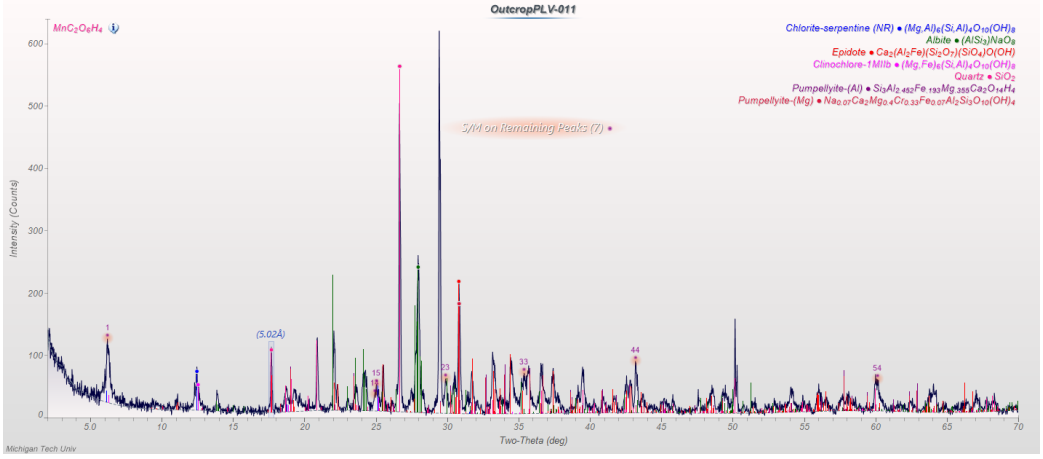

Figure I-2l

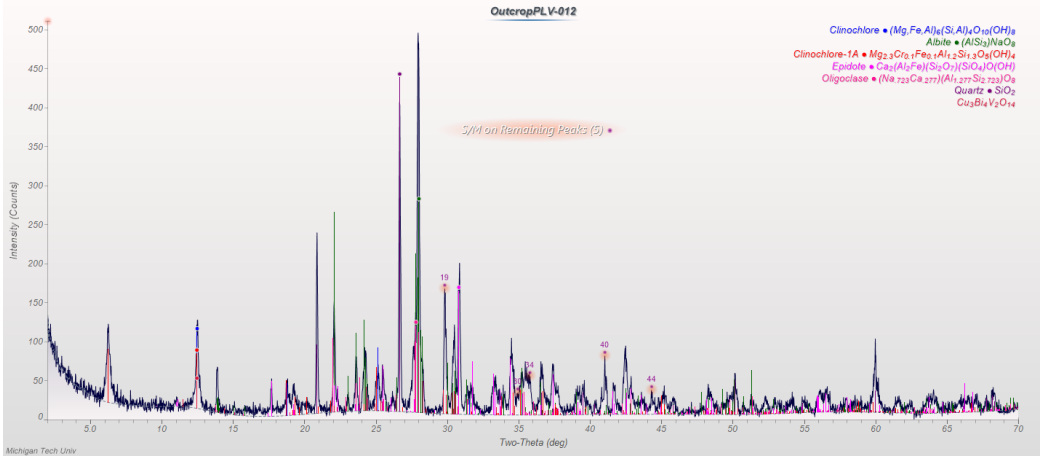

Figure I-2m

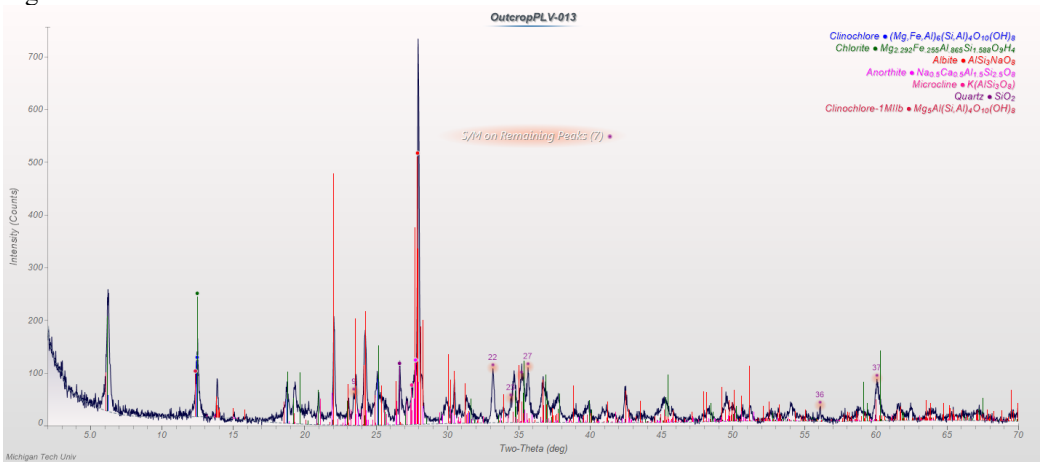

Figure I-2n

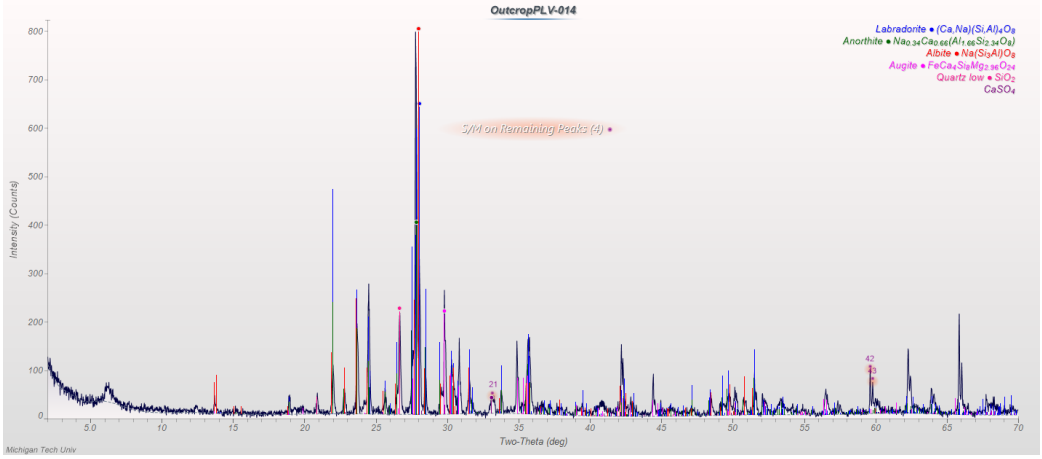

Figure I-2o

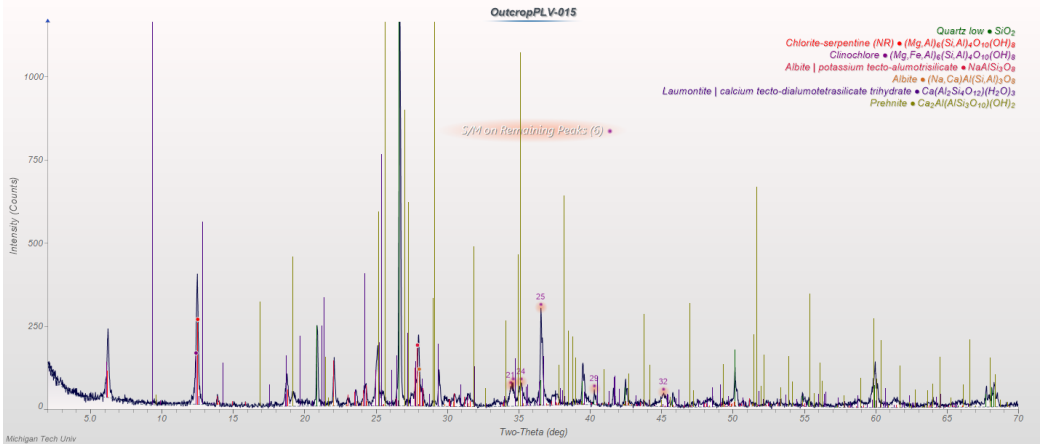

Figure I-2p

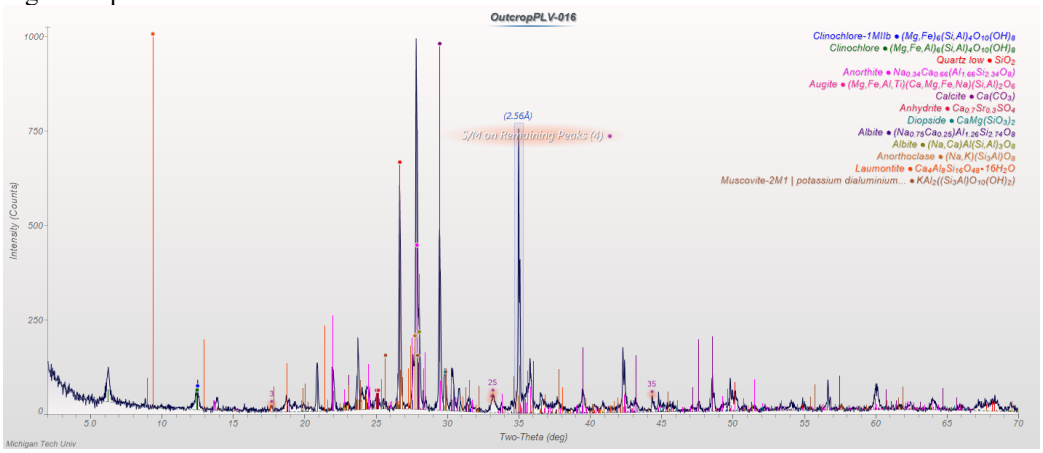

Figure I-2q

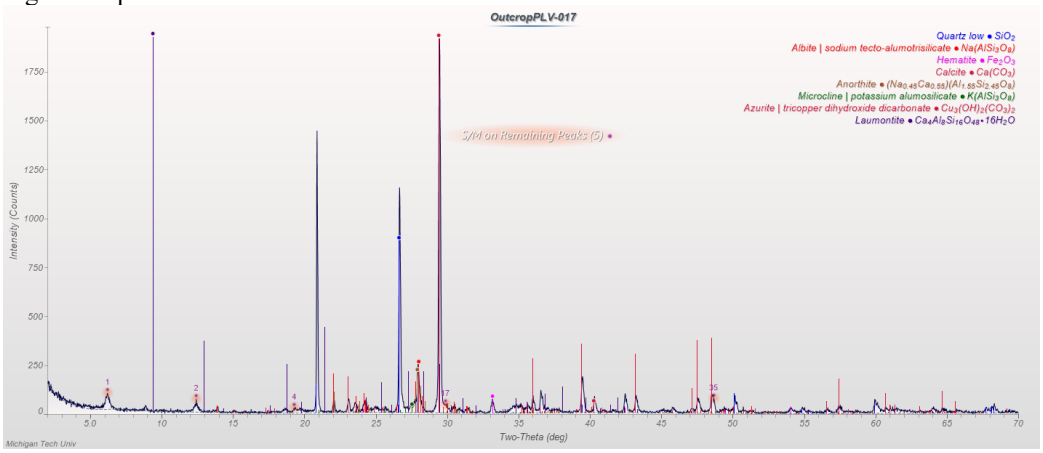

Figure I-2r

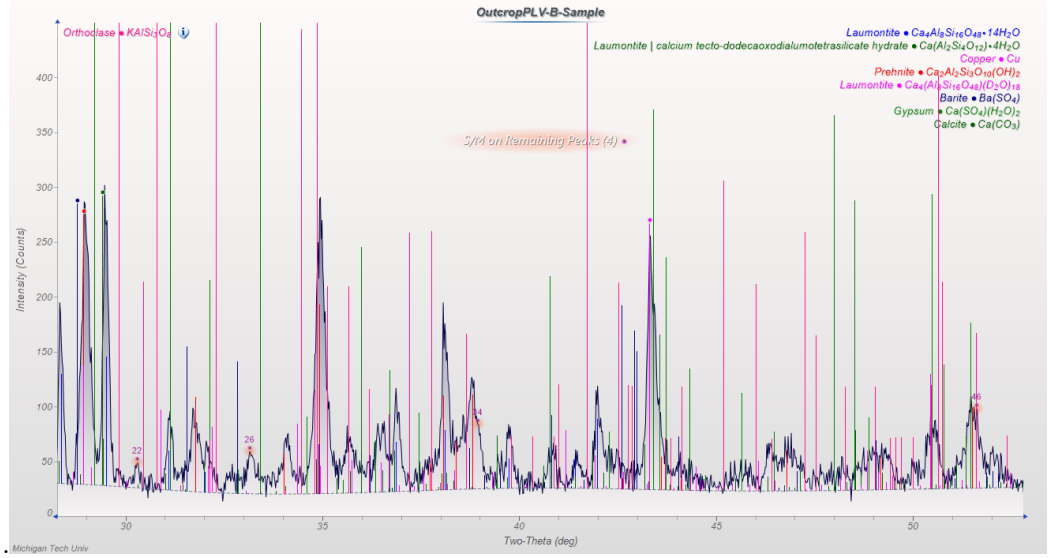

Figures I-2a/r: XRD data results for the newly collected outcrop samples. The middle to upper right of each figure lists the minerals that were identified as being present in each sample. The peaks of those minerals are shown in the same color that the mineral names are displayed.

5 Appendix II: Bulk Raw Stable Isotope Data

Appendix II contains the compiled light stable isotope data from Livnat (1983), Bornhorst and Woodruff (1997), and Püschner (2001). Stable isotope data was analyzed and collected for a selection of minerals: Livnat (1983) analyzed data from all over the Keweenaw Peninsula, with stable isotope data for the minerals calcite, chlorite, epidote, pumpellyite, ankerite, potassium feldspar, muscovite, and hematite. Bornhorst and Woodruff (1997) focused on analyzing calcite within the Kearsarge deposit. Püschner (2001) analyzed data from 3 drill core sections from the Ahmeek, Eagle Harbor, and Copper Harbor area for the minerals calcite, clinochlore, quartz, and epidote. All mineral data for oxygen, carbon or hydrogen stable isotopes were compiled. Whole-rock data were not compiled. Each data set is labelled with Identification (Id) letter and number as well as other information as described in the Legend below.

The tables in this appendix are only compiled raw data. Each source provided different sets of information from one another, resulting in blank areas in some sections of the tables. The tables are organized to keep the sources together, i.e., Livnat data are all in one portion, followed by Püschner and Bornhorst and Woodruff. Püschner (2001) didn't list minerals specifically per sample description, instead he displayed the minerals found associated per sample section in a drill core profile figure, and the associated minerals for each sample were derived from his figures. The legend for the spreadsheets is given below.

5.1 Legend for Table

I.D.:
Labeled data source and numbered in order they were compiled:
A1-158 = Livnat (1983) data
B1-112 = Püschner (2001) data
C1-41 = Bornhorst and Woodruff (1997) data

Source:
Secondary assigned ranking to identify which source the data comes from:
PP1 = Püschner (2001), PL1 = Livnat (1983), PW1 = Bornhorst and Woodruff (1997).

Published Sample Number:
Sample numbers from original published data.
Similar to the mine section for Bornhorst and Woodruff (1997) and Püschner (2001); Livnat (1983) sample numbers include abbreviations for location and a number with abbreviations being: AHM = Ahmeek, ALL= Allouez, ASH= Ashbed, BAL = Baltic, BOH = Bohemia, CCF = Copper City Flow, CHF = Copper Harbor Formation, CEN = Central, CF = Copper Falls, DEL = Delaware, EH = Eagle Harbor, EVR = Evergreen Lode, GRA = Gratoit-Lake, GRN = Greenstone, HC = Hills Creek, HGH = Houghton Conglomerate, IRQ = Iroquois Lode, ISR = Isle-Royale Lode, KRS = Kearsarge, MB =

Mt. Bohemia, MH = Mt. Houghton, OJB = Ojibway, PEW = Pewabic Lode, PNX = Phoenix, U = Union, WIN = Winona.

Bornhorst and Woodruff (1997) sample numbers are ###CL# (example: 221CL2). The first three numbers differentiate the samples, the ending number is 1-3, to indicate when there is more than one sample from the same source. So, example number 221CL2, the 2 after CL is saying it is the 2nd of the 221CL# samples.

Püschner (2001) samples are numbered by him to denote different depths of the drill core, each range of depth (###) for a given core are labeled in groups. From increasing depth: the Ahmeek core sample numbers are in groups S10-###, AH8-###, and G7-###; Eagle Harbor core labels are in groups EH04-###, C89-###, and D56-###; and the Copper Harbor core labels are in groups CL14-###, CL11-###, and ST7-###. All sample groups are followed by numbers to denote different samples.

Sample Location:
Where in the Keweenaw the data was collected from is shown in this section. The labels are recorded as the location provided by the original publication, which is why some are put into groups while others are more mine specific. Livnat (1983) categorized the location in groups: Baltic Veins, Isle Royale Veins, Ojibway Veins, Lac La Bell Fissures, Kearsarge Arsenide fissures, Mass copper fissures, Shear Veins, Lakeshore Veins, Copper Harbor Cement, and Amygdular/Cementing. Püschner (2001) analyses came from 3 separate drill core locations: Ahmeek, Eagle Harbor, and Copper Harbor. Bornhorst and Woodruff (1997) collected samples within the Kearsarge flow: La Salle, Ahmeek, Centennial, Seneca, North and South Kearsarge, Central, and Mohawk mines.

Source Page:
Denotes where in the previous works each set of data was taken from. Lists the page and if given the table that the data originally came from.

Type:
This was assigned based on Livnat's (1983) tables. Since Püschner's (2001) samples were all drill core, they are labeled as DH.
M = mine, W = waste pile, DH = drill hole, S= surface.

Host Rock:
Terms applied by Püschner (2001) for the different parts of a vertical section of a typical basaltic flow from the PLV, described in his pages 11-12 and Figure 3.
FT = Flow top, TZ = transition zone, MF = massive flow interior.

Vein/Amygdule:
V= Vein, A = Amygdule.

Associated Minerals:
Lists the minerals that are found with each sample as recorded by the original publication.
Abbreviations for the minerals:
ca = calcite, cc = chalcocite, cp= chalcopyrite, qz = quartz, mv = muscovite, ank = ankerite, pp = pumpellyite, Ag = silver, chl = chlorite, cu = copper, hm = hematite, ba = barite, bn = bornite, ep = epidote, ksp = potassium feldspar, dat = datolite, lm = laumontite, orn = orientite, prl = pyrolusite, fl = fluorite, pr = prehnite, nat = natrolite. Calcite specific labels: Ca(E) = early, Ca(L) = Late, Ca(P) = Pink, Ca(W) = White.

The raw bulk stable isotope data for each sample is given in per mil. The mineral analyzed is separated into different columns as follows:

$\delta^{18}O_{qz}$ are quartz oxygen stable isotope data, $\delta^{18}O_{pr}$ are prehnite oxygen stable isotope data, $\delta^{18}O_{chl/cln}$ are chlorite/clinochlore oxygen stable isotope data, $\delta^{18}O_{ksp}$ are potassium feldspar oxygen stable isotope data, $\delta^{18}O_{mv}$ are muscovite oxygen stable isotope data, $\delta^{18}O_{hm}$ are hematite oxygen stable isotope data, $\delta^{18}O_{ca}$ are calcite oxygen stable isotope data, $\delta^{18}O_{epi}$ are epidote oxygen stable isotope data, $\delta^{18}O_{ank}$ are ankerite oxygen stable isotope data, $\delta^{13}C_{ca}$ are calcite carbon stable isotope data, $\delta^{13}C_{ank}$ are ankerite carbon stable isotope data, δD_{epi} are epidote hydrogen stable isotope data, δD_{pmp} are pumpellyite hydrogen stable isotope data, and $\delta D_{chl/cln}$ are chlorite/clinochlore hydrogen stable isotope data.

Clinochlore and chlorite stable isotope $\delta^{18}O$ data are in the same column as they are equivalent to one another but in the original reference they are listed as either chlorite or clinochlore, with Livnat's (1983) data all listed to be chlorite and Püschner's data all listed as clinochlore.

I.D.	Source	Published Sample Number	Sample Location	Source Page	Type	Host Rock	Vein/ Amygdule	Associated Minerals	$\delta^{18}O_{qz}$	$\delta^{18}O_{pr}$	$\delta^{18}O_{CH/cln}$	$\delta^{18}O_{ksp}$	$\delta^{18}O_{mv}$	$\delta^{18}O_{hm}$	$\delta^{18}O_{ca}$	$\delta^{18}O_{epi}$	$\delta^{18}O_{ank}$	$\delta^{13}C_{cs}$	$\delta^{13}C_{smk}$	δD_{epi}	δD_{prnp}	$\delta D_{CH/cln}$
A1	Pt1	BAL-6	Baltic Veins	tablet7/p127	M		V	ca,qz,cc	17.2													
A2	Pt1	BAL-7	Baltic Veins	tablet7/p127	M		V	cc,ca,mv,ank,pp						14		17		15.7	-2.2	-2.2		
A3	Pt1	BAL-8	Baltic Veins	tablet7/p127	M		V	qz,cc,Ag	17.7							14.3			-0.7			
A4	Pt1	BAL-10	Baltic Veins	tablet7/p127	M		V	ca								13.8			-3.1			
A5	Pt1	BAL-11	Baltic Veins	tablet7/p127	M		V	chl,qz,hm,cc,Cu	17.6							16.8			-2.2			
A6	Pt1	BAL-11(2)	Baltic Veins	tablet7/p127			V	Top=w,bottom=p								22.7			-3.4			
A7	Pt1	BAL-12	Baltic Veins	tablet7/p127	M		V	ca								18		16.1	-2.7	-2.6		
A8	Pt1	BAL-14	Baltic Veins	tablet7/p127	M		V	qz,cal (i),cc,Cu								14.80 €			-2.5			
A9	Pt1	BAL-22	Baltic Veins	tablet7/p127	M		V	cal(i),qz,Cu	17.9							16.8			-2.4			
A10	Pt1	BAL-23	Baltic Veins	tablet7/p127	M		V	ca,qz,cc,Cu	17.5							13.7			-3			
A11	Pt1	BAL25	Baltic Veins	tablet7/p127	M		V	qz,ca,Cu								14.4			-3.3			
A12	Pt1	BAL-26	Baltic Veins	tablet7/p127	M		V	mv,chl,cal (i),qz,cc,Cu	17.7							13.7		14.4	-2.4	-3.1		
A13	Pt1	BAL-27	Baltic Veins	tablet7/p127	M		V	chl,cal (i),cc			8					14.7			-2.6			
A14	Pt1	ISR-2	Isle Noyale Veins	tablet7/p127	W		V	pp,ba,qz	17.8													
A15	Pt1	ISR-4	Isle Noyale Veins	tablet7/p127	W		V	qz,ca,ba,cc								15.1		14.4	-1.6	-1.3		
A16	Pt1	ISR-4A	Isle Noyale Veins	tablet7/p127	W		V	ank,qz,mv,chl,hm,cc	17.2				12.6									
A17	Pt1	ISR-5	Isle Noyale Veins	tablet7/p127	W		V	ba,qz	17.1													
A18	Pt1	ISR-21	Isle Noyale Veins	tablet7/p127	M		V	ca,ank,qz,chl,hm,cc	16.8													
A19	Pt1	OJB-11,1812	Ojibway Veins	tablet7/p127	DH		V	pp,qz	17.1													
A20	Pt1	BOH-12	Lac a belle Fissure	tablet7/p127	M		V	qz,chl,mv,ca,cc,ep	16.8		7.2		11.4		14				-1.9			
A21	Pt1	BOH-14	Lac a belle Fissure	tablet7/p127	M		V	cal (i)							15.3				-2.1			
A22	Pt1	BOH-14,2)?	Lac a belle Fissure	tablet7/p127	M		V	cal(i)							23.5				-2.2			
A23	Pt1	BOH-17	Lac a belle Fissure	tablet7/p127	M		V	chl,ksp,cc,qz,ca(P)			12.6				14.6				-2.8			
A24	Pt1	BOH-19	Lac a belle Fissure	tablet7/p127	W		V	mv,ca,hm							12.4				-3.1			
A25	Pt1	CEN-105,1374	Lac a belle Fissure	tablet7/p127	DH		V	qz,ca							14.3				-6.8			
A26	Pt1	DEL-109,348	Lac a belle Fissure	tablet7/p127	DH		V	ep,ca,ch,cc,qz							17.3				-1.2			
A27	Pt1	DEL-109,594	Lac a belle Fissure	tablet7/p127	DH		V	chl,ca							14.5				-2.8			
A28	Pt1	MB-810,144	Lac a belle Fissure	tablet7/p127	DH		V	chl,cc,qz			6.9											
A29	Pt1	AHM-UG-4,409	Keweenaw Fissures	tablet7/p127	DH		V	ep,qz	9.7													
A30	Pt1	KRS-69	Keweenaw Fissures	tablet7/p127	M		V	ank,hm,ksp,Cu						-3.8	15.3				-3.9			
A31	Pt1	KRS-71	Keweenaw Fissures	tablet7/p127	M		V	ca,ank,chl,copper arsenides			13.6				13.6				-3.5			
A32	Pt1	KRS-108	Keweenaw Fissures	tablet7/p127	M		V	qz,Cu,copper arsenides	16.9													
A33	Pt1	KRS-109	Keweenaw Fissures	tablet7/p127	M		V	ca,copper arsenides							10.3				2.8			
A34	Pt1	AHM-21,333.5	Mass copper Fissures	tablet7/p128	DH		V	ep,mv,hm,cc,ca,Cu	12.8						12.7				-3.1			
A35	Pt1	AHM-UG-4,3847	Mass copper Fissures	tablet7/p128	DH		V	ep,pp,ksp,ca							11.5				-3.7			
A36	Pt1	ASH-11	Mass copper Fissures	tablet7/p128	W		V	pr,dol,ch,Cu			8.9											
A37	Pt1	BVR-31	Mass copper Fissures	tablet7/p128	M		V	ca,Ag,Cu							12.9				-4			
A38	Pt1	KRS-58	Mass copper Fissures	tablet7/p128	W		V	pr,Cu		9.2												
A39	Pt1	PEW-5	Mass copper Fissures	tablet7/p128	M		V	ca,Cu							21.8				-2.3			
A40	Pt1	Pew-6(2)?	Mass copper Fissures	table 7/p128				ca, chl, cu, mv							19.4				-2.3			
A41	Pt1	PWC-UG-2,321	Mass copper Fissures	table 7/p128	DH		V	ca,qz,ep,chl,Cu	8.6													
A42	Pt1	CEN-105,134	Sheer veins	tablet7/p128	DH		V	hm,ca							14.7				-6.2			
A43	Pt1	**_337	Sheer veins	tablet7/p128	DH		V	ca							16.1				-11.8			
A44	Pt1	**_744	Sheer veins	tablet7/p128	DH		V	ca							12.5				-1.9			
A45	Pt1	**_888	Sheer veins	tablet7/p128	DH		V	hm,chl			13.1											
A46	Pt1	**_1201	Sheer veins	tablet7/p128	DH		V	hm,chl			6.1											
A47	Pt1	**_1292	Sheer veins	tablet7/p128	DH		V	hm,ca							15.2				-1.1			
A48	Pt1	**_1528	Sheer veins	tablet7/p128	DH		V	hm,ca							13.8				-9.8			
A49	Pt1	DEL-109,204	Sheer veins	tablet7/p128	DH		V	hm,ca						2.5	18.1				-4			
A50	Pt1	**_834	Sheer veins	tablet7/p128	DH		V	hm,ca							15				-3.9			
A51	Pt1	**_1702	Sheer veins	tablet7/p128	DH		V	hm,ca							20.6				-2			
A52	Pt1	HC-1,186	Sheer veins	tablet7/p128	DH		V	qz,hm,ca							22.2				-0.5			
A53	Pt1	UM-1,573	Sheer veins	tablet7/p128	DH		V	qz							6				-5.5			
A54	Pt1	MC-145,324.5	Sheer veins	tablet7/p128	DH		V	ca,ars,prl														
A55	Pt1	CHF-4	Lakeshore Veins	tablet7/p128	S		V	pr,chl,qz			5.9											
A56	Pt1	CHF-11	Lakeshore Veins	tablet7/p128	S		V	ca,qz							17.8				2.5			
A57	Pt1	CHF-11(2)	Lakeshore Veins	tablet7/p128	S		V	ca,ba,cc							22.4				-3.2			
A58	Pt1	CHF-18	Lakeshore Veins	tablet7/p128	S		V	ca,ba,cc							13.2				-3.4			
A59	Pt1	CHF-22A	Lakeshore Veins	tablet7/p128	S		V	ca,hm							18.5				-3.5			
A60	Pt1	CHF-27	Lakeshore Veins	tablet7/p128	S		V	ca							14.2				-2.4			
A61	Pt1	CHF-28	Lakeshore Veins	tablet7/p128	S		V	ca							23.1				-2.5			
A62	Pt1	AHM-UG-4,1800	Amygdular/Cementing	table16/p125	DH		A	ca,cc,prl							18.5				-5.5		-75	
A63	Pt1	ASH-2	Amygdular/Cementing	table16/p125	W		A	ca, chl, pp							15.6				-3			
A64	Pt1	ASH-7	Amygdular/Cementing	table16/p125	W		A	ca, chl, cu, pr, qz							15.1				-3			
A65	Pt1	ASH7(11)	Amygdular/Cementing	table16/p125	W		A	ca, chl, cu, pr, qz							15.4				-3			
A66	Pt1	ASH-17	Amygdular/Cementing	table16/p125	W		A	ca, cu, ksp, mv, pp, qz							15				-2.7			
A67	Pt1	ASH-21	Amygdular/Cementing	table16/p125	W		A	ca, cu, hm,mv, pr							21.5				-3.9			
A68	Pt1	ASH-25	Amygdular/Cementing	table16/p125	W		A	ca							12.6				-3.7			
A69	Pt1	ASH-25	Amygdular/Cementing	table16/p125	W		A	ca,mv							20.6				-2.8			
A70	Pt1	BOH-7	Amygdular/Cementing	table16/p125	W		A	ca,cu,qz							14.9				-3.1			
A71	Pt1	CCF-5	Amygdular/Cementing	table16/p125	S		A	ca, cu, pp, pr, qz							17.7				-3.2			
A72	Pt1	CEN-105,2526	Amygdular/Cementing	table16/p125	W		A	ca,chl,cu,ep, pr, qz							11.2				-1.7			
A73	Pt1	**_661	Amygdular/Cementing	table16/p125	DH		A	ca, chl, ep, Im, mv, pp							13				-4.9		-69	
A74	Pt1	**_990	Amygdular/Cementing	table16/p125	DH		A	ca, chl, ep, pp							18				-2.9			
A75	Pt1	**_1093	Amygdular/Cementing	table16/p125	DH		A	ca, chl, ep, qz							12.2				-2.6			
A76	Pt1	**_1096	Amygdular/Cementing	table16/p125	DH		A	ca, chl, ep, ksp							14.5				-1.9			
A77	Pt1	CF-1,787	Amygdular/Cementing	table16/p125	DH		A	ca, pp, pr							17.2				-4.3			
A78	Pt1	CHF-9	Copper Harbor cement	table16/p125	DH		A	ca, cu							20.7				-4.6			

I.D.	Source	Published Sample Number	Sample Location	Source Page	Type	Host Rock	Vein/ Amygdule	Associated Minerals	$\delta^{18}O_{qz}$	$\delta^{18}O_{pr}$	$\delta^{18}O_{chl/cln}$	$\delta^{18}O_{ksp}$	$\delta^{18}O_{mv}$	$\delta^{18}O_{hm}$	$\delta^{18}O_{ca}$	$\delta^{18}O_{epi}$	$\delta^{18}O_{ank}$	$\delta^{13}C_{ca}$	$\delta^{13}C_{ank}$	δD_{epi}	δD_{pmp}	$\delta D_{chl/cln}$
A79	PL1	CHF-20A	Copper Harbor cement	table16/p125	S		A	ca, chl							23.2			-1.7				
A80	PL1	CFHF-20B	Copper Harbor cement	table16/p125	S		A	ca							21			-2.1				
A81	PL1	CHF-21A	Copper Harbor cement	table16/p125	S		A	ca, lm							22			-2.8				
A82	PL1	CHF-22B	Copper Harbor cement	table16/p125	S		A	ca							21			-1.6				
A83	PL1	CHF-29	Copper Harbor cement	table16/p125	S		A	ca							22			-2.3				
A84	PL1	DEL-109,20	Amygdular/Cementing	table16/p125	S		A	ca, ep, qz							12			-3.5				
A85	PL1	***,63	Amygdular/Cementing	table16/p125	DH		A	ca, chl, ep, ksp, pr							15.5			-2.4				
A86	PL1	***,911	Amygdular/Cementing	table16/p125	DH		A	ca, cu, ep, pp, qz							13.1			-3.2				
A87	PL1	***,914	Amygdular/Cementing	table16/p125	DH		A	ca, chl, ksp							16.9			-3.1				
A88	PL1	***,1079	Amygdular/Cementing	table16/p125	DH		A	ca, ep, qz							13.5			-2.5				
A89	PL1	***,1157	Amygdular/Cementing	table16/p125	DH		A	ca, chl							14			-2.8				
A90	PL1	GRN-3	Amygdular/Cementing	table16/p125	DH		A	ca							21			-13.4				
A91	PL1	HC-1,80	Amygdular/Cementing	table16/p125	W		A	ca, cu, lm							21.2			-2				
A92	PL1	***,236	Amygdular/Cementing	table16/p125	DH		A	ca, lm							21.8			-2.1				
A93	PL1	***,1214	Amygdular/Cementing	table16/p125	DH		A	ca, cu, lm							19.7			-3				
A94	PL1	***,1229	Amygdular/Cementing	table16/p125	DH		A	ca, ep, lm, mv, pp, pr							20.3			-2.9				
A95	PL1	***,1725	Amygdular/Cementing	table16/p125	DH		A	chl, cu, pp, pr, qz							20.1			-3.7			-75	
A96	PL1	***,3227	Amygdular/Cementing	table16/p125	DH		A	ca, cu, pr							16.2			-3.7				
A97	PL1	***,4236	Amygdular/Cementing	table16/p125	DH		A	ca, cu, ep, lm, pp, qz							17.9			-2.6				
A98	PL1	***,4401	Amygdular/Cementing	table16/p125	DH		A	ca							18			-3.1				
A99	PL1	***,4492	Amygdular/Cementing	table16/p125	DH		A	ca, cu, ep, mv							19.9			-3.1				
A100	PL1	***,4644	Amygdular/Cementing	table16/p125	DH		A	ca, cu, ep, pp, pr, qz							16.3			-3.2				
A101	PL1	HC-1,4958	Amygdular/Cementing	table16/p126	DH		A	ca							18			-3.4				
A102	PL1	HC-1,5024	Amygdular/Cementing	table16/p126	DH		A	ca, cu, ep, pp, qz							17.2			-1.9				
A103	PL1	HGH-1	Amygdular/Cementing	table16/p126	M		A	ca, ep, qz							13.6			-2				
A104	PL1	IRQ-12	Amygdular/Cementing	table16/p126	M		A	ca, cu, ep, pp, pr, qz							14.9			-2.9				
A105	PL1	ISR-20	Amygdular/Cementing	table16/p126	M		A	ca, ep, pp, qz							13.9			0.3				
A106	PL1	ISR-22,Pink	Amygdular/Cementing	table16/p126	M		A	ca, cu, ep, pr, qz							16.7			-0.8				
A107	PL1	KSR-20	Amygdular/Cementing	table16/p126	W		A	ca, chl, cu, ep, qz							20.1			-4.1				
A108	PL1	KRS-21	Amygdular/Cementing	table16/p126	W		A	ca, chl, cu, qz							13.2			-3.7				
A109	PL1	KRS-30	Amygdular/Cementing	table16/p126	W		A	ca, ep							17.9			-3.8				
A110	PL1	KRS-34	Amygdular/Cementing	table16/p126	W		A	ca, chl, cu, ep, qz							13.3			-4				
A111	PL1	KRS-37	Amygdular/Cementing	table16/p126	W		A	ca, chl, cu, ksp, qz							15.3			-4.4				
A112	PL1	KRS-39	Amygdular/Cementing	table16/p126	W		A	ca, chl, pp, qz							11.3			-4.2				
A113	PL1	KRS-42	Amygdular/Cementing	table16/p126	W		A	ca, chl, ksp, qz							12.4			-4.5				
A114	PL1	KRS-43	Amygdular/Cementing	table16/p126	W		A	ca, chl, ksp, qz							15.4			-2.4				
A115	PL1	KRS-57	Amygdular/Cementing	table16/p126	W		A	ca, ep, pr							12.9			-3.2				
A116	PL1	KRS-61	Amygdular/Cementing	table16/p126	W		A	ca, ep							13.1			-2.9				
A117	PL1	KRS-63	Amygdular/Cementing	table16/p126	W		A	ca, cu, ep, pp, pr							13			-3.3			-83	
A118	PL1	KRS-66	Amygdular/Cementing	table16/p126	W		A	ca, chl, ksp, pr, qz							12.9			-3				
A119	PL1	KRS-89	Amygdular/Cementing	table16/p126	M		A	ca, chl, ksp							15.3			-3.8				
A120	PL1	KRS-101	Amygdular/Cementing	table16/p126	W		A	ca, chl, cu, ep, ksp, pr							14.1			-3.4				
A121	PL1	OJB-43,624	Amygdular/Cementing	table16/p126	DH		A	ca, pp, qz							16.7			-2.6				
A122	PL1	OJB-43,624,,	Amygdular/Cementing	table16/p126	DH		A	ca, pp, qz							15			-2.5				
A123	PL1	PNX-25,112early	Amygdular/Cementing	table16/p126	DH		A	ca, cu, pr, qz							21.9			-2.6				
A124	PL1	PNX-25,112late	Amygdular/Cementing	table16/p126	DH		A	ca, cu, pr, qz							14.9			-2.9				
A125	PL1	WIN-3	Amygdular/Cementing	table16/p126	W		A	ca, ep, pp, qz							13			-4.7				
A126	PL1	WIN-4	Amygdular/Cementing	table16/p126	W		A	ca, ep, pp							16.9			-4.1				
A127	PL1	WIN-9	Amygdular/Cementing	table16/p126	W		A	ca, ep, pp, qz							19.3			-3.5				
A128	PL1	CEN-105.1096	Cell.rAmygdule	table15/p118	DH			ksp, ep,ca, hm			6.1											-55
A129	PL1	KRS-56	cell footy amg	table15/p118	W			qz, ep			7.2											-55
A130	PL1	MH-1.124	Frag. Amg.	table15/p118	DH			Ep, qz, ksp, py			7.8											-41
A131	PL1	OJB-8.1833	cell footy	table15/p118	DH			amg, ca			7											-45
A132	PL1	PNX-18.1738	Cell footy Amg	table15/p118	DH			chl, mv			7.2											-60
A133	PL1	U-16.3216	Cell footy,	table15/p118	DH			ab, chl, pr			6.7											-54
A134	PL1	U-16.3217.5	Cell foot	table15/p118	DH			ca, chl, lm, pp, pr														-62
A135	PL1	U-16.3332	Flow interior	table15/p118	DH			chl, mv, qz			6.2											-77
A136	PL1	U-16.3455	Flow interire	table15/p118	DH			chl, mv			8											-84
A137	PL1	ASH-22/24	Mass Copper Fissures	p138	W			ca, chl, cu, ep, ksp, pp, pr														-48
A138	PL1	BOH-26	cell amg. indike,	table15/p118	DH			bn amd cc														-41
A139	PL1	CHC-5		table15/p119	M			chloritized qz-porphyry pebble			6.3											-25
A140	PL1	HC-1.80	cell, amg,	table15/p120	DH			lm, wk?, hm, Cu			8.4											-50
A141	PL1	CEN-105.1201	Shear Veins	p138	DH			lm, chl, hm														-55
A142	PL1	MB-81C.528	Shear Veins	p138	DH			lm, pr, bn														-70
A143	PL1	OJB-44.355	Shear Veins	p138	DH			lm, pr, qz, Cu														-61
A144	PL1	GRA-6.467	pumpellyite-domains	table19/p144	DH			ep, Cu, qz													-88	
A145	PL1	GRA-6.1094	pumpellyite-domains	table19/p144	DH			ep, pp, chl, pr, ep, ca													-82	
A146	PL1	GRA-6.1925	pumpellyite-domains	table19/p144	DH			ep, hm, ep, qz, ca, pr													-69	
A147	PL1	OJB-44.355	pumpellyite-domains	table19/p144	DH			pr, chl, pp, qz													-66	
A148	PL1	U-16.301	pumpellyite-domains	table19/p144	DH			chl, pr, lm, ca, Cu													-98	
A149	PL1	EVR-24	Pumpellyite-basalts	table19/p144	W			qz, pp													-79	
A150	PL1	U-16.399	Pumpellyite-basalts	table19/p144	DH			pr, ca, Cu													-91	
A151	PL1	U-16.3226	Pumpellyite-basalts	table19/p144	DH			chl													-76	
A152	PL1	AHM-UG-4.1546	table20p146	table20/p146	DH			qz, ep								5.9				-20		
A153	PL1	CEN-105.246	table20p146	table20/p146	DH			qz,ep												-29		
A154	PL1	CEN-105.346	table20p146	table20/p146	DH			qz,ep								5.4				-34		
A155	PL1	CEN-105.379	table20p146	table20/p146	DH			ep,qz,chl,ca												-37		
A156	PL1	CEN-105.399	table20p146	table20/p146	DH			qz,ep								4.8				-35		

I.D.	Source	Published Sample Number	Sample Location	Source Page	Type	Host Rock	Vein/ Amygdule	Associated Minerals	$\delta^{18}O_{qz}$	$\delta^{18}O_{pr}$	$\delta^{18}O_{chl/cln}$	$\delta^{18}O_{ksp}$	$\delta^{18}O_{mv}$	$\delta^{18}O_{hm}$	$\delta^{18}O_{ca}$	$\delta^{18}O_{epi}$	$\delta^{18}O_{ank}$	$\delta^{13}C_{ca}$	$\delta^{13}C_{ank}$	δD_{epi}	δD_{pmp}	$\delta D_{chl/cln}$
A157	PL1	DEL-109.20	table20p146	table20/p146	DH			ebasalt												-26		
A158	PL1	HC-1.4501	table20p146	table20/p146	DH			ep,qz								6.1				-7		
B1	PP1	S10-10AV	Ahmeek	Table2/p34	DH	FT	A								27.7			-3.9				
B2	PP1	S10-25B	Ahmeek	Table2/p34	DH	TZ	A				7.1											-75.4
B3	PP1	S10-25B/2	Ahmeek	Table2/p34	DH	TZ	A				7.6											-75.4
B4	PP1	S10-31V	Ahmeek	Table2/p34	DH	FT	V		18.3													
B5	PP1	S10-37V	Ahmeek	Table2/p34	DH	FT	V								29.3			-3.7				
B6	PP1	S10-37V/2	Ahmeek	Table2/p34	DH	FT	V								25.9			-4				
B7	PP1	S10-37Vqtz	Ahmeek	Table2/p34	DH	FT	V		13.8													
B8	PP1	S10-43V	Ahmeek	Table2/p34	DH	MF	V				9.5											
B9	PP1	S10-70V	Ahmeek	Table2/p34	DH	TZ	V				6											-76.4
B10	PP1	AH8-10BB	Ahmeek	Table2/p34	DH	FT	A				8.1											-47.7
B11	PP1	AH8-12BB	Ahmeek	Table2/p34	DH	TZ	A				6.5											
B12	PP1	AH8-18V	Ahmeek	Table2/p34	DH	TZ	V								25.5			-3				
B13	PP1	AH8-21V	Ahmeek	Table2/p34	DH	FT	V				4.2											
B14	PP1	AH821V	Ahmeek	Table2/p34	DH	FT	V								26.7			-2.7				
B15	PP1	AH8-21V	Ahmeek	Table2/p34	DH	FT	V									8.7						
B16	PP1	AH8-23V	Ahmeek	Table2/p34	DH	MF	V				7.5											-62.6
B17	PP1	AH823V1	Ahmeek	Table2/p34	DH	MF	V				8.8											
B18	PP1	AH8-23V2	Ahmeek	Table2/p34	DH	MF	V				7.7											
B19	PP1	AH8-27B	Ahmeek	Table2/p34	DH	TZ	A				7.2											
B20	PP1	AH8-27B/2	Ahmeek	Table2/p34	DH	TZ	A				9.1											
B21	PP1	AH8-28BV	Ahmeek	Table2/p34	DH	MF	V/A				6.8											
B22	PP1	AH8-36B	Ahmeek	Table2/p34	DH	TZ	A		6.2													
B23	PP1	AH8-IV	Ahmeek	Table2/p34	DH	MF	V				8.7											
B24	PP1	AH8-IVrim	Ahmeek	Table2/p34	DH	MF	V				7.6											
B25	PP1	AH8-JV	Ahmeek	Table2/p34	DH	FT	V								25.5			-2.6				
B26	PP1	AH8-JVq/2	Ahmeek	Table2/p34	DH	FT	V		15.2													
B27	PP1	AH8-LB	Ahmeek	Table2/p34	DH	TZ	A				6.3											
B28	PP1	G7-06B/V	Ahmeek	Table2/p34	DH	TZ	V/A				5.6											
B29	PP1	G7-06V	Ahmeek	Table2/p34	DH	TZ	V/A									7						
B30	PP1	G7-08B	Ahmeek	Table2/p34	DH	TZ	V/A				5.6											
B31	PP1	G7-10V	Ahmeek	Table2/p34	DH	MF	V				8.8											
B32	PP1	G7-11V	Ahmeek	Table2/p34	DH	MF	A				6.2											
B33	PP1	G7-12BB	Ahmeek	Table2/p34	DH	FT	V/A				15.3											
B34	PP1	G7-18B	Ahmeek	Table2/p34	DH	FT	A								19.6			-3.7				
B35	PP1	G7-22V	Ahmeek	Table2/p34	DH	MF	V				10.5											
B36	PP1	G7-28B	Ahmeek	Table2/p34	DH	TZ	A				5.9											
B37	PP1	G7-36V	Ahmeek	Table2/p34	DH	MF	V				4.5											-54.4
B38	PP1	G7-45dom	Ahmeek	Table2/p34	DH	MF	V									9.3						
B39	PP1	G7-56V	Ahmeek	Table2/p34	DH	MF	V				9.3											-26.5
B40	PP1	G7-56V	Ahmeek	Table2/p34	DH	MF	V								24.6			-3.5				
B41	PP1	G7-62V	Ahmeek	Table2/p34	DH	TZ	V								18.1			-1.9				
B42	PP1	G7-63B	Ahmeek	Table2/p34	DH	TZ	A				7											-42.2
B43	PP1	G7-64V	Ahmeek	Table2/p34	DH	TZ	A								22			-3.2				
B44	PP1	G7-68V	Ahmeek	Table2/p34	DH	MF	V				4.3											
B45	PP1	G7-68V	Ahmeek	Table2/p34	DH	MF	V								20			-2.7				
B46	PP1	EH02-08B	Eagle Harbor	Table2/p35	DH	TZ	A				9.8											-41.2
B47	PP1	EH02-16BB	Eagle Harbor	Table2/p35	DH	MF	A				10.9											
B48	PP1	EH02-16V	Eagle Harbor	Table2/p35	DH	MF	V				10.7											
B49	PP1	EH04-06V	Eagle Harbor	Table2/p35	DH	TZ	V								27.9			-4.9				
B50	PP1	EH04-09BB	Eagle Harbor	Table2/p35	DH	TZ	A				11.5											-51.8
B51	PP1	EH04-10B	Eagle Harbor	Table2/p35	DH	FT	A				9.5											
B52	PP1	EH04-11B	Eagle Harbor	Table2/p35	DH	TZ	A				9											
B53	PP1	EH04-11V	Eagle Harbor	Table2/p35	DH	TZ	V				12.4											
B54	PP1	EH04-16B	Eagle Harbor	Table2/p35	DH	TZ	A				10.7											
B55	PP1	EH04-19B	Eagle Harbor	Table2/p35	DH	TZ	A								25.3			-1.9				
B56	PP1	C89-09V	Eagle Harbor	Table2/p35	DH	MF	A								25.4			-5.9				
B57	PP1	C89-12ABB	Eagle Harbor	Table2/p35	DH	TZ	A				18.3											
B58	PP1	C89-15V	Eagle Harbor	Table2/p35	DH	MF	A								17.7			-7.1				
B59	PP1	C89-20B	Eagle Harbor	Table2/p35	DH	FT	A				10.7											-37
B60	PP1	C89-29V	Eagle Harbor	Table2/p35	DH	TZ	V		17.4													
B61	PP1	C89-38	Eagle Harbor	Table2/p35	DH	TZ	A				5.9											-42.9
B62	PP1	C89-40B	Eagle Harbor	Table2/p35	DH	TZ	A				7.6											-44.5
B63	PP1	D56-09BB	Eagle Harbor	Table2/p35	DH	TZ	A				11											
B64	PP1	D56-20V	Eagle Harbor	Table2/p35	DH	MF	V				11											-65.5
B65	PP1	D56-20V	Eagle Harbor	Table2/p35	DH	MF	V				8.5											
B66	PP1	D56-26V	Eagle Harbor	Table2/p35	DH	MF	V		13.8													
B67	PP1	D56-28V	Eagle Harbor	Table2/p35	DH	MF	V				5.9											
B68	PP1	D56-29V	Eagle Harbor	Table2/p35	DH	MF	V				11.8											
B69	PP1	D56-33V	Eagle Harbor	Table2/p35	DH	MF	V								22.1			-3.3				
B70	PP1	D56-34AV	Eagle Harbor	Table2/p35	DH	MF	A								23.2			-0.2				
B71	PP1	D57-07V	Eagle Harbor	Table2/p35	DH	TZ	V				5.8											
B72	PP1	D57-13VB	Eagle Harbor	Table2/p35	DH	TZ	V/A				5.5											
B73	PP1	D57-18BA	Eagle Harbor	Table2/p35	DH	(FT)	A				10.9											
B74	PP1	D57-20V	Eagle Harbor	Table2/p35	DH	MF	V								22.2			-2.5				
B75	PP1	D57-26Vdom	Eagle Harbor	Table2/p35	DH	MF	V									6.4						
B76	PP1	D52-76V	Eagle Harbor	Table2/p35	DH	MF	V									6.8						

I.D.	Source	Published Sample Number	Sample Location	Source Page	Type	Host Rock	Vein/ Amygdule	Associated Minerals	$\delta^{18}O_{qz}$	$\delta^{18}O_{pr}$	$\delta^{18}O_{chl/cln}$	$\delta^{18}O_{ksp}$	$\delta^{18}O_{mv}$	$\delta^{18}O_{hm}$	$\delta^{18}O_{ca}$	$\delta^{18}O_{epi}$	$\delta^{18}O_{ank}$	$\delta^{13}C_{ca}$	$\delta^{13}C_{ank}$	δD_{epi}	δD_{pmp}	$\delta D_{chl/cln}$
B77	PP1	D52-76V	Eagle Harbor	Table2/p35	DH	MF	V		13.9													
B78	PP1	D57-28VA	Eagle Harbor	Table2/p35	DH	MF	V								22.8			-2.4				
B79	PP1	D57-28VB	Eagle Harbor	Table2/p35	DH	MF	V								21.7			-2.1				
B80	PP1	D57-31B	Eagle Harbor	Table2/p35	DH	TZ	V				5.9											
B81	PP1	D57-41dom	Eagle Harbor	Table2/p35	DH	MF	V									4.9						
B82	PP1	D57-42B	Eagle Harbor	Table2/p35	DH	TZ	A				5.5											-59.4
B83	PP1	CL14-02V	Copper Harbor	Table2/p36	DH	MF	V								28.9			-2				
B84	PP1	CL14-18V	Copper Harbor	Table2/p36	DH	FT	V				13.8											
B85	PP1	CL14-20V	Copper Harbor	Table2/p36	DH	TZ	V								23.1			-2.8				
B86	PP1	CL14-22B	Copper Harbor	Table2/p36	DH	FT	A				10.6											
B87	PP1	CL14-23B	Copper Harbor	Table2/p36	DH	FT	A				9.5											
B88	PP1	CL14-25V	Copper Harbor	Table2/p36	DH	FT	A				15.8											
B89	PP1	CL14-28V	Copper Harbor	Table2/p36	DH	FT	V								29.6			-3				
B90	PP1	CL14-30V	Copper Harbor	Table2/p36	DH	MF	V				12.9											
B91	PP1	CL14-32B	Copper Harbor	Table2/p36	DH	FT	A				9.9											
B92	PP1	CL14-45V	Copper Harbor	Table2/p36	DH	TZ	V								27.5			-2.9				
B93	PP1	CL14-48V	Copper Harbor	Table2/p36	DH	MF	V															15.9
B94	PP1	CL14-63B	Copper Harbor	Table2/p36	DH	TZ	A				8.8											
B95	PP1	CL14-72V	Copper Harbor	Table2/p36	DH	MF	V								24.5			-2.3				
B96	PP1	CL14-83V	Copper Harbor	Table2/p36	DH	MF	V				6.4											
B97	PP1	CL14-83V/1	Copper Harbor	Table2/p36	DH	MF	V								23.3			-3.7				
B98	PP1	CL14-83V/2	Copper Harbor	Table2/p36	DH	MF	V								22.9			-3.7				
B99	PP1	CL11-06B	Copper Harbor	Table2/p36	DH	FT	A								28.7			-3.7				
B100	PP1	CL11-10V	Copper Harbor	Table2/p36	DH	TZ	V								21.1			-2				
B101	PP1	CL11-12B	Copper Harbor	Table2/p36	DH	TZ	A				5.8											
B102	PP1	CL11-25AB	Copper Harbor	Table2/p36	DH	TZ	A				9.9											
B103	PP1	CL11-27V	Copper Harbor	Table2/p36	DH	MF	V								24.1			-2.7				
B104	PP1	CL11-31V	Copper Harbor	Table2/p36	DH	FT	V								26			-2.8				
B105	PP1	CL11-35V	Copper Harbor	Table2/p36	DH	MF	V				19.4											
B106	PP1	CL11-38B	Copper Harbor	Table2/p36	DH	TZ	A				7.2											
B107	PP1	CL11-48V	Copper Harbor	Table2/p36	DH	MF	V				9.7											
B108	PP1	ST7-07B	Copper Harbor	Table2/p36	DH	TZ	A				5.3											
B109	PP1	ST7-13BE	Copper Harbor	Table2/p36	DH	TZ	A				8.7											
B110	PP1	ST7-20V	Copper Harbor	Table2/p36	DH	MF	V				13.4											
B111	PP1	ST7-38V	Copper Harbor	Table2/p36	DH	FT	V				6.8											
B112	PP1	ST7-38V	Copper Harbor	Table2/p36	DH	FT	V								19.7			-3.4				
C1	PW1	227CL2	LaSalle #3-4				V	ksp,ca,ep							19.3			-3.04				
C2	PW1	218CL1	LaSalle #3-4				V/A	ksp,ca,ep							15.27			-2.92				
C3	PW1	228CL2	Centennial #1				A	ep,ca,Cu							13.12			-2.78				
C4	PW1	214CL3	Centennial #1				A	ep,qtz,Cu,ca							12.68			-2.37				
C5	PW1	214CL2	South Kearsarge #1				A	ep,ca							13.61			-2.89				
C6	PW1	215CL2	South Kearsarge #1				A	ksp,ca,ep,Cu							13.92			-2.28				
C7	PW1	226CL1	Wolverine #3				A	Cu,ca,ep,qtz							14.09			-2.18				
C8	PW1	219CL1	Wolverine #3				A	ep,ksp,ca							12.71			-2.9				
C9	PW1	216CL1	Wolverine #2				A	ep,ca,Ag,ksp							14.1			-2.48				
C10	PW1	216CL3	Wolverine #2				A	ksp,ca,Cu							13.68			-2.67				
C11	PW1	216CL2	Wolverine #2				A	ca,ep,ksp							14.24			-3.19				
C12	PW1	222CL1	North Kearsarge #1				A	ca,ksp,ep,qtz							16.5			-3.12				
C13	PW1	223CL1	North Kearsarge #3				A	ca,Cu							12.95			-2.79				
C14	PW1	229CL1	North Kearsarge #3				A	ca,Cu,qtz							17			-2.72				
C15	PW1	221CL2	North Kearsarge #3				A	ca,ksp,ep							13.63			-1.68				
C16	PW1	230CL1	North Kearsarge #4				A	chl,ca,Cu							18.29			-3.2				
C17	PW1	228CL1	North Kearsarge #4				A	ca,ep,ksp							12.99			-3.01				
C18	PW1	218CL3	Ahmeek #1				A	ca,ep,Cu							17.78			-3.37				
C19	PW1	217CL2	Ahmeek #1				A	ksp,ep,ca							13.78			-3.09				
C20	PW1	219CL3	Ahmeek #1					ca,ep,Cu							18.14			-3.18				
C21	PW1	225CL2	Ahmeek #2				A	ca,Cu							13.8			-2.82				
C22	PW1	225CL1	Ahmeek #2				A	chl,ep,Cu,ca							19.14			-3.89				
C23	PW1	220CL2	Mohawk#6				A	ep,ca							18.1			-3.06				
C24	PW1	224CL3	Mohawk#5				V	ksp,ca,pr,Cu							17.55			-2.81				
C25	PW1	224CL2	Mohawk#5				A	ca,ksp,Cu							13.17			-3.15				
C26	PW1	221CL3	Mohawk#4				A	ca							12.62			-3.42				
C27	PW1	218CL2	Mohawk#4				A	ca,ksp,ep							14.01			-2.94				
C28	PW1	219CL2	Mohawk#4					ca,pr,Cu							13.69			-2.43				
C29	PW1	215CL3	Mohawk#4				A	ksp,ca							13.78			-3.41				
C30	PW1	215CL1	Mohawk#4				A	ksp,ca							14.19			-2.13				
C31	PW1	223CL2	Mohawk#3				A	ca,laum							16.67			-2.72				
C32	PW1	220CL3	Mohawk#3				A	ca,Cu							15.28			-2.2				
C33	PW1	228CL3	Mohawk#2				V	ca							16.63			-4.43				
C34	PW1	222CL3	Mohawk#2				A	ca,Cu							18.67			-3.53				
C35	PW1	224CL1	Mohawk#2				A	ksp,ca							13.91			-3.66				
C36	PW1	225CL3	Seneca # 2 (Gratiot?)				A	ca,pr,Cu							14.78			-3.38				
C37	PW1	221CL1	Seneca # 2 (Gratiot?)				A	ca,pr,Cu							13.83			-2.54				
C38	PW1	222CL2	Seneca #3 (Gratiot?)				V	Cu,ca							13.76			-2.88				
C39	PW1	226CL3	Seneca #3 (Gratiot?)				A	ep,ksp,ca,Cu,Ag							13.18			-2.95				
C40	PW1	223CL3	Central #58				A	ca,ep							15.99			-3.23				
C41	PW1	227CL3	Central #32				A	ca							17.91			-2.63				

6 Appendix III: SIMS Raw Stable Isotope Data

Appendix III contains light stable isotope oxygen and carbon data that was analyzed for this study. The measurements were made by the SIMS method described in the text. Three samples were analyzed for this study, two from the Kearsarge flow, and one from the Quincy mine. The spot analyses were done by Florence Bégué, Institute of Earth Sciences University of Lausanne Switzerland. The spot size for oxygen isotope measurements was between 12 and 14µm and for carbon isotope measurements about 18µm with a 10µm raster.

The mounted polished chips are shown in cathodoluminescence image (Figure III.1). Figures III.1-4 provide a detailed view showing the location of the spot analyses. Small circles and each image represent spot location for oxygen and carbon isotopic determinations. The raw data for each spot is given in this appendix after the images.

6.1 Spot Analysis Cathodoluminescence Images:

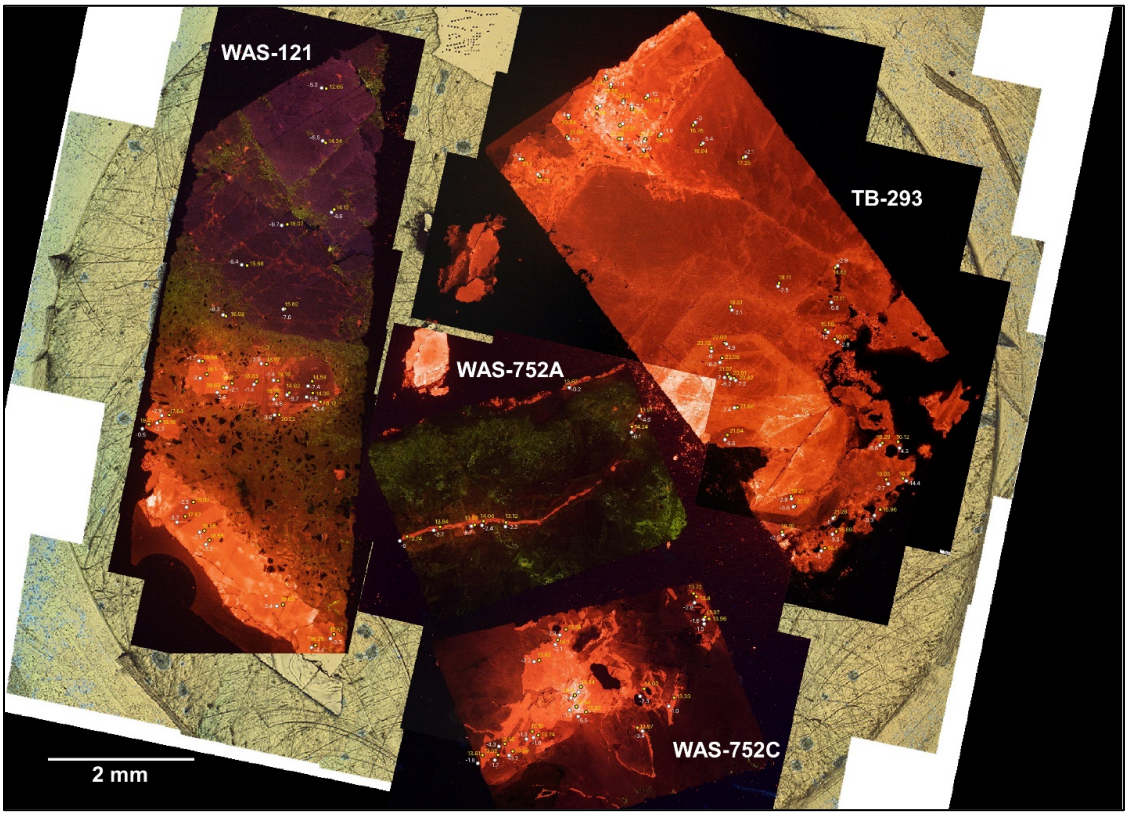

Figure III.1: Cathodoluminescence image of the three samples analyzed for this study using the SIMS method. Small circles represent spot location for oxygen and carbon isotopic determinations. Figures III.2-4 are more detailed images of each sample showing SIMS spot analysis locations and isotopic values.

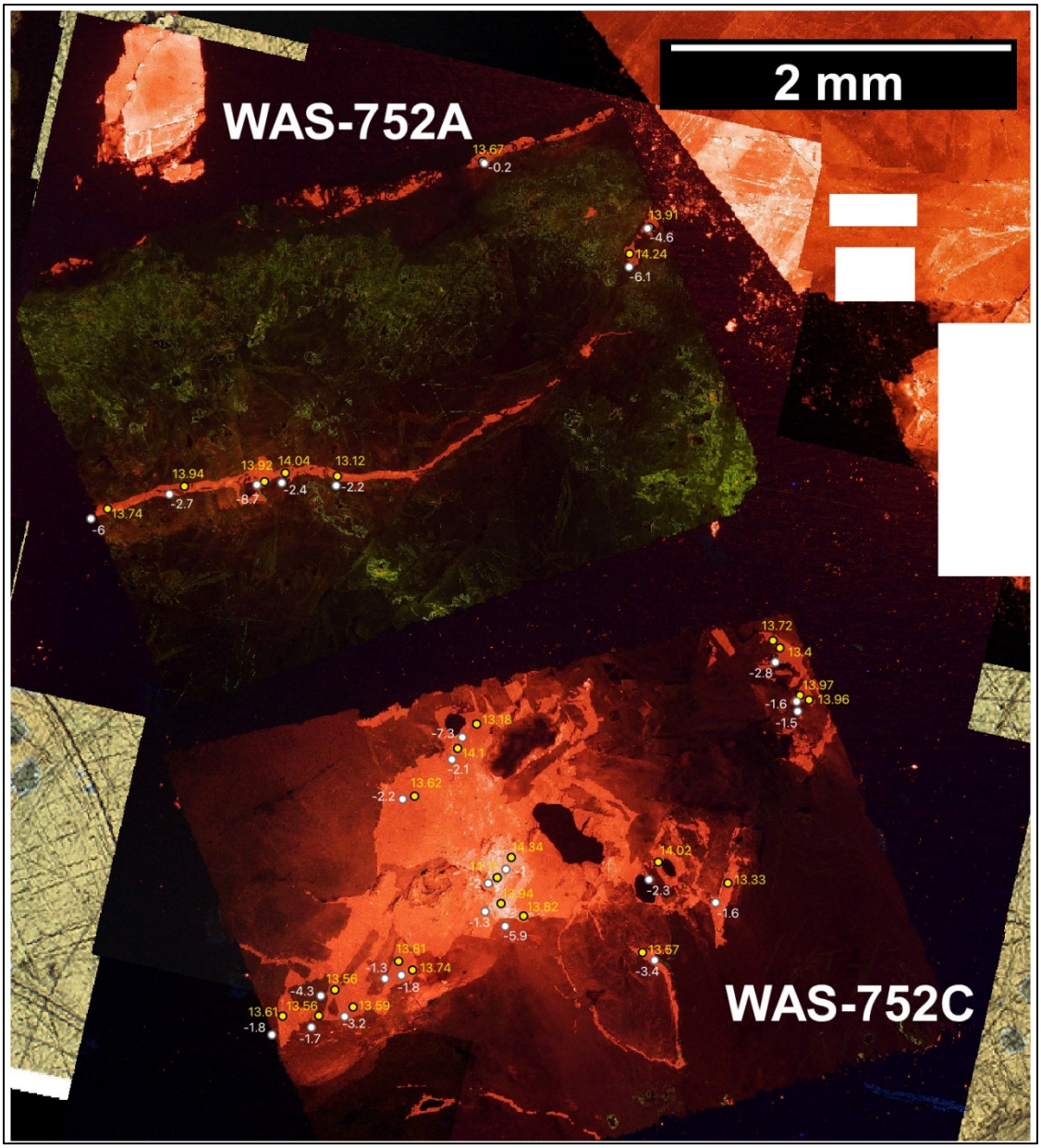

Figure III.2: Cathodoluminescence image of WAS-752. This sample is from the Kearsarge Wolverine mine. Small circles represent spot location for oxygen and carbon isotopic determinations. Figure III.2 is a more detailed image of the WAS-752 sample showing SIMS spot analysis locations and isotopic values. Based on mineral association it is a main-stage sample.

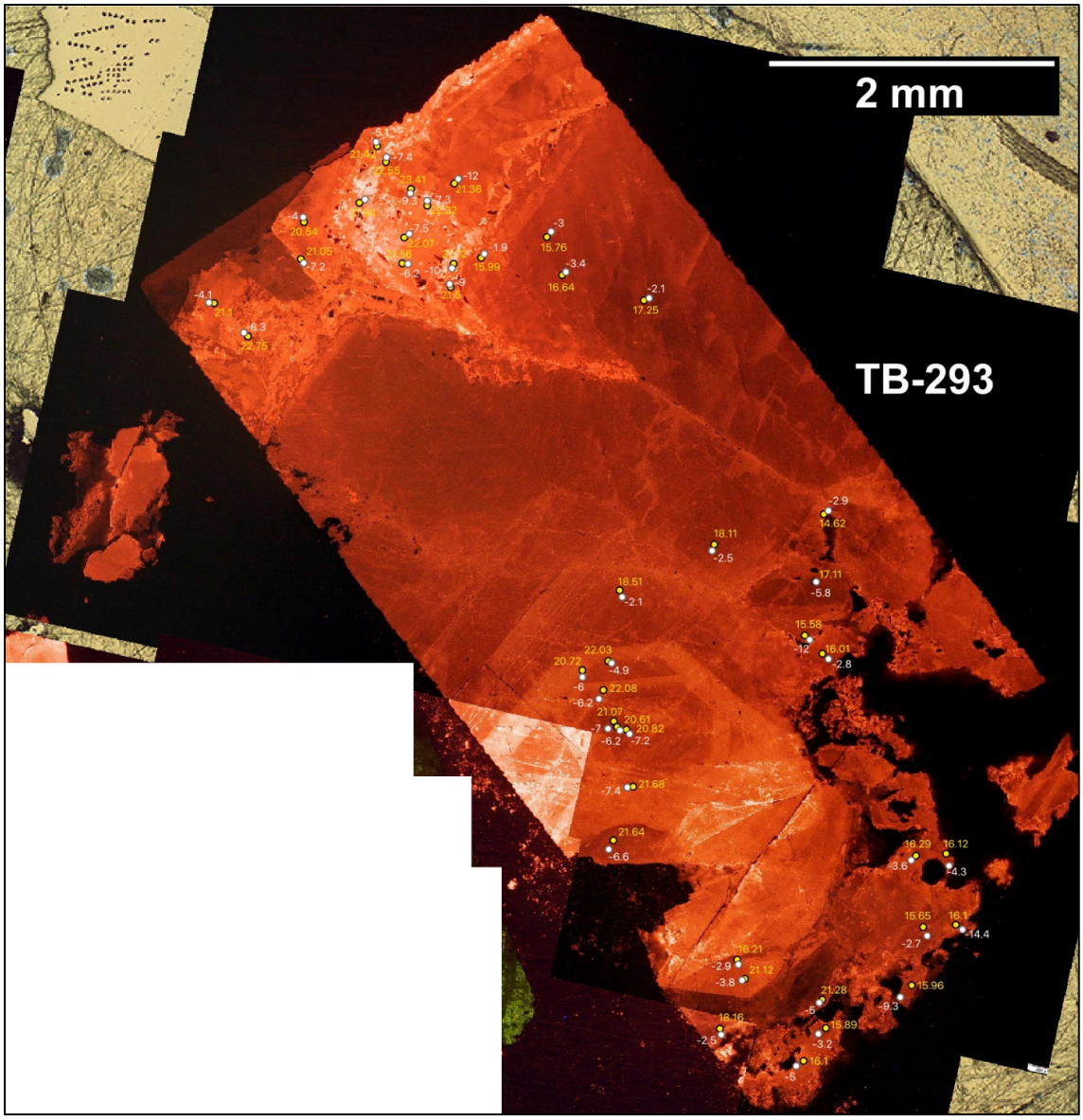

Figure III.3: Spot Analysis Cathodoluminescence image of TB-293. This sample is from the Quincy mine. Small circles represent spot location for oxygen and carbon isotopic determinations. Figure III.3 is a more detailed image of the TB-293 sample showing SIMS spot analysis locations and isotopic values. Based on mineral association it is a main-stage sample.

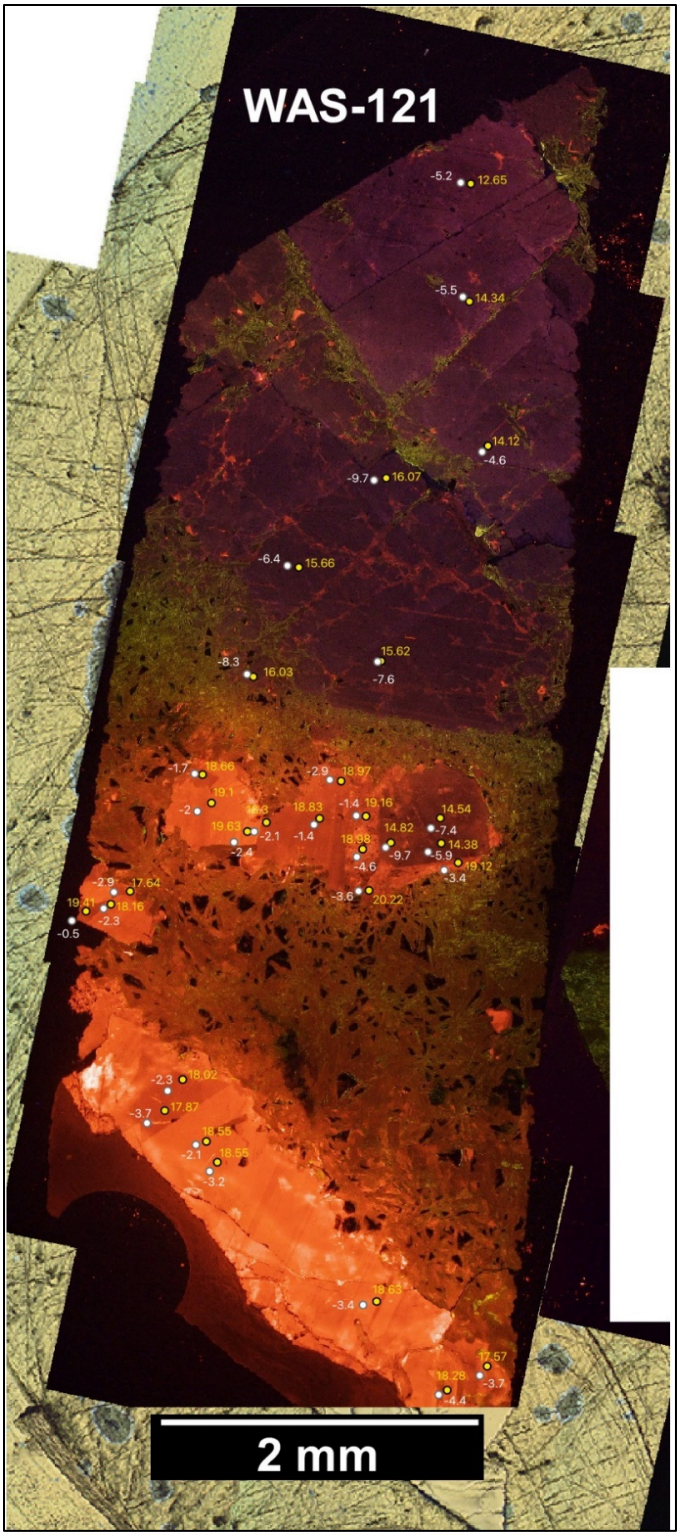

Figure III.4: Spot Analysis Cathodoluminescence image of WAS-121. This sample is from the Kearsarge Seneca mine. Small circles represent spot location for oxygen and carbon isotopic determinations. Figure III.4 is a more detailed image of the WAS-121 sample showing SIMS spot analysis locations and isotopic values. Based on mineral association (natrolite and laumontite) it is late-stage.

6.2 Legend for Table

I.D.:
Labeled data source and numbered in order they were compiled:
SIMS1-103 for Spot analysis data

Source:
Secondary assigned ranking to identify which source the data comes from:
PS1 = spot isotopic SIMS analysis from this study.

Sample Number:
TB-292 was a thick section cut from an approximately 2 cm tall vug-filling calcite crystal that has inclusions of native copper. This sample was provided for study by the A. E. Seaman Mineral Museum from its Keweenaw Research Suite. The crystal was among a suite of about 30 calcite crystals with inclusions of native copper donated to the museum by the late Arthur Moretta. These crystals all looked quite similar to one another and therefore likely were recovered from the same pocket. The samples were only labeled as from the Quincy mine, but were likely recovered from above the 7th level in the mine some time after the mine officially closed.

WAS-752 was calcite filling an open space along with prehnite and epidote. The is the Kearsarge Wolverine sample which was associated with prehnite and epidote. This sample was provided for study by the A. E. Seaman Mineral Museum from its Keweenaw Research Suite. The sample was collected by W. A. Seaman May 1, 1938 from underground at the Wolverine mine accessing the Kearsarge flow top deposit. W. A. Seaman notes that the sample was from a native copper bearing fracture/fault.

WAS-121 was calcite from a 3 cm wide vein also containing mostly natrolite and laumontite. This sample was provided for study by the A. E. Seaman Mineral Museum from its Keweenaw Research Suite. The vein clearly cross-cut the host rock which contains main-stage amygdule filling minerals. The sample was collected by W. A. Seaman from underground at the Seneca Mine accessing the Kearsarge flow top deposit.

The sample numbers provided given above are followed by an @ and an increasing number, indicating the order of completion of the analyses.

Sample Location:
Where in the Keweenaw the data was collected from is shown in this section. There are three samples that were analyzed using the SIMS method, they are noted as Kearsarge Wolverine, Kearsarge Seneca, and Quincy Mine.

Associated Minerals:
ca = calcite, cu = copper, ep = epidote, lm = laumontite, pr = prehnite, nat = natrolite.

Temp of Precipitation Error (°C):
This column lists the absolute value of the probable error in the inferred temperature of precipitation as discussed in the text.

Analytical Error Values for Calcite:
An estimate of the analytical error is given. The error for the bulk analyses was assumed to be 0.20‰ as stated by Actlabs. For SIMS spot analysis data, values were recorded for each analysis.

"Error ‰ $\delta^{18}O_{H2O}$ ca":
The analytical error of $\delta^{18}O_{H2O}$ ca for calcite, given in per mil (*‰).*

"Error ‰ $\delta^{13}C_{CO2}$ ca":
The analytical error of $\delta^{13}C_{CO2}$ ca for calcite, given in per mil (*‰).*

Raw spot stable isotope data was collected from calcites by the SIMS method described in the text.

						Analytical Error Values for Calcite			
I.D.	Source	Sample Number	Sample Location	Associated Minerals	Temp of Precipitation Error (°C)	Error ‰ $\delta^{18}O_{H2O}$ ca	Error ‰ $\delta^{13}C_{CO2}$ ca	$\delta^{18}O_{ca}$	$\delta^{13}C_{ca}$
SIMS1	PS1	TB-293-A@1	Quincy Mine	ca, cu	37.5	0.31	1.50	18.16	-2.5
SIMS2	PS1	TB-293-A@02	Quincy Mine	ca, cu	37.5	0.33	1.50	21.28	-5
SIMS3	PS1	TB-293-A@03	Quincy Mine	ca, cu	37.5	0.32	1.50	15.89	-3.2
SIMS4	PS1	TB-293-A@04	Quincy Mine	ca, cu	37.5	0.26	1.50	16.1	-5
SIMS5	PS1	TB-293-A@05	Quincy Mine	ca, cu	37.5	0.34	1.50	15.96	-9.3
SIMS6	PS1	TB-293-A@06	Quincy Mine	ca, cu	37.5	0.31	1.50	15.65	-2.7
SIMS7	PS1	TB-293-A@07	Quincy Mine	ca, cu	37.5	0.31	1.50	16.1	
SIMS8	PS1	TB-293-A@08	Quincy Mine	ca, cu	37.5	0.31	1.50	16.29	-3.6
SIMS9	PS1	TB-293-A@09	Quincy Mine	ca, cu	37.5	0.33	1.50	16.12	-4.3
SIMS10	PS1	TB-293-A@10	Quincy Mine	ca, cu	37.5	0.29	1.50	21.12	-3.8
SIMS11	PS1	TB-293-A@11	Quincy Mine	ca, cu	37.5	0.29	1.50	16.21	-2.9
SIMS12	PS1	TB-293-A@12	Quincy Mine	ca, cu	37.5	0.29	1.50	21.64	-6.6
SIMS13	PS1	TB-293-A@13	Quincy Mine	ca, cu	37.5	0.28	1.50	21.68	-7.4
SIMS14	PS1	TB-293-A@14	Quincy Mine	ca, cu	37.5	0.21	1.50	20.82	-7.2
SIMS15	PS1	TB-293-A@15	Quincy Mine	ca, cu	37.5	0.34	1.50	20.61	-6.2
SIMS16	PS1	TB-293-A@16	Quincy Mine	ca, cu	37.5	0.41	1.50	21.07	-7
SIMS17	PS1	TB-293-A@17	Quincy Mine	ca, cu	37.5	0.25	1.50	22.08	-6.2
SIMS18	PS1	TB-293-A@18	Quincy Mine	ca, cu	37.5	0.23	1.50	20.72	-4.9
SIMS19	PS1	TB-293-A@19	Quincy Mine	ca, cu	37.5	0.30	1.50	22.03	-6
SIMS20	PS1	TB-293-A@20	Quincy Mine	ca, cu	37.5	0.26	1.50	18.51	-2.1
SIMS21	PS1	TB-293-A@21	Quincy Mine	ca, cu	37.5	0.41	1.50	18.11	-2.5
SIMS22	PS1	TB-293-A@22	Quincy Mine	ca, cu	37.5	0.31	1.50	14.62	-2.9
SIMS23	PS1	TB-293-A@23	Quincy Mine	ca, cu	37.5	0.23	1.50	17.11	-5.8
SIMS24	PS1	TB-293-A@24	Quincy Mine	ca, cu	37.5	0.30	1.50	15.58	
SIMS25	PS1	TB-293-A@25	Quincy Mine	ca, cu	37.5	0.25	1.50	16.01	-2.8
SIMS26	PS1	TB-293-A@26	Quincy Mine	ca, cu	37.5	0.33	1.50	17.25	-2.1
SIMS27	PS1	TB-293-A@27	Quincy Mine	ca, cu	37.5	0.24	1.50	16.64	-3.4
SIMS28	PS1	TB-293-A@28	Quincy Mine	ca, cu	37.5	0.25	1.50	15.76	-3
SIMS29	PS1	TB-293-A@29	Quincy Mine	ca, cu	37.5	0.28	1.50	15.99	-1.9
SIMS30	PS1	TB-293-A@30	Quincy Mine	ca, cu	37.5	0.30	1.50	21.56	-6.2
SIMS31	PS1	TB-293-A@31	Quincy Mine	ca, cu	37.5	0.29	1.50	22.07	-7.5
SIMS32	PS1	TB-293-A@32	Quincy Mine	ca, cu	37.5	0.28	1.50	22.22	-7.3
SIMS33	PS1	TB-293-A@33	Quincy Mine	ca, cu	37.5	0.33	1.50	21.72	-10.1
SIMS34	PS1	TB-293-A@34	Quincy Mine	ca, cu	37.5	0.33	1.50	21.5	-9
SIMS35	PS1	TB-293-A@35	Quincy Mine	ca, cu	37.5	0.33	1.50	21.36	
SIMS36	PS1	TB-293-A@36	Quincy Mine	ca, cu	37.5	0.31	1.50	23.41	-9.3
SIMS37	PS1	TB-293-A@37	Quincy Mine	ca, cu	37.5	0.30	1.50	22.55	-7.4
SIMS38	PS1	TB-293-A@38	Quincy Mine	ca, cu	37.5	0.35	1.50	21.42	-5.1
SIMS39	PS1	TB-293-A@39	Quincy Mine	ca, cu	37.5	0.24	1.50	21.94	-7.8
SIMS40	PS1	TB-293-A@40	Quincy Mine	ca, cu	37.5	0.28	1.50	20.54	-4
SIMS41	PS1	TB-293-A@41	Quincy Mine	ca, cu	37.5	0.39	1.50	21.05	-7.2
SIMS42	PS1	TB-293-A@42	Quincy Mine	ca, cu	37.5	0.20	1.50	21.86	
SIMS43	PS1	TB-293-A@43	Quincy Mine	ca, cu	37.5	0.28	1.50	23.53	
SIMS44	PS1	TB-293-A@44	Quincy Mine	ca, cu	37.5	0.26	1.50	21.1	-4.1
SIMS45	PS1	TB-293-A@45	Quincy Mine	ca, cu	37.5	0.26	1.50	22.75	-6.3
SIMS46	PS1	WAS121-A@1	Seneca Mine (Kearsarge Deposit)	ca, qz, lm, nat	25	0.28	1.50	14.12	-4.6
SIMS47	PS1	WAS121-A@2	Seneca Mine (Kearsarge Deposit)	ca, qz, lm, nat	25	0.32	1.50	16.07	-9.7
SIMS48	PS1	WAS121-A@3	Seneca Mine (Kearsarge Deposit)	ca, qz, lm, nat	25	0.24	1.50	15.62	-7.6
SIMS49	PS1	WAS121-A@4	Seneca Mine (Kearsarge Deposit)	ca, qz, lm, nat	25	0.28	1.50	15.66	-6.4
SIMS50	PS1	WAS121-A@5	Seneca Mine (Kearsarge Deposit)	ca, qz, lm, nat	25	0.23	1.50	16.03	-8.3
SIMS51	PS1	WAS121-A@6	Seneca Mine (Kearsarge Deposit)	ca, qz, lm, nat	25	0.36	1.50	14.54	-7.4
SIMS52	PS1	WAS121-A@7	Seneca Mine (Kearsarge Deposit)	ca, qz, lm, nat	25	0.30	1.50	14.38	-5.9

						Analytical Error Values for Calcite			
I.D.	Source	Sample Number	Sample Location	Associated Minerals	Temp of Precipitation Error (°C)	Error ‰ $\delta^{18}O_{H2O}$ ca	Error ‰ $\delta^{13}C_{CO2}$ ca	$\delta^{18}O_{ca}$	$\delta^{13}C_{ca}$
SIMS53	PS1	WAS121-A@8	Seneca Mine (Kearsarge Deposit)	ca, qz, lm, nat	25	0.29	1.50	14.82	-9.7
SIMS54	PS1	WAS121-A@9	Seneca Mine (Kearsarge Deposit)	ca, qz, lm, nat	25	0.25	1.50	18.98	-4.6
SIMS55	PS1	WAS121-A@10	Seneca Mine (Kearsarge Deposit)	ca, qz, lm, nat	25	0.27	1.50	20.22	-3.6
SIMS56	PS1	WAS121-A@11	Seneca Mine (Kearsarge Deposit)	ca, qz, lm, nat	25	0.29	1.50	19.12	-3.4
SIMS57	PS1	WAS121-A@12	Seneca Mine (Kearsarge Deposit)	ca, qz, lm, nat	25	0.23	1.50	19.16	-1.4
SIMS58	PS1	WAS121-A@13	Seneca Mine (Kearsarge Deposit)	ca, qz, lm, nat	25	0.31	1.50	18.97	-2.9
SIMS59	PS1	WAS121-A@14	Seneca Mine (Kearsarge Deposit)	ca, qz, lm, nat	25	0.36	1.50	18.83	-1.4
SIMS60	PS1	WAS121-A@15	Seneca Mine (Kearsarge Deposit)	ca, qz, lm, nat	25	0.35	1.50	18.3	-2.1
SIMS61	PS1	WAS121-A@16	Seneca Mine (Kearsarge Deposit)	ca, qz, lm, nat	25	0.25	1.50	19.63	-2.4
SIMS62	PS1	WAS121-A@17	Seneca Mine (Kearsarge Deposit)	ca, qz, lm, nat	25	0.26	1.50	19.1	-2
SIMS63	PS1	WAS121-A@18	Seneca Mine (Kearsarge Deposit)	ca, qz, lm, nat	25	0.30	1.50	18.66	-1.7
SIMS64	PS1	WAS121-A@19	Seneca Mine (Kearsarge Deposit)	ca, qz, lm, nat	25	0.31	1.50	17.64	-2.9
SIMS65	PS1	WAS121-A@20	Seneca Mine (Kearsarge Deposit)	ca, qz, lm, nat	25	0.28	1.50	18.16	-2.3
SIMS66	PS1	WAS121-A@21	Seneca Mine (Kearsarge Deposit)	ca, qz, lm, nat	25	0.31	1.50	19.41	-0.5
SIMS67	PS1	WAS121-A@22	Seneca Mine (Kearsarge Deposit)	ca, qz, lm, nat	25	0.25	1.50	18.02	-2.3
SIMS68	PS1	WAS121-A@23	Seneca Mine (Kearsarge Deposit)	ca, qz, lm, nat	25	0.29	1.50	17.87	-3.7
SIMS69	PS1	WAS121-A@24	Seneca Mine (Kearsarge Deposit)	ca, qz, lm, nat	25	0.26	1.50	18.55	-2.1
SIMS70	PS1	WAS121-A@25	Seneca Mine (Kearsarge Deposit)	ca, qz, lm, nat	25	0.34	1.50	18.55	-3.2
SIMS71	PS1	WAS121-A@26	Seneca Mine (Kearsarge Deposit)	ca, qz, lm, nat	25	0.23	1.50	18.63	-3.4
SIMS72	PS1	WAS121-A@27	Seneca Mine (Kearsarge Deposit)	ca, qz, lm, nat	25	0.32	1.50	18.28	-4.4
SIMS73	PS1	WAS121-A@28	Seneca Mine (Kearsarge Deposit)	ca, qz, lm, nat	25	0.34	1.50	17.57	-3.7
SIMS74	PS1	WAS121-A@29	Seneca Mine (Kearsarge Deposit)	ca, qz, lm, nat	25	0.26	1.50	12.65	-5.2
SIMS75	PS1	WAS121-A@30	Seneca Mine (Kearsarge Deposit)	ca, qz, lm, nat	25	0.28	1.50	14.34	-5.5
SIMS76	PS1	WAS752-A@1	Wolverine Mine (Kearsarge Deposit)	ca, cu, pr, ep	25	0.29	1.50	13.74	-6
SIMS77	PS1	WAS752-A@2	Wolverine Mine (Kearsarge Deposit)	ca, cu, pr, ep	25	0.31	1.50	13.94	-2.7
SIMS78	PS1	WAS752-A@3	Wolverine Mine (Kearsarge Deposit)	ca, cu, pr, ep	25	0.31	1.50	13.92	-8.7
SIMS79	PS1	WAS752-A@4	Wolverine Mine (Kearsarge Deposit)	ca, cu, pr, ep	25	0.25	1.50	14.04	-2.4
SIMS80	PS1	WAS752-A@5	Wolverine Mine (Kearsarge Deposit)	ca, cu, pr, ep	25	0.29	1.50	13.12	-2.2
SIMS81	PS1	WAS752-A@6	Wolverine Mine (Kearsarge Deposit)	ca, cu, pr, ep	25	0.32	1.50	13.91	-4.6
SIMS82	PS1	WAS752-A@7	Wolverine Mine (Kearsarge Deposit)	ca, cu, pr, ep	25	0.30	1.50	14.24	-6.1
SIMS83	PS1	WAS752-A@8	Wolverine Mine (Kearsarge Deposit)	ca, cu, pr, ep	25	0.28	1.50	13.67	-0.2
SIMS84	PS1	WAS752-C@1	Wolverine Mine (Kearsarge Deposit)	ca, cu, pr, ep	25	0.20	1.50	13.18	-7.3
SIMS85	PS1	WAS752-C@2	Wolverine Mine (Kearsarge Deposit)	ca, cu, pr, ep	25	0.33	1.50	14.1	-2.1
SIMS86	PS1	WAS752-C@3	Wolverine Mine (Kearsarge Deposit)	ca, cu, pr, ep	25	0.30	1.50	13.62	-2.2
SIMS87	PS1	WAS752-C@4	Wolverine Mine (Kearsarge Deposit)	ca, cu, pr, ep	25	0.30	1.50	14.34	-1
SIMS88	PS1	WAS752-C@5	Wolverine Mine (Kearsarge Deposit)	ca, cu, pr, ep	25	0.30	1.50	14.11	-2
SIMS89	PS1	WAS752-C@6	Wolverine Mine (Kearsarge Deposit)	ca, cu, pr, ep	25	0.34	1.50	13.94	-1.3
SIMS90	PS1	WAS752-C@7	Wolverine Mine (Kearsarge Deposit)	ca, cu, pr, ep	25	0.29	1.50	13.82	-5.9
SIMS91	PS1	WAS752-C@8	Wolverine Mine (Kearsarge Deposit)	ca, cu, pr, ep	25	0.28	1.50	14.02	-2.3
SIMS92	PS1	WAS752-C@9	Wolverine Mine (Kearsarge Deposit)	ca, cu, pr, ep	25	0.25	1.50	13.33	-1.6
SIMS93	PS1	WAS752-C@10	Wolverine Mine (Kearsarge Deposit)	ca, cu, pr, ep	25	0.32	1.50	13.57	-3.4
SIMS94	PS1	WAS752-C@11	Wolverine Mine (Kearsarge Deposit)	ca, cu, pr, ep	25	0.33	1.50	13.81	-1.3
SIMS95	PS1	WAS752-C@12	Wolverine Mine (Kearsarge Deposit)	ca, cu, pr, ep	25	0.28	1.50	13.74	-1.8
SIMS96	PS1	WAS752-C@13	Wolverine Mine (Kearsarge Deposit)	ca, cu, pr, ep	25	0.26	1.50	13.59	-3.2
SIMS97	PS1	WAS752-C@14	Wolverine Mine (Kearsarge Deposit)	ca, cu, pr, ep	25	0.29	1.50	13.56	-4.3
SIMS98	PS1	WAS752-C@15	Wolverine Mine (Kearsarge Deposit)	ca, cu, pr, ep	25	0.34	1.50	13.61	-1.8
SIMS99	PS1	WAS752-C@16	Wolverine Mine (Kearsarge Deposit)	ca, cu, pr, ep	25	0.26	1.50	13.56	-1.7
SIMS100	PS1	WAS752-C@17	Wolverine Mine (Kearsarge Deposit)	ca, cu, pr, ep	25	0.28	1.50	13.72	-2.8
SIMS101	PS1	WAS752-C@18	Wolverine Mine (Kearsarge Deposit)	ca, cu, pr, ep	25	0.26	1.50	13.4	-1.6
SIMS102	PS1	WAS752-C@19	Wolverine Mine (Kearsarge Deposit)	ca, cu, pr, ep	25	0.29	1.50	13.97	-1.5
SIMS103	PS1	WAS752-C@20	Wolverine Mine (Kearsarge Deposit)	ca, cu, pr, ep	25	0.32	1.50	13.96	

7 Appendix IV: Assigned Paragenetic Stage and Calculated Stable Isotope Data

Appendix IV contains the calculated mineral stable isotope data in equilibrium with water, the paragenetic stage that is assigned for each sample, and the temperature and analytical error for the calculated values. Each raw value was assigned to a paragenetic stage, main- or late-stage, when possible following the protocol as discussed in the text. For main-stage minerals the assumed temperature of precipitation was based on the temperature zonation map for the Keweenaw Peninsula (Figure 1.6). For late-stage minerals, a constant temperature of precipitation was used as discussed in the text. Raw mineral values were used to calculate the composition of H_2O or CO_2 in equilibrium with the mineral at the time of precipitation using temperature dependency of fractionation as described below.

7.1 Legend for Table

I.D.:
Labeled data source and numbered in order they were compiled:
A1-158 = Livnat (1983) data
B1-112 = Püschner (2001) data
C1-41 = Bornhorst and Woodruff (1997) data
SIMS1-103 = New SIMS collected data

Source:
Secondary assigned ranking to identify which source the data comes from:
PP1 = Püschner (2001), PL1 = Livnat (1983), PS1 = SIMS data from this study, PW1 = Bornhorst and Woodruff (1997)

Sample Number:
Labels assigned from original published data.
Livnat samples are labeled with locations and number: AHM = Ahmeek, ALL= Allouez, ASH= Ashbed, BAL = Baltic, BOH = Bohemia, CCF = Copper City Flow, CHF = Copper Harbor Formation, CEN = Central, CF = Copper Falls, DEL = Delaware, EH = Eagle Harbor, EVR = Evergreen Lode, GRA = Gratoit-Lake, GRN = Greenstone, HC = Hills Creek, HGH = Houghton Conglomerate, IRQ = Iroquois Lode, ISR = Isle-Royale Lode, KRS = Kearsarge, MB = Mt. Bohemia, MH = Mt. Houghton, OJB = Ojibway, PEW = Pewabic Lode, PNX = Phoenix, U = Union, WIN = Winona. SIMS samples are followed by an @ and an increasing number, indicating the order that the order that the analyses were done.

Bornhorst and Woodruff (1997) sample numbers are ###CL# (example: 221CL2). The first three numbers differentiate the samples, the ending number is 1-3, to indicate when there is more than one sample from the same source. So, example number 221CL2, the 2 after CL is saying it is the 2nd of the 221CL# samples.

Püschner (2001) samples are numbered by him to denote different depths of the drill core, each range of depth (###) for a given core are labeled in groups. From increasing depth: the Ahmeek core sample numbers are in groups S10-###, AH8-###, and G7-###; Eagle Harbor core labels are in groups EH04-###, C89-###, and D56-###; and the Copper Harbor core labels are in groups CL14-###, CL11-###, and ST7-###. All sample groups are followed by numbers to denote different samples.

There are three SIMS spot analysis samples: TB-292 is the Quincy mine sample which was a vug-filling calcite crystal, WAS-752 is the Kearsarge Wolverine sample which was associated with prehnite and epidote, and WAS-121 is the Kearsarge Seneca sample which was selected because it was part of a cross-cutting vein closely associated with laumontite. These are followed by an @ and an increasing number, indicating the order that the analyses were done.

Sample Location:
Indicates where in the Keweenaw the data was collected from. Livnat (1983) categorized the location in groups: Baltic Veins, Isle Royale Veins, Ojibway Veins, Lac La Bell Fissures, Kearsarge Arsenide fissures, Mass copper fissures, Shear Veins, Lakeshore Veins, Copper Harbor Cement, and Amygdular/Cementing. Püschner (2001) analyses came from 3 separate drill core locations: Ahmeek, Eagle Harbor, and Copper Harbor. Bornhorst and Woodruff (1997) collected samples within the Kearsarge flow: La Salle, Ahmeek, Centennial, Seneca, North and South Kearsarge, Central, and Mohawk mines. There are three samples that were analyzed using the SIMS method, they are noted as Kearsarge Wolverine, Kearsarge Seneca, and Quincy Mine.

Assigned Paragenetic Stage:
Stages were assigned based on minerals present in the sample. Main-stage and late-stage minerals are indicated in Figure 2.2 (paragenetic diagram). The number 1 represents main-stage in the table, 2 represents late-stage, and the stage is labeled 3 if assignment of the analyses were not possible or unsure.

Confidence of Assigned Paragenetic Stage:
The confidence levels represent the level of confidence in assigning stages to each analysis in order of most to least confident: confident, less confident, and uncertain. Uncertain level of confidence was only used when it was not possible to assign a sample to a paragenetic stage.

Basis of Paragenetic Stage Assignment:
This section lists minerals (by abbreviation) that were used to determine stage, some areas also list details for the samples such as if they are in crosscutting veins. Püschner (2001) only analyzed main-stage minerals for stable isotopes.

Mineral abbreviations are: cc = chalcocite, cp= chalcopyrite, mv = muscovite, ank = ankerite, pp = pumpellyite, Ag = silver, chl = chlorite, cu = copper, hm = hematite, ba =

barite, bn = bornite, ep = epidote, ksp = potassium feldspar, dat = datolite, lm = laumontite, orn = orientite, prl = pyrolusite, fl = fluorite, pr = prehnite, nat = natrolite.

Temp of Precipitation (°C):
This is the inferred temperature of precipitation in Celsius based on the metamorphic zone temperatures in Chapter 1 as indicated in Figure 1.6 or as discussed in the "Metamorphic Mineral Zones/Temperatures" section of chapter 1.

Temp of Precipitation (K):
This is the inferred temperature of precipitation presented as Kelvin.

Temp of Precipitation Error (°C):
This column lists the absolute value of the probable error in the inferred temperature of precipitation as discussed in the text.

Analytical Error Values for Calcite:
An estimate of the analytical error is given. The error for the bulk analyses was assumed to be 0.20‰ as stated by Actlabs (Activation Laboratories, LTD. 41 Bittern Street Ancaster, Ontario, Canada L9G 4V5, https://actlabs.com). For SIMS spot analysis data, values were recorded for each analysis.

"Error ‰ $\delta^{18}O_{H2O}$ ca":
The analytical error of $\delta^{18}O_{H2O}$ for calcite, given in per mil (*‰).*

"Error ‰ $\delta^{13}C_{CO2}$ ca":
The analytical error of $\delta^{13}C_{CO2}$ for calcite, given in per mil (*‰).*

Raw Mineral Data in ‰:
The raw stable isotope data for each sample is given here as well as in Appendix II and III in per mil. The abbreviations are as follows:
$\delta^{18}O_{ca}$ are calcite oxygen stable isotope data, $\delta^{13}C_{ca}$ are calcite carbon stable isotope data, $\delta^{18}O_{qz}$ are quartz oxygen stable isotope data, $\delta^{18}O_{chl/cln}$ are chlorite/clinochlore oxygen stable isotope data, $\delta D_{chl/cln}$ are chlorite/clinochlore hydrogen stable isotope data, δD_{epi} are epidote hydrogen stable isotope data, and δD_{pmp} are pumpellyite hydrogen stable isotope data.

Calculated Isotopic Composition of H_2O or CO_2:
This section includes the calculated isotopic composition of H_2O or CO2 using the raw mineral data. For each mineral, the raw stable isotope values and temperature of precipitation are used in fractionation equations to determine the isotopic composition of H_2O or CO_2 ($\delta^{18}O_{H2O}$, $\delta^{13}C_{CO2}$, and δD_{H2O}) The fractionation equations are given below; all temperatures are in degrees K:

The header "$\delta^{18}O_{H2O}$ ca" uses the water fractionation equation for calcite as discussed by O'Neil et al. (1969) and later corrected in Friedman and O'Neil (1977):

($\delta^{18}O_{H2O}$‰) = (δ^{18}O‰ of calcite) – ((2.78*10^6)/T^2)) + 2.89

The header "$\delta^{18}O_{H2O}$ qz" uses the water fractionation equation for quartz discussed by White (2013):

($\delta^{18}O_{H2O}$‰) = (δ^{18}O‰ of quartz) – ((1.63*10^6)/T^2)) + 5.44

The header "$\delta^{18}O_{H2O}$ chl/cln" uses the water fractionation equation for chlorite and clinochlore as discussed by Clayton et al. (1972):

($\delta^{18}O_{H2O}$‰) = (δ^{18}O‰ of chlorite) – ((3.38*10^6)/T^2)) + 3.4

The header "$\delta^{13}C_{CO2}$ ca" uses the carbon dioxide fractionation equation for calcite discussed by Sheele and Hoefs (1992):

($\delta^{13}C_{CO2}$‰) = (δ^{13}C‰ of calcite) –((3.46*10^6)/T^2)) + ((9.58 *10^3)/T)-2.72

δD_{H2O} chl/cln was calculated using the following approach: Graham and Harmon (1987) "Figure 3" shows ranges for the fractionation between chlorite and δD_{H2O} as: 125-150°C = add 17‰, 212.5°C = add 33‰, and 250-275°C = add 38‰.

The header "δD_{H2O} epi" uses the fractionation equation for epidote from Graham et al (1980):

(δD_{H2O}‰) = (δD‰ of Epidote) - (29.2*(10^6/T^2)-138.8)

Livnat proposed that it was appropriate to use the zoisite fractionation equation to calculate δD_{H2O} from pumpellyite raw mineral data. The header "δD_{H2O} pmp" uses the fractionation equation for zoisite from Graham et al. (1980):

(δD_{H2O}‰) = (δD‰ of Pumpellyite) - (-15.07*(10^6/T^2)-27.73)

Calculated Isotopic Composition of H_2O and CO_2 for Maximum and Minimum Analytical Error:

This section shows the calculated water or carbon dioxide composition when analytical error is added or subtracted from the raw mineral value. The subtracted and added values are presented in this section with the following headers:

Error + $\delta^{18}O_{H2O}$ ca, Error - $\delta^{18}O_{H2O}$ ca, Error + $\delta^{13}C_{CO2}$ ca, Error - $\delta^{13}C_{CO2}$ ca. These sections are showing the calculated error when you add (+) or subtract (-) the "Analytical Error Values for Calcite" from the calculated calcite stable isotope $\delta^{18}O_{H2O}$ and $\delta^{13}C_{CO2}$ data.

Calculated Isotopic Composition of H2O and CO2 for Expected Maximum and Minimum Temperature of Precipitation:

The calculated isotopic composition of water or carbon dioxide is reliant on the temperature of precipitation. Each inferred temperature of precipitation is based on mapping of mineral assemblages with precipitation within a range of temperatures which is termed the temperature of precipitation error. This section calculates the isotopic compositions in ‰ of H_2O or CO_2 by adding or subtracting the temperature of precipitation error from the temperature of precipitation in the fractionation equations given above. These ‰ values can be directly compared to the Calculated Isotopic Composition of H_2O or CO_2 ‰ values. This calculated temperature of precipitation error for each mineral is as follows:

"Temp + $\delta^{18}O_{H2O}$ ca" and "Temp - $\delta^{18}O_{H2O}$ ca" are for the calcite oxygen stable isotope data.

"Temp + $\delta^{13}C_{CO2}$ ca" and "Temp - $\delta^{13}C_{CO2}$ ca" for the calcite carbon stable isotope data.

"Temp + $\delta^{18}O_{H2O}$ qz" and "Temp - $\delta^{18}O_{H2O}$ qz" are for the quartz oxygen stable isotope data.

"Temp + $\delta^{18}O_{H2O}$ chl/cln" and "Temp - $\delta^{18}O_{H2O}$ chl/cln" are for the chlorite/clinochlore oxygen stable isotope data.

"Temp + δD_{H2O} chl/cln" and "Temp - δD_{H2O} chl/cln" are for the chlorite/clinochlore hydrogen stable isotope data.

"Temp + δD_{H2O} epi" and "Temp - δD_{H2O} epi" are for the epidote hydrogen stable isotope data.

"Temp + δD_{H2O} pmp" and "Temp - δD_{H2O} pmp" are for the pumpellyite hydrogen stable isotope data.

I.D.	Source	Sample Number	Sample Location	Assigned Paragenetic Stage	Confidence of Assigned Paragenetic Stage	Basis of Paragenetic Stage Assignment	Temp of Precipitation (°C)	Temp of Precipitation (K)	Temp of Precipitation Error (°C)
A1	PL1	BAL-6	Baltic Veins	2	less confident	cc, veins crosscut main-stage	125.00	398.15	25
A2	PL1	BAL-7	Baltic Veins	2	uncertain	cc,mv,ank,pp, veins crosscut main-stage	125.00	398.15	25
A3	PL1	BAL-8	Baltic Veins	2	uncertain	qz,cc,Ag, veins crosscut main-stage	125.00	398.15	25
A4	PL1	BAL-10	Baltic Veins	2	uncertain	veins crosscut main-stage	125.00	398.15	25
A5	PL1	BAL-11	Baltic Veins	2	uncertain	chl,cc,Cu, veins crosscut main-stage	125.00	398.15	25
A6	PL1	BAL-11(2)	Baltic Veins	2	uncertain	veins crosscut main-stage	125.00	398.15	25
A7	PL1	BAL-12	Baltic Veins	2	uncertain	veins crosscut main-stage	125.00	398.15	25
A8	PL1	BAL-14	Baltic Veins	2	uncertain	cc,Cu, veins crosscut main-stage	125.00	398.15	25
A9	PL1	BAL-22	Baltic Veins	2	uncertain	Cu, veins crosscut main-stage	125.00	398.15	25
A10	PL1	BAL-23	Baltic Veins	2	uncertain	cc,Cu,veins crosscut main-stage	125.00	398.15	25
A11	PL1	BAL25	Baltic Veins	2	uncertain	Cu,veins crosscut main-stage	125.00	398.15	25
A12	PL1	BAL-26	Baltic Veins	2	uncertain	chl,cc,Cu,veins crosscut main-stage	125.00	398.15	25
A13	PL1	BAL-27	Baltic Veins	2	uncertain	chl,cc,veins crosscut main-stage	125.00	398.15	25
A14	PL1	ISR-2	Isle Royale Veins	2	less confident	pp,ba,veins crosscut main-stage	125.00	398.15	25
A15	PL1	ISR-4	Isle Royale Veins	2	uncertain	pp,ba,veins crosscut main-stage	125.00	398.15	25
A16	PL1	ISR-4A	Isle Royale Veins	2	less confident	ank,mv,chl,cc,veins crosscut main-stage	125.00	398.15	25
A17	PL1	ISR-5	Isle Royale Veins	2	less confident	ba,veins crosscut main-stage	125.00	398.15	25
A18	PL1	ISR-21	Isle Royale Veins	2	less confident	ank,chl,cc,veins crosscut main-stage	125.00	398.15	25
A19	PL1	OJB-11,1812	Ojibway Veins	1	less confident	pp	212.50	485.65	37.5
A20	PL1	BOH-12	Lac La belle Fissure	3	uncertain	chl,mv,cc,cp	125.00	398.15	25
A21	PL1	BOH-14	Lac La belle Fissure	3	uncertain	ca(E)	125.00	398.15	25
A22	PL1	BOH-14(2)?	Lac La belle Fissure	3	uncertain	ca(L)	125.00	398.15	25
A23	PL1	BOH-17	Lac La belle Fissure	3	uncertain	chl,ksp,cc,cp	125.00	398.15	25
A24	PL1	BOH-19	Lac La belle Fissure	3	uncertain	mv,cc	125.00	398.15	25
A25	PL1	CEN-105,1374	Lac La belle Fissure	3	uncertain	qz	125.00	398.15	25
A26	PL1	DEL-109,343	Lac La belle Fissure	3	uncertain	ep,chl,cc,cp	125.00	398.15	25
A27	PL1	DEL-109,554	Lac La belle Fissure	3	uncertain	chl	125.00	398.15	25
A28	PL1	MB-810,144	Lac La belle Fissure	2	less confident	chl,cc,cp	125.00	398.15	25
A29	PL1	AHM-UG-4,409	Kearsarge Arsenide fissures	2	less confident	ep,qz	125.00	398.15	25
A30	PL1	KRS-69	Kearsarge Arsenide fissures	2	confident	ank,ksp,Cu	125.00	398.15	25
A31	PL1	KRS-71	Kearsarge Arsenide fissures	2	confident	ank,chl,copper arsenides	125.00	398.15	25
A32	PL1	KRS-108	Kearsarge Arsenide fissures	2	confident	Cu,copper arsenides	125.00	398.15	25
A33	PL1	KRS-109	Kearsarge Arsenide fissures	2	confident	copper arsenides	125.00	398.15	25
A34	PL1	AHM-21,333.5	Mass copper fissures	2	confident	ep,mv,cc,Cu	125.00	398.15	25
A35	PL1	AHM-UG-4,1847	Mass copper fissures	1	confident	ep,pp,ksp	275.00	548.15	25
A36	PL1	ASH-11	Mass copper fissures	1	confident	pr,dat,chl,Cu	212.50	485.65	37.5
A37	PL1	EVR-31	Mass copper fissures	1	confident	Ag,Cu	212.50	485.65	37.5
A38	PL1	KRS-58	Mass copper fissures	1	confident	pr,Cu	250.00	523.15	25
A39	PL1	PEW-6	Mass copper fissures	1	confident	Cu	212.50	485.65	37.5
A40	PL1	Pew-6(2)?	Mass copper fissures	1	confident	chl, Cu, mv	212.50	485.65	37.5
A41	PL1	PNX-UG-2,1321	Mass copper fissures	1	confident	ep,chl,Cu	212.50	485.65	37.5
A42	PL1	CEN-105,174	Shear veins	2	confident	lm,veins crosscut main-stage	125.00	398.15	25
A43	PL1	CEN-105,337	Shear veins	2	uncertain	veins crosscut main-stage	125.00	398.15	25
A44	PL1	CEN-105,744	Shear veins	2	confident	veins crosscut main-stage	125.00	398.15	25
A45	PL1	CEN-105,888	Shear veins	2	confident	hm,chl,veins crosscut main-stage	125.00	398.15	25
A46	PL1	CEN-105,1201	Shear veins	2	confident	lm,chl,veins crosscut main-stage	125.00	398.15	25
A47	PL1	CEN-105,1292	Shear veins	2	confident	veins crosscut main-stage	125.00	398.15	25
A48	PL1	CEN-105,1528	Shear veins	2	confident	lm,veins crosscut main-stage	125.00	398.15	25
A49	PL1	DEL-109,204	Shear veins	2	confident	lm,veins crosscut main-stage	125.00	398.15	25
A50	PL1	DEL-109,814	Shear veins	2	confident	lm,veins crosscut main-stage	125.00	398.15	25
A51	PL1	DEL-109,1702	Shear veins	2	confident	lm,veins crosscut main-stage	125.00	398.15	25
A52	PL1	HC-1,186	Shear veins	2	confident	lm,veins crosscut main-stage	125.00	398.15	25
A53	PL1	MM-4,573	Shear veins	2	uncertain	veins crosscut main-stage	125.00	398.15	25
A54	PL1	U-16,3252.5	Shear veins	2	confident	pr,chl,cp,veins crosscut main-stage	125.00	398.15	25
A55	PL1	CHF-4	Lakeshore Veins	3	uncertain	cc	150.00	423.15	25
A56	PL1	CHF-11	Lakeshore Veins	3	uncertain	ba,cc	150.00	423.15	25
A57	PL1	CHF-11(2)	Lakeshore Veins	3	uncertain	ba,cc	150.00	423.15	25
A58	PL1	CHF-18	Lakeshore Veins	3	uncertain	fl	150.00	423.15	25
A59	PL1	CHF-22A	Lakeshore Veins	3	uncertain	lm	150.00	423.15	25
A60	PL1	CHF-27	Lakeshore Veins	3	uncertain		150.00	423.15	25
A61	PL1	CHF-28	Lakeshore Veins	3	uncertain	orn,prl	150.00	423.15	25
A62	PL1	AHM UG-4,1800	Amygdular/Cementing	1	less confident	cu	275.00	548.15	25
A63	PL1	ASH-2	Amygdular/Cementing	1	uncertain	chl, pp	212.50	485.65	37.5
A64	PL1	ASH-7	Amygdular/Cementing	1	uncertain	chl, Cu, pr	212.50	485.65	37.5
A65	PL1	ASH7(11)	Amygdular/Cementing	1	uncertain	chl, Cu, pr	212.50	485.65	37.5
A66	PL1	ASH-17	Amygdular/Cementing	1	uncertain	Cu, ksp, mv, pp	212.50	485.65	37.5
A67	PL1	ASH-21	Amygdular/Cementing	1	uncertain	Cu, lm, mv, pr	212.50	485.65	37.5
A68	PL1	ASH-25	Amygdular/Cementing	1	uncertain	samples from same area are main	212.50	485.65	37.5
A69	PL1	ASH-25	Amygdular/Cementing	1	uncertain	mv	212.50	485.65	37.5
A70	PL1	BOH-7	Amygdular/Cementing	1	confident	Cu	212.50	485.65	37.5
A71	PL1	CCF-5	Amygdular	1	confident	Cu, pp, pr	275.00	548.15	25
A72	PL1	CEN-105,250/6	Amygdular/Cementing	1	confident	chl,Cu,ep, pr	275.00	548.15	25
A73	PL1	CEN-105, 661	Amygdular	1	confident	chl, ep, lm, mv, pp	275.00	548.15	25
A74	PL1	CEN-105, 990	Amygdular	1	confident	chl, ep, pp	275.00	548.15	25
A75	PL1	CEN-105, 1093	Amygdular	1	confident	chl, ep	275.00	548.15	25
A76	PL1	CEN-105,1096	Amygdular	1	confident	chl, ep, ksp	275.00	548.15	25
A77	PL1	CF-1,787	Amygdular	1	confident	pp, pr	212.50	485.65	37.5
A78	PL1	CHF-9	Copper Harbor cement	3	uncertain	Cu	150.00	423.15	25
A79	PL1	CHF-20A	Copper Harbor cement	3	uncertain	chl	150.00	423.15	25
A80	PL1	CHF-20B	Copper Harbor cement	3	uncertain		150.00	423.15	25
A81	PL1	CHF-21A	Copper Harbor cement	3	uncertain	lm	150.00	423.15	25
A82	PL1	CHF-22B	Copper Harbor cement	3	uncertain		150.00	423.15	25
A83	PL1	CHF-29	Copper Harbor cement	3	uncertain		150.00	423.15	25
A84	PL1	DEL-109,20	Amygdular	1	confident	ep	212.50	485.65	37.5
A85	PL1	DEL-109,63	Amygdular	1	confident	chl, ep, ksp, pr	212.50	485.65	37.5
A86	PL1	DEL-109,911	Amygdular	1	confident	Cu, ep, pp	212.50	485.65	37.5
A87	PL1	DEL-109,914	Amygdular	1	confident	chl, ksp	212.50	485.65	37.5
A88	PL1	DEL-109,1079	Amygdular	1	confident	ep	212.50	485.65	37.5
A89	PL1	DEL-109,1157	Amygdular	1	confident	chl	212.50	485.65	37.5
A90	PL1	GRN-3	Amygdular/Cementing	3	uncertain		212.50	485.65	37.5
A91	PL1	HC-1,80	Amygdular	1	confident	Cu, lm	212.50	485.65	37.5
A92	PL1	HC-1,286	Amygdular	1	confident	lm	212.50	485.65	37.5
A93	PL1	HC-1,1214	Amygdular	1	confident	cu, lm	212.50	485.65	37.5
A94	PL1	HC-1,1229	Amygdular	1	confident	ep, lm, mv, pp, pr	212.50	485.65	37.5
A95	PL1	HC-1,1725	Amygdular	1	confident	chl, Cu, pp, pr,	212.50	485.65	37.5
A96	PL1	HC-1,3227	Amygdular	1	confident	Cu, pr	212.50	485.65	37.5
A97	PL1	HC-1,4236	Amygdular	1	confident	Cu, ep, lm, pp	212.50	485.65	37.5
A98	PL1	HC-1,4401	Amygdular	1	confident	samples from same area are main	212.50	485.65	37.5
A99	PL1	HC-1,4492	Amygdular	1	confident	Cu, ep, mv	212.50	485.65	37.5

I.D.	Analytical Error Values for Calcite: Error ‰ $\delta^{18}O_{H2O}$ ca	Error ‰ $\delta^{13}C_{CO2}$ ca	Raw Mineral Data in ‰: Raw $\delta^{18}O_{ca}$	Raw $\delta^{13}C_{ca}$	Raw $\delta^{18}O_{qz}$	Raw $\delta^{18}O_{chl/cln}$	Raw $\delta D_{chl/cln}$	Raw δD_{epi}	Raw δD_{pmp}	Calculated Isotopic Composition of H_2O or CO_2: $\delta^{18}O_{H2O}$ ca	$\delta^{18}O_{H2O}$ qz	$\delta^{18}O_{H2O}$ chl/cln	$\delta^{13}C_{CO2}$ ca	δD_{H2O} chl/cln	δD_{H2O} epi	δD_{H2O} pmp
A1					17.20						-0.72					
A2	0.20	0.20	17	-2.2						2.35			-2.69			
A3	0.20	0.20	14.3	-0.7	17.70					-0.35	-0.22		-1.19			
A4	0.20	0.20	13.8	-3.1						-0.85			-3.59			
A5	0.20	0.20	16.8	-2.2	17.60					2.15	-0.32		-2.69			
A6	0.20	0.20	22.7	-3.4						8.05			-3.89			
A7	0.20	0.20	18	-2.7						3.35			-3.19			
A8	0.20	0.20	14.80	-2.5						0.15			-2.99			
A9	0.20	0.20	16.8	-2.4						2.15			-2.89			
A10	0.20	0.20	13.7	-3						-0.95			-3.49			
A11	0.20	0.20	14.4	-3.3						-0.25			-3.79			
A12	0.20	0.20	13.7	-2.4		8.00				-0.95		2.86	-2.89			
A13	0.20	0.20	14.7	-2.6						0.05			-3.09			
A14					17.80						-0.12					
A15	0.20	0.20	15.1	-1.6						0.45			-2.09			
A16					17.20						-0.72					
A17					17.10						-0.82					
A18					16.80						-1.12					
A19					17.10						6.17					
A20	0.20	0.20	14	-1.9	14.80	7.20				-0.65	-3.12	2.06	-2.39			
A21	0.20	0.20	15.3	-2.1						0.65			-2.59			
A22	0.20	0.20	23.5	-2.2						8.85			-2.69			
A23	0.20	0.20	14.6	-2.8						-0.05			-3.29	cal		
A24	0.20	0.20	12.4	-3.1						-2.25			-3.59			
A25	0.20	0.20	14.3	-6.8						-0.35			-7.29			
A26	0.20	0.20	17.3	-1.2						2.65			-1.69			
A27	0.20	0.20	14.5	-2.8						-0.15			-3.29			
A28						6.90						1.76				
A29					9.70						-8.22					
A30	0.20	0.20	15.3	-3.9						0.65			-4.39			
A31	0.20	0.20	13.6	-3.5						-1.05			-3.99			
A32					16.90						-1.02					
A33	0.20	0.20	10.3	-2.8						-4.35			-3.29			
A34	0.20	0.20	12.7	-3.1						-1.95			-3.59			
A35	0.20	0.20	11.5	-3.7	12.80					5.14	4.95		-0.46			
A36						8.90						6.99				
A37	0.20	0.20	12.9	-4						4.00			-1.66			
A38																
A39	0.20	0.20	21.8	-2.3						12.90			0.04			
A40	0.20	0.20	19.4	-2.3						10.50			0.04			
A41					8.6						-2.33		2.34			
A42	0.20	0.20	14.7	-6.2						0.05			-6.69			
A43	0.20	0.20	16.1	-11.8						1.45			-12.29			
A44	0.20	0.20	12.5	-1.9						-2.15			-2.39			
A45						13.10						7.96				
A46						6.10						0.96				
A47			15.2	-1.1						0.55			-1.59			
A48	0.20	0.20	13.8	-9.8						-0.85			-10.29			
A49	0.20	0.20	18.1	-4						3.45			-4.49			
A50	0.20	0.20	15	-3.9						0.35			-4.39			
A51	0.20	0.20	20.6	-2						5.95			-2.49			
A52	0.20	0.20	22.2	-0.5						7.55			-0.99			
A53	0.20	0.20	6	-5.5						-8.65			-5.99			
A54						5.90						0.76				
A55	0.20	0.20	17.8	-2.5						5.16			-1.90			
A56	0.20	0.20	22.4	-3.2						9.76			-2.60			
A57	0.20	0.20	13.2	-3.4						0.56			-2.80			
A58	0.20	0.20	18.5	-1.5						5.86			-0.90			
A59	0.20	0.20	14.2	-3.4						1.56			-2.80			
A60	0.20	0.20	23.1	-2.5						10.46			-1.90			
A61	0.20	0.20	20.7	-2.7						8.06			-2.10			
A62	0.20	0.20	18.5	-5.5					-75	12.14			-2.26			2.89
A63	0.20	0.20	15.6	-3						6.70			-0.66			
A64	0.20	0.20	15.1	-3						6.20			-0.66			
A65	0.20	0.20	15.4	-3						6.50			-0.66			
A66	0.20	0.20	15	-2.7						6.10			-0.36			
A67	0.20	0.20	21.5	-1.9						12.60			0.44			
A68	0.20	0.20	12.6	-3.7						3.70			-1.36			
A69	0.20	0.20	20.6	-2.8						11.70			-0.46			
A70	0.20	0.20	14.9	-3.1						6.00			-0.76			
A71	0.20	0.20	17.7	-3.2						11.34			0.04			
A72	0.20	0.20	11.2	-1.7						4.84			1.54			
A73	0.20	0.20	13	-4.9					-69	6.64			-1.66			8.89
A74	0.20	0.20	18	-2.9						11.64			0.34			
A75	0.20	0.20	12.2	-2.6						5.84			0.64			
A76	0.20	0.20	14.5	-1.9						8.14			1.34			
A77	0.20	0.20	17.2	-4.3						8.30			-1.96			
A78	0.20	0.20	20.7	-4.6						8.06			-4.00			
A79	0.20	0.20	23.2	-1.7						10.56			-1.10			
A80	0.20	0.20	21	-2.1						8.36			-1.50			
A81	0.20	0.20	22	-2.8						9.36			-2.20			
A82	0.20	0.20	21	-1.6						8.36			-1.00			
A83	0.20	0.20	22	-2.3						9.36			-1.70			
A84	0.20	0.20	12	-3.5						3.10			-1.16			
A85	0.20	0.20	15.5	-2.4						6.60			-0.06			
A86	0.20	0.20	13.1	-3.2						4.20			-0.86			
A87	0.20	0.20	16.9	-3.1						8.00			-0.76			
A88	0.20	0.20	13.5	-2.5						4.60			-0.16			
A89	0.20	0.20	14	-2.8						5.10			-0.46			
A90	0.20	0.20	21	-13.4						12.10			-11.06			
A91	0.20	0.20	21.2	-2						12.30			0.34			
A92	0.20	0.20	21.8	-2.1						12.90			0.24			
A93	0.20	0.20	19.7	-3						10.80			-0.66			
A94	0.20	0.20	20.3	-2.9						11.40			-0.56			
A95	0.20	0.20	20.1	-3.7					-75	11.20			-1.36			16.62
A96	0.20	0.20	16.2	-3.7						7.30			-1.36			
A97	0.20	0.20	17.9	-2.6						9.00			-0.26			
A98	0.20	0.20	18	-3.1						9.10			-0.76			
A99	0.20	0.20	19.9	-3.1						11.00			-0.76			

I.D.	Calculated Isotopic Composition of H_2O and CO_2 for Maximum and Minimum Analytical Error: Error + $\delta^{18}O_{H2O}$ ca	Error - $\delta^{18}O_{H2O}$ ca	Error + $\delta^{13}C_{CO2}$ ca	Error - $\delta^{13}C_{CO2}$ ca	Calculated Isotopic Composition of H2O and CO2 for Expected Maximum and Minimum Temperature of Precipitation: Temp + $\delta^{18}O_{H2O}$ ca	Temp - $\delta^{18}O_{H2O}$ ca	Temp + $\delta^{13}C_{CO2}$ ca	Temp - $\delta^{13}C_{CO2}$ ca	Temp + $\delta^{18}O_{H2O}$ qz	Temp - $\delta^{18}O_{H2O}$ qz	Temp + $\delta^{18}O_{H2O}$ chl/cln	Temp - $\delta^{18}O_{H2O}$ chl/cln	Temp + δD_{H2O} chl/cln	Temp - δD_{H2O} chl/cln	Temp + δD_{H2O} epi	Temp - δD_{H2O} epi	Temp + δD_{H2O} pmp	Temp - δD_{H2O} pmp
A1									1.72	-3.67								
A2	2.55	2.15	-2.49	-2.89	4.36	-0.08	-1.60	-4.10										
A3	-0.15	-0.55	-0.99	-1.39	1.66	-2.78	-0.10	-2.60	2.22	-3.17								
A4	-0.65	-1.05	-3.39	-3.79	1.16	-3.28	-2.50	-5.00										
A5	2.35	1.95	-2.49	-2.89	4.16	-0.28	-1.60	-4.10	2.12	-3.27								
A6	8.25	7.85	-3.69	-4.09	10.06	5.62	-2.80	-5.30										
A7	3.55	3.15	-2.99	-3.39	5.36	0.92	-2.10	-4.60										
A8	0.35	-0.05	-2.79	-3.19	2.16	-2.28	-1.90	-4.40										
A9	2.35	1.95	-2.69	-3.09	4.16	-0.28	-1.80	-4.30										
A10	-0.75	-1.15	-3.29	-3.69	1.06	-3.38	-2.40	-4.90										
A11	-0.05	-0.45	-3.59	-3.99	1.76	-2.68	-2.70	-5.20										
A12	-0.75	-1.15	-2.69	-3.09	1.06	-3.38	-1.80	-4.30			3.99	1.50						
A13	0.25	-0.15	-2.89	-3.29	2.06	-2.38	-2.00	-4.50										
A14									2.32	-3.07								
A15	0.65	0.25	-1.89	-2.29	2.46	-1.98	-1.00	-3.50										
A16									1.72	-3.67								
A17									1.62	-3.77								
A18									1.32	-4.07								
A19									8.15	3.67								
A20	-0.45	-0.85	-2.19	-2.59	1.36	-3.08	-1.30	-3.80	-0.68	-6.07	3.19	0.70						
A21	0.85	0.45	-2.39	-2.79	2.66	-1.78	-1.50	-4.00										
A22	9.05	8.65	-2.49	-2.89	10.86	6.42	-1.60	-4.10										
A23	0.15	-0.25	-3.09	-3.49	1.96	-2.48	-2.20	-4.70										
A24	-2.05	-2.45	-3.39	-3.79	-0.24	-4.68	-2.50	-5.00										
A25	-0.15	-0.55	-7.09	-7.49	1.66	-2.78	-6.20	-8.70										
A26	2.85	2.45	-1.49	-1.89	4.66	0.22	-0.60	-3.10										
A27	0.05	-0.35	-3.09	-3.49	1.86	-2.58	-2.20	-4.70										
A28											2.89	0.40						
A29									-5.78	-11.17								
A30	0.85	0.45	-4.19	-4.59	2.66	-1.78	-3.30	-5.80										
A31	-0.85	-1.25	-3.79	-4.19	0.96	-3.48	-2.90	-5.40										
A32									1.42	-3.97								
A33	-4.15	-4.55	-3.09	-3.49	-2.34	-6.78	-2.20	-4.70										
A34	-1.75	-2.15	-3.39	-3.79	0.06	-4.38	-2.50	-5.00										
A35	5.34	4.94	-0.26	-0.66	5.93	4.23	-0.24	-0.75	5.91	3.85								
A36											7.90	5.83						
A37	4.20	3.80	-1.46	-1.86	5.63	1.95	-1.05	-2.57										
A38																		
A39	13.10	12.70	0.24	-0.16	14.53	10.85	0.65	-0.87										
A40	10.70	10.30	0.24	-0.16	12.13	8.45	0.65	-0.87										
A41									-0.35	-4.83								
A42	0.25	-0.15	-6.49	-6.89	2.06	-2.38	-5.60	-8.10										
A43	1.65	1.25	-12.09	-12.49	3.46	-0.98	-11.20	-13.70										
A44	-1.95	-2.35	-2.19	-2.59	-0.14	-4.58	-1.30	-3.80										
A45											9.09	6.60						
A46											2.09	-0.40						
A47																		
A48	-0.65	-1.05	-10.09	-10.49	1.16	-3.28	-9.20	-11.70										
A49	3.65	3.25	-4.29	-4.69	5.46	1.02	-3.40	-5.90										
A50	0.55	0.15	-4.19	-4.59	2.36	-2.08	-3.30	-5.80										
A51	6.15	5.75	-2.29	-2.69	7.96	3.52	-1.40	-3.90										
A52	7.75	7.35	-0.79	-1.19	9.56	5.12	0.10	-2.40										
A53	-8.45	-8.85	-5.79	-6.19	-6.64	-11.08	-4.90	-7.40										
A54											1.89	-0.60						
A55	5.36	4.96	-1.70	-2.10	6.85	3.15	-1.07	-2.99										
A56	9.96	9.56	-2.40	-2.80	11.45	7.75	-1.77	-3.69										
A57	0.76	0.36	-2.60	-3.00	2.25	-1.45	-1.97	-3.89										
A58	6.06	5.66	-0.70	-1.10	7.55	3.85	-0.07	-1.99										
A59	1.76	1.36	-2.60	-3.00	3.25	-0.45	-1.97	-3.89										
A60	10.66	10.26	-1.70	-2.10	12.15	8.45	-1.07	-2.99										
A61	8.26	7.86	-1.90	-2.30	9.75	6.05	-1.27	-3.19										
A62	12.34	11.94	-2.06	-2.46	12.93	11.23	-2.04	-2.55									-1.39	7.79
A63	6.90	6.50	-0.46	-0.86	8.33	4.65	-0.05	-1.57										
A64	6.40	6.00	-0.46	-0.86	7.83	4.15	-0.05	-1.57										
A65	6.70	6.30	-0.46	-0.86	8.13	4.45	-0.05	-1.57										
A66	6.30	5.90	-0.16	-0.56	7.73	4.05	0.25	-1.27										
A67	12.80	12.40	0.64	0.24	14.23	10.55	1.05	-0.47										
A68	3.90	3.50	-1.16	-1.56	5.33	1.65	-0.75	-2.27										
A69	11.90	11.50	-0.26	-0.66	13.33	9.65	0.15	-1.37										
A70	6.20	5.80	-0.56	-0.96	7.63	3.95	-0.15	-1.67										
A71	11.54	11.14	0.24	-0.16	12.48	9.93	0.35	-0.43										
A72	5.04	4.64	1.74	1.34	5.98	3.43	1.85	1.07										
A73	6.84	6.44	-1.46	-1.86	7.43	5.73	-1.44	-1.95									4.61	13.79
A74	11.84	11.44	0.54	0.14	12.43	10.73	0.56	0.05										
A75	6.04	5.64	0.84	0.44	6.63	4.93	0.86	0.35										
A76	8.34	7.94	1.54	1.14	8.93	7.23	1.56	1.05										
A77	8.50	8.10	-1.76	-2.16	9.93	6.25	-1.35	-2.87										
A78	8.26	7.86	-3.80	-4.20	9.75	6.05	-3.17	-5.09										
A79	10.76	10.36	-0.90	-1.30	12.25	8.55	-0.27	-2.19										
A80	8.56	8.16	-1.30	-1.70	10.05	6.35	-0.67	-2.59										
A81	9.56	9.16	-2.00	-2.40	11.05	7.35	-1.37	-3.29										
A82	8.56	8.16	-0.80	-1.20	10.05	6.35	-0.17	-2.09										
A83	9.56	9.16	-1.50	-1.90	11.05	7.35	-0.87	-2.79										
A84	3.30	2.90	-0.96	-1.36	4.73	1.05	-0.55	-2.07										
A85	6.80	6.40	0.14	-0.26	8.23	4.55	0.55	-0.97										
A86	4.40	4.00	-0.66	-1.06	5.83	2.15	-0.25	-1.77										
A87	8.20	7.80	-0.56	-0.96	9.63	5.95	-0.15	-1.67										
A88	4.80	4.40	0.04	-0.36	6.23	2.55	0.45	-1.07										
A89	5.30	4.90	-0.26	-0.66	6.73	3.05	0.15	-1.37										
A90	12.30	11.90	-10.86	-11.26	13.73	10.05	-10.45	-11.97										
A91	12.50	12.10	0.54	0.14	13.93	10.25	0.95	-0.57										
A92	13.10	12.70	0.44	0.04	14.53	10.85	0.85	-0.67										
A93	11.00	10.60	-0.46	-0.86	12.43	8.75	-0.05	-1.57										
A94	11.60	11.20	-0.36	-0.76	13.03	9.35	0.05	-1.47										
A95	11.40	11.00	-1.16	-1.56	12.83	9.15	-0.75	-2.27									7.79	27.77
A96	7.50	7.10	-1.16	-1.56	8.93	5.25	-0.75	-2.27										
A97	9.20	8.80	-0.06	-0.46	10.63	6.95	0.35	-1.17										
A98	9.30	8.90	-0.56	-0.96	10.73	7.05	-0.15	-1.67										
A99	11.20	10.80	-0.56	-0.96	12.63	8.95	-0.15	-1.67										

										Analytical Error Values for Calcite		Raw Mineral Data in ‰							Calculated Isotopic Composition of H_2O or CO_2							Calculated Isotopic Composition of H_2O and CO_2 for Maximum and Minimum Analytical Error				Calculated Isotopic Composition of H2O and CO2 for Expected Maximum and Minimum Temperature of Precipitation													
I.D.	Source	Sample Number	Sample Location	Assigned Paragenetic Stage	Confidence of Assigned Paragenetic Stage	Basis of Paragenetic Stage Assignment	Temp of Precipitation (°C)	Temp of Precipitation (K)	Temp of Precipitation Error (°C)	Error ‰ $\delta^{18}O_{H2O}$ ca	Error ‰ $\delta^{13}C_{CO2}$ ca	Raw $\delta^{18}O_{ca}$	Raw $\delta^{13}C_{ca}$	Raw $\delta^{18}O_{qz}$	Raw $\delta^{18}O_{chl/cln}$	Raw $\delta D_{chl/cln}$	Raw δD_{epi}	Raw δD_{pmp}	$\delta^{18}O_{H2O}$ ca	$\delta^{18}O_{H2O}$ qz	$\delta^{18}O_{H2O}$ chl/cln	$\delta^{13}C_{CO2}$ ca	δD_{H2O} chl/cln	δD_{H2O} epi	δD_{H2O} pmp	Error + $\delta^{18}O_{H2O}$ ca	Error - $\delta^{18}O_{H2O}$ ca	Error + $\delta^{13}C_{CO2}$ ca	Error - $\delta^{13}C_{CO2}$ ca	Temp + $\delta^{18}O_{H2O}$ ca	Temp - $\delta^{18}O_{H2O}$ ca	Temp + $\delta^{13}C_{CO2}$ ca	Temp - $\delta^{13}C_{CO2}$ ca	Temp + $\delta^{18}O_{H2O}$ qz	Temp - $\delta^{18}O_{H2O}$ qz	Temp + $\delta^{18}O_{H2O}$ chl/cln	Temp - $\delta^{18}O_{H2O}$ chl/cln	Temp + δD_{H2O} chl/cln	Temp - δD_{H2O} chl/cln	Temp + δD_{H2O} epi	Temp - δD_{H2O} epi	Temp + δD_{H2O} pmp	Temp - δD_{H2O} pmp
B48	PP1	EH02-16V	Eagle Harbor	1	confident	pp,pr,ep,lm traces, paragenesis determined by Püschner	212.50	485.65	37.5						10.70						8.79															9.70	7.63						
B49	PP1	EH04-06V	Eagle Harbor	1	less confident	pp,pr,ep,lm traces, paragenesis determined by Püschner	212.50	485.65	37.5	0.20	0.20	27.9	-4.9						19.00			-2.56				19.20	18.80	-2.36	-2.76	20.63	16.95	-1.95	-3.47										
B50	PP1	EH04-09BB	Eagle Harbor	1	confident	pp,pr,ep,lm traces, paragenesis determined by Püschner	212.50	485.65	37.5						11.50	-51.8					9.59		-18.80													10.50	8.43	-13.80	-18.80				
B51	PP1	EH04-10B	Eagle Harbor	1	confident	pp,pr,ep,lm traces, paragenesis determined by Püschner	212.50	485.65	37.5						9.50						7.59															8.50	6.43						
B52	PP1	EH04-11B	Eagle Harbor	1	confident	pp,pr,ep,lm traces, paragenesis determined by Püschner	212.50	485.65	37.5						9.00						7.09															8.00	5.93						
B53	PP1	EH04-11V	Eagle Harbor	1	confident	pp,pr,ep,lm traces, paragenesis determined by Püschner	212.50	485.65	37.5						12.40						10.49															11.40	9.33						
B54	PP1	EH04-16B	Eagle Harbor	1	confident	pp,pr,ep,lm traces, paragenesis determined by Püschner	212.50	485.65	37.5						10.70						8.79															9.70	7.63						
B55	PP1	EH04-19B	Eagle Harbor	1	less confident	pp,pr,ep,lm traces, paragenesis determined by Püschner	212.50	485.65	37.5	0.20	0.20	25.3	-1.9						16.40			0.44				16.60	16.20	0.64	0.24	18.03	14.35	1.05	-0.47										
B56	PP1	C89-09V	Eagle Harbor	1	less confident	pp,pr,ep,lm traces, paragenesis determined by Püschner	212.50	485.65	37.5	0.20	0.20	25.4	-5.9						16.50			-3.56				16.70	16.30	-3.36	-3.76	18.13	14.45	-2.95	-4.47										
B57	PP1	C89-12ABB	Eagle Harbor	1	confident	pp,pr,ep,lm traces, paragenesis determined by Püschner	212.50	485.65	37.5						18.30						16.39															17.30	15.23						
B58	PP1	C89-15V	Eagle Harbor	1	less confident	pp,pr,ep,lm traces, paragenesis determined by Püschner	212.50	485.65	37.5	0.20	0.20	17.7	-7.1						8.80			-4.76				9.00	8.60	-4.56	-4.96	10.43	6.75	-4.15	-5.67										
B59	PP1	C89-20B	Eagle Harbor	1	confident	pp,pr,ep,lm traces, paragenesis determined by Püschner	212.50	485.65	37.5						10.70	-37					8.79		-4.00													9.70	7.63	1.00	-4.00				
B60	PP1	C89-29V	Eagle Harbor	1	confident	pp,pr,ep,lm traces, paragenesis determined by Püschner	212.50	485.65	37.5					17.40						6.47														8.45	3.97								
B61	PP1	C89-38	Eagle Harbor	1	confident	pp,pr,ep,lm traces, paragenesis determined by Püschner	212.50	485.65	37.5						5.90	-42.9					3.99		-9.90													4.90	2.83	-4.90	-9.90				
B62	PP1	C89-40B	Eagle Harbor	1	confident	pp,pr,ep,lm traces, paragenesis determined by Püschner	212.50	485.65	37.5						7.60	-44.5					5.69		-11.50													6.60	4.53	-6.50	-11.50				
B63	PP1	D56-09BB	Eagle Harbor	1	confident	pp,pr,ep,lm traces, paragenesis determined by Püschner	212.50	485.65	37.5						11.00						9.09															10.00	7.93						
B64	PP1	D56-20V	Eagle Harbor	1	confident	pp,pr,ep,lm traces, paragenesis determined by Püschner	212.50	485.65	37.5						11.00	-65.5					9.09		-32.50													10.00	7.93	-27.50	-32.50				
B65	PP1	D56-20V	Eagle Harbor	1	confident	pp,pr,ep,lm traces, paragenesis determined by Püschner	212.50	485.65	37.5						8.50						6.59															7.50	5.43						
B66	PP1	D56-26V	Eagle Harbor	1	confident	pp,pr,ep,lm traces, paragenesis determined by Püschner	212.50	485.65	37.5					13.80						2.87														4.85	0.37								
B67	PP1	D56-28V	Eagle Harbor	1	confident	pp,pr,ep,lm traces, paragenesis determined by Püschner	212.50	485.65	37.5						5.90						3.99															4.90	2.83						
B68	PP1	D56-29V	Eagle Harbor	1	confident	pp,pr,ep,lm traces, paragenesis determined by Püschner	212.50	485.65	37.5						11.80						9.89															10.80	8.73						
B69	PP1	D56-33V	Eagle Harbor	1	less confident	pp,pr,ep,lm traces, paragenesis determined by Püschner	212.50	485.65	37.5	0.20	0.20	22.1	-3.3						13.20			-0.96				13.40	13.00	-0.76	-1.16	14.83	11.15	-0.35	-1.87										
B70	PP1	D56-34AV	Eagle Harbor	1	less confident	pp,pr,ep,lm traces, paragenesis determined by Püschner	212.50	485.65	37.5	0.20	0.20	23.2	-0.2						14.30			2.14				14.50	14.10	2.34	1.94	15.93	12.25	2.75	1.23										
B71	PP1	D57-07V	Eagle Harbor	1	confident	pp,pr,ep,lm traces, paragenesis determined by Püschner	212.50	485.65	37.5						5.80						3.89															4.80	2.73						
B72	PP1	D57-13VB	Eagle Harbor	1	confident	pp,pr,ep,lm traces, paragenesis determined by Püschner	212.50	485.65	37.5						5.50						3.59															4.50	2.43						
B73	PP1	D57-18BA	Eagle Harbor	1	confident	pp,pr,ep,lm traces, paragenesis determined by Püschner	212.50	485.65	37.5						10.90						8.99															9.90	7.83						
B74	PP1	D57-20V	Eagle Harbor	1	less confident	pp,pr,ep,lm traces, paragenesis determined by Püschner	212.50	485.65	37.5	0.20	0.20	22.2	-2.5						13.30			-0.16				13.50	13.10	0.04	-0.36	14.93	11.25	0.45	-1.07										
B75	PP1	D57-26Vdom	Eagle Harbor	1	confident	pp,pr,ep,lm traces, paragenesis determined by Püschner	212.50	485.65	37.5																																		
B76	PP1	D52-76V	Eagle Harbor	1	confident	pp,pr,ep,lm traces, paragenesis determined by Püschner	212.50	485.65	37.5																																		
B77	PP1	D52-76V	Eagle Harbor	1	confident	pp,pr,ep,lm traces, paragenesis determined by Püschner	212.50	485.65	37.5					13.90						2.97														4.95	0.47								
B78	PP1	D57-28VA	Eagle Harbor	1	less confident	pp,pr,ep,lm traces, paragenesis determined by Püschner	212.50	485.65	37.5	0.20	0.20	22.8	-2.4						13.90			-0.06				14.10	13.70	0.14	-0.26	15.53	11.85	0.55	-0.97										
B79	PP1	D57-28VB	Eagle Harbor	1	less confident	pp,pr,ep,lm traces, paragenesis determined by Püschner	212.50	485.65	37.5	0.20	0.20	21.7	-2.1						12.80			0.24				13.00	12.60	0.44	0.04	14.43	10.75	0.85	-0.67										
B80	PP1	D57-31B	Eagle Harbor	1	confident	pp,pr,ep,lm traces, paragenesis determined by Püschner	212.50	485.65	37.5						5.90						3.99															4.90	2.83						
B81	PP1	D57-41dom	Eagle Harbor	1	confident	pp,pr,ep,lm traces, paragenesis determined by Püschner	212.50	485.65	37.5																																		
B82	PP1	D57-42B	Eagle Harbor	1	confident	pp,pr,ep,lm traces, paragenesis determined by Püschner	150.00	423.15	25						5.50	-59.4					1.49		-42.40													2.43	0.36	-21.40	-26.40				
B83	PP1	CL14-02V	Copper Harbor	1	less confident	pp,pr,ep,lm traces, paragenesis determined by Püschner	150.00	423.15	25	0.20	0.20	28.9	-2						16.26			-1.40				16.46	16.06	-1.20	-1.60	17.95	14.25	-0.57	-2.49										
B84	PP1	CL14-18V	Copper Harbor	1	confident	pp,pr,ep,lm traces, paragenesis determined by Püschner	150.00	423.15	25						13.80						9.79															10.73	8.66						
B85	PP1	CL14-20V	Copper Harbor	1	less confident	pp,pr,ep,lm traces, paragenesis determined by Püschner	150.00	423.15	25	0.20	0.20	23.1	-2.8						10.46			-2.20				10.66	10.26	-2.00	-2.40	12.15	8.45	-1.37	-3.29										
B86	PP1	CL14-22B	Copper Harbor	1	confident	pp,pr,ep,lm traces, paragenesis determined by Püschner	150.00	423.15	25						10.60						6.59															7.53	5.46						
B87	PP1	CL14-23B	Copper Harbor	1	confident	pp,pr,ep,lm traces, paragenesis determined by Püschner	150.00	423.15	25						9.50						5.49															6.43	4.36						
B88	PP1	CL14-25V	Copper Harbor	1	confident	pp,pr,ep,lm traces, paragenesis determined by Püschner	150.00	423.15	25						15.80						11.79															12.73	10.66						
B89	PP1	CL14-28V	Copper Harbor	1	less confident	pp,pr,ep,lm traces, paragenesis determined by Püschner	150.00	423.15	25	0.20	0.20	29.6	-3						16.96			-2.40				17.16	16.76	-2.20	-2.60	18.65	14.95	-1.57	-3.49										
B90	PP1	CL14-30V	Copper Harbor	1	confident	pp,pr,ep,lm traces, paragenesis determined by Püschner	150.00	423.15	25						12.90						8.89															9.83	7.76						
B91	PP1	CL14-32B	Copper Harbor	1	confident	pp,pr,ep,lm traces, paragenesis determined by Püschner	150.00	423.15	25						9.90						5.89															6.83	4.76						
B92	PP1	CL14-45V	Copper Harbor	1	less confident	pp,pr,ep,lm traces, paragenesis determined by Püschner	150.00	423.15	25	0.20	0.20	27.5	-2.9						14.86			-2.30				15.06	14.66	-2.10	-2.50	16.55	12.85	-1.47	-3.39										
B93	PP1	CL14-48V	Copper Harbor	1	less confident	pp,pr,ep,lm traces, paragenesis determined by Püschner	150.00	423.15	25							15.9			-12.64			0.60	32.90			-12.64	-12.64	0.60	0.60									53.90	48.90				
B94	PP1	CL14-63B	Copper Harbor	1	confident	pp,pr,ep,lm traces, paragenesis determined by Püschner	150.00	423.15	25						8.80						4.79															5.73	3.66						
B95	PP1	CL14-72V	Copper Harbor	1	less confident	pp,pr,ep,lm traces, paragenesis determined by Püschner	150.00	423.15	25	0.20	0.20	24.5	-2.3						11.86			-1.70				12.06	11.66	-1.50	-1.90	13.55	9.85	-0.87	-2.79										
B96	PP1	CL14-83V	Copper Harbor	1	confident	pp,pr,ep,lm traces, paragenesis determined by Püschner	150.00	423.15	25						6.40						2.39															3.33	1.26						
B97	PP1	CL14-83V/1	Copper Harbor	1	less confident	pp,pr,ep,lm traces, paragenesis determined by Püschner	150.00	423.15	25	0.20	0.20	23.3	-3.7						10.66			-3.10				10.86	10.46	-2.90	-3.30	12.35	8.65	-2.27	-4.19										
B98	PP1	CL14-83V/2	Copper Harbor	1	less confident	pp,pr,ep,lm traces, paragenesis determined by Püschner	150.00	423.15	25	0.20	0.20	22.9	-3.7						10.26			-3.10				10.46	10.06	-2.90	-3.30	11.95	8.25	-2.27	-4.19										
B99	PP1	CL11-06B	Copper Harbor	1	less confident	pp,pr,ep,lm traces, paragenesis determined by Püschner	150.00	423.15	25	0.20	0.20	28.7	-3.7						16.06			-3.10				16.26	15.86	-2.90	-3.30	17.75	14.05	-2.27	-4.19										
B100	PP1	CL11-10V	Copper Harbor	1	less confident	pp,pr,ep,lm traces, paragenesis determined by Püschner	150.00	423.15	25	0.20	0.20	21.1	-2						8.46			-1.40				8.66	8.26	-1.20	-1.60	10.15	6.45	-0.57	-2.49										
B101	PP1	CL11-12B	Copper Harbor	1	confident	pp,pr,ep,lm traces, paragenesis determined by Püschner	150.00	423.15	25						5.80						1.79															2.73	0.66						
B102	PP1	CL11-25AB	Copper Harbor	1	confident	pp,pr,ep,lm traces, paragenesis determined by Püschner	150.00	423.15	25						9.90						5.89															6.83	4.76						
B103	PP1	CL11-27V	Copper Harbor	1	less confident	pp,pr,ep,lm traces, paragenesis determined by Püschner	150.00	423.15	25	0.20	0.20	24.1	-2.7						11.46			-2.10				11.66	11.26	-1.90	-2.30	13.15	9.45	-1.27	-3.19										
B104	PP1	CL11-31V	Copper Harbor	1	less confident	pp,pr,ep,lm traces, paragenesis determined by Püschner	150.00	423.15	25	0.20	0.20	26	-2.8						13.36			-2.20				13.56	13.16	-2.00	-2.40	15.05	11.35	-1.37	-3.29										
B105	PP1	CL11-35V	Copper Harbor	1	confident	pp,pr,ep,lm traces, paragenesis determined by Püschner	150.00	423.15	25						19.40						15.39															16.33	14.26						
B106	PP1	CL11-38B	Copper Harbor	1	confident	pp,pr,ep,lm traces, paragenesis determined by Püschner	150.00	423.15	25						7.20						3.19															4.13	2.06						
B107	PP1	CL11-48V	Copper Harbor	1	confident	pp,pr,ep,lm traces, paragenesis determined by Püschner	150.00	423.15	25						9.70						5.69															6.63	4.56						
B108	PP1	ST7-07B	Copper Harbor	2	confident	pp,pr,ep,lm traces, paragenesis determined by Püschner	125.00	398.15	25						5.30						0.16															1.29	-1.20						
B109	PP1	ST7-13BE	Copper Harbor	2	confident	pp,pr,ep,lm traces, paragenesis determined by Püschner	125.00	398.15	25						8.70						3.56															4.69	2.20						
B110	PP1	ST720V	Copper Harbor	1	confident	pp,pr,ep,lm traces, paragenesis determined by Püschner	150.00	423.15	25						13.40						9.39															10.33	8.26						
B111	PP1	ST738V	Copper Harbor	1	confident	pp,pr,ep,lm traces, paragenesis determined by Püschner	150.00	423.15	25						6.80						2.79															3.73	1.66						
B112	PP1	ST7-38V	Copper Harbor	1	less confident	pp,pr,ep,lm traces, paragenesis determined by Püschner	150.00	423.15	25	0.20	0.20	19.7	-3.4						7.06			-2.80				7.26	6.86	-2.60	-3.00	8.75	5.05	-1.97	-3.89										
C1	PW1	227CL2	LaSalle #3-4	1	confident	ksp,ep	275.00	548.15	25	0.20	0.20	19.3	-3.04						12.94			0.20				13.14	12.74	0.40	0.00	13.73	12.03	0.42	-0.09										
C2	PW1	218CL1	LaSalle #3-4	1	confident	ksp,ep	275.00	548.15	25	0.20	0.20	15.27	-2.92						8.91			0.32				9.11	8.71	0.52	0.12	9.70	8.00	0.54	0.03										
C3	PW1	228CL2	Centennial #1	1	confident	ep,Cu	275.00	548.15	25	0.20	0.20	13.12	-2.78						6.76			0.46				6.96	6.56	0.66	0.26	7.55	5.85	0.68	0.17										
C4	PW1	214CL3	Centennial #1	1	confident	ep,Cu	275.00	548.15	25	0.20	0.20	12.68	-2.37						6.32			0.87				6.52	6.12	1.07	0.67	7.11	5.41	1.09	0.58										
C5	PW1	214CL2	South Kearsarge #1	1	confident	ep,ca	250.00	523.15	25	0.20	0.20	13.61	-2.89						6.34			0.06				6.54	6.14	0.26	-0.14	7.25	5.30	0.35	-0.32										
C6	PW1	215CL2	South Kearsarge #1	1	confident	ksp,ep,Cu	250.00	523.15	25	0.20	0.20	13.92	-2.28						6.65			0.67				6.85	6.45	0.87	0.47	7.56	5.61	0.96	0.29										
C7	PW1	226CL1	Wolverine #3	1	confident	Cu,ep	250.00	523.15	25	0.20	0.20	14.09	-2.18						6.82			0.77				7.02	6.62	0.97	0.57	7.73	5.78	1.06	0.39										
C8	PW1	219CL1	Wolverine #3	1	confident	ep,ksp	250.00	523.15	25	0.20	0.20	12.71	-2.9						5.44			0.05				5.64	5.24	0.25	-0.15	6.35	4.40	0.34	-0.33										
C9	PW1	216CL1	Wolverine #2	1	confident	ep,Ag,ksp	250.00	523.15	25	0.20	0.20	14.1	-2.48						6.83			0.47				7.03	6.63	0.67	0.27	7.74	5.79	0.76	0.09										
C10	PW1	216CL3	Wolverine #2	1	confident	ksp,Cu	250.00	523.15	25	0.20	0.20	13.68	-2.67						6.41			0.28				6.61	6.21	0.48	0.08	7.32	5.37	0.57	-0.10										
C11	PW1	216CL2	Wolverine #2	1	confident	ep,ksp	250.00	523.15	25	0.20	0.20	14.24	-3.19						6.97			-0.24				7.17	6.77	-0.04	-0.44	7.88	5.93	0.05	-0.62										
C12	PW1	222CL1	North Kearsarge #1	1	confident	ksp,ep	250.00	523.15	25	0.20	0.20	16.5	-3.12						9.23			-0.17				9.43	9.03	0.03	-0.37	10.14	8.19	0.12	-0.55										
C13	PW1	223CL1	North Kearsarge #3	1	confident	Cu	250.00	523.15	25	0.20	0.20	12.95	-2.79						5.68			0.16				5.88	5.48	0.36	-0.04	6.59	4.64	0.45	-0.22										
C14	PW1	229CL1	North Kearsarge #3	1	confident	Cu	250.00	523.15	25	0.20	0.20	17	-2.72						9.73			0.23				9.93	9.53	0.43	0.03	10.64	8.69	0.52	-0.15										
C15	PW1	221CL2	North Kearsarge #3	1	confident	ksp,ep	250.00	523.15	25	0.20	0.20	13.63	-1.68						6.36			1.27				6.56	6.16	1.47	1.07	7.27	5.32	1.56	0.89										
C16	PW1	230CL1	North Kearsarge #4	1	confident	chl,Cu	250.00	523.15	25	0.20	0.20	18.29	-3.2						11.02			-0.25				11.22	10.82	-0.05	-0.45	11.93	9.98	0.04	-0.63										
C17	PW1	228CL1	North Kearsarge #4	1	confident	ep,ksp	250.00	523.15	25	0.20	0.20	12.99	-3.01						5.72			-0.06				5.92	5.52	0.14	-0.26	6.63	4.68	0.23	-0.44										
C18	PW1	218CL3	Ahmeek #1	1	confident	ep,Cu	275.00	548.15	25	0.20	0.20	17.78	-3.37						11.42			-0.13				11.62	11.22	0.07	-0.33	12.21	10.51	0.09	-0.42										
C19	PW1	217CL2	Ahmeek #1	1	confident	ksp,ep	275.00	548.15	25	0.20	0.20	13.78	-3.09						7.42			0.15				7.62	7.22	0.35	-0.05	8.21	6.51	0.37	-0.14										
C20	PW1	219CL3	Ahmeek #1	1	confident	ep,Cu	275.00	548.15	25	0.20	0.20	18.14	-3.18						11.78			0.06				11.98	11.58	0.26	-0.14	12.57	10.87	0.28	-0.23										
C21	PW1	225CL2	Ahmeek #2	1	confident	Cu	275.00	548.15	25	0.20	0.20	13.8	-2.82						7.44			0.42				7.64	7.24	0.62	0.22	8.23	6.53	0.64	0.13										
C22	PW1	225CL1	Ahmeek #2	1	confident	chl,ep,Cu	275.00	548.15	25	0.20	0.20	19.14	-3.89						12.78			-0.65				12.98	12.58	-0.45	-0.85	13.57	11.87	-0.43	-0.94										
C23	PW1	220CL2	Mohawk#6	1	confident	ep	250.00	523.15	25	0.20	0.20	18.1	-3.06						10.83			-0.11				11.03	10.63	0.09	-0.31	11.74	9.79	0.18	-0.49										
C24	PW1	224CL3	Mohawk#5	1	confident	ksp,pr,Cu	250.00	523.15	25	0.20	0.20	17.55	-2.81						10.28			0.14				10.48	10.08	0.34	-0.06	11.19	9.24	0.43	-0.24										
C25	PW1	224CL2	Mohawk#5	1	confident	ksp,Cu	250.00	523.15	25	0.20	0.20	13.17	-3.15						5.90			-0.20				6.10	5.70	0.00	-0.40	6.81	4.86	0.09	-0.58										
C26	PW1	221CL3	Mohawk#4	1	confident	samples from same area are main	250.00	523.15	25	0.20	0.20	12.62	-3.42						5.35			-0.47				5.55	5.15	-0.27	-0.67	6.26	4.31	-0.18	-0.85										
C27	PW1	218CL2	Mohawk#4	1	confident	ksp,ep	250.00	523.15	25	0.20	0.20	14.01	-2.94						6.74			0.01				6.94	6.54	0.21	-0.19	7.65	5.70	0.30	-0.37										
C28	PW1	219CL2	Mohawk#4	1	confident	pr,Cu	250.00	523.15	25	0.20	0.20	13.69	-2.43						6.42			0.52				6.62	6.22	0.72	0.32	7.33	5.38	0.81	0.14										
C29	PW1	215CL3	Mohawk#4	1	confident	ksp	250.00	523.15	25	0.20	0.20	13.78	-3.41						6.51			-0.46				6.71	6.31	-0.26	-0.66	7.42	5.47	-0.17	-0.84										
B36	PP1	G7-28B	Ahmeek	1	confident	pp,pr,ep,lm traces, paragenesis determined by Püschner	275.00	548.15	25						5.90						5.41															5.85	4.90						
B37	PP1	G7-36V	Ahmeek	1	confident	pp,pr,ep,lm traces, paragenesis determined by Püschner	275.00	548.15	25						4.50	-54.4					4.01		-21.40													4.45	3.50	-16.40	-16.40				
B38	PP1	G7-45dom	Ahmeek	1	confident	pp,pr,ep,lm traces, paragenesis determined by Püschner	275.00	548.15	25																																		
B39	PP1	G7-56V	Ahmeek	1	confident	pp,pr,ep,lm traces, paragenesis determined by Püschner	275.00	548.15	25						9.30	-26.5					8.81		11.50													9.25	8.30	11.50	11.50				
B40	PP1	G7-56V	Ahmeek	1	less confident	pp,pr,ep,lm traces, paragenesis determined by Püschner	275.00	548.15	25	0.20	0.20	24.6	-3.5						18.24			-0.26				18.44	18.04	-0.06	-0.46	19.03	17.33	-0.04	-0.55										
B41	PP1	G7-62V	Ahmeek	1	less confident	pp,pr,ep,lm traces, paragenesis determined by Püschner	275.00	548.15	25	0.20	0.20	18.1	-1.9						11.74			1.34				11.94	11.54	1.54	1.14	12.53	10.83	1.56	1.05										

										Analytical Error Values for Calcite		Raw Mineral Data in ‰							Calculated Isotopic Composition of H_2O or CO_2							Calculated Isotopic Composition of H_2O and CO_2 for Maximum and Minimum Analytical Error				Calculated Isotopic Composition of H2O and CO2 for Expected Maximum and Minimum Temperature of Precipitation													
I.D.	Source	Sample Number	Sample Location	Assigned Paragenetic Stage	Confidence of Assigned Paragenetic Stage	Basis of Paragenetic Stage Assignment	Temp of Precipitation (°C)	Temp of Precipitation (K)	Temp of Precipitation Error (°C)	Error ‰ $\delta^{18}O_{H2O}$ ca	Error ‰ $\delta^{13}C_{CO2}$ ca	Raw $\delta^{18}O_{ca}$	Raw $\delta^{13}C_{ca}$	Raw $\delta^{18}O_{qz}$	Raw $\delta^{18}O_{chl/cln}$	Raw $\delta D_{chl/cln}$	Raw δD_{epi}	Raw δD_{pmp}	$\delta^{18}O_{H2O}$ ca	$\delta^{18}O_{H2O}$ qz	$\delta^{18}O_{H2O}$ chl/cln	$\delta^{13}C_{CO2}$ ca	δD_{H2O} chl/cln	δD_{H2O} epi	δD_{H2O} pmp	Error + $\delta^{18}O_{H2O}$ ca	Error - $\delta^{18}O_{H2O}$ ca	Error + $\delta^{13}C_{CO2}$ ca	Error - $\delta^{13}C_{CO2}$ ca	Temp + $\delta^{18}O_{H2O}$ ca	Temp - $\delta^{18}O_{H2O}$ ca	Temp + $\delta^{13}C_{CO2}$ ca	Temp - $\delta^{13}C_{CO2}$ ca	Temp + $\delta^{18}O_{H2O}$ qz	Temp - $\delta^{18}O_{H2O}$ qz	Temp + $\delta^{18}O_{H2O}$ chl/cln	Temp - $\delta^{18}O_{H2O}$ chl/cln	Temp + δD_{H2O} chl/cln	Temp - δD_{H2O} chl/cln	Temp + δD_{H2O} epi	Temp - δD_{H2O} epi	Temp + δD_{H2O} pmp	Temp - δD_{H2O} pmp
C36	PW1	225CL3	Seneca # 2 (Gratiot?)	1	confident	pr,Cu	250.00	523.15	25	0.20	0.20	14.78	-3.38						7.51			-0.43				7.71	7.31	-0.23	-0.63	8.42	6.47	-0.14	-0.81										
C37	PW1	221CL1	Seneca # 2 (Gratiot?)	1	confident	pr,Cu	250.00	523.15	25	0.20	0.20	13.83	-2.54						6.56			0.41				6.76	6.36	0.61	0.21	7.47	5.52	0.70	0.03										
C38	PW1	222CL2	Seneca #3 (Gratiot?)	1	confident	Cu	250.00	523.15	25	0.20	0.20	13.76	-2.88						6.49			0.07				6.69	6.29	0.27	-0.13	7.40	5.45	0.36	-0.31										
C39	PW1	226CL3	Seneca #3 (Gratiot?)	1	confident	ep,ksp,Cu,Ag	250.00	523.15	25	0.20	0.20	13.18	-2.95						5.91			0.00				6.11	5.71	0.20	-0.20	6.82	4.87	0.29	-0.38										
C40	PW1	223CL3	Central #58	1	confident	ep	212.50	485.65	37.5	0.20	0.20	15.99	-3.23						7.09			-0.89				7.29	6.89	-0.69	-1.09	8.72	5.04	-0.28	-1.80										
C41	PW1	227CL3	Central #32	1	confident	samples from same area are main	212.50	485.65	37.5	0.20	0.20	17.91	-2.63						9.01			-0.29				9.21	8.81	-0.09	-0.49	10.64	6.96	0.32	-1.20										
SIMS1	PS1	TB-293-A@1	Quincy Mine	1	confident	Cu	212.50	485.65	37.5	0.31	1.50	18.16	-2.50						9.26			-0.16				9.57	8.95	1.34	-1.66	10.89	7.21	0.45	-1.07										
SIMS2	PS1	TB-293-A@02	Quincy Mine	1	confident	Cu	212.50	485.65	37.5	0.33	1.50	21.28	-5.00						12.38			-2.66				12.71	12.05	-1.16	-4.16	14.01	10.33	-2.05	-3.57										
SIMS3	PS1	TB-293-A@03	Quincy Mine	1	confident	Cu	212.50	485.65	37.5	0.32	1.50	15.89	-3.20						6.99			-0.86				7.32	6.67	0.64	-2.36	8.62	4.94	-0.25	-1.77										
SIMS4	PS1	TB-293-A@04	Quincy Mine	1	confident	Cu	212.50	485.65	37.5	0.26	1.50	16.10	-5.00						7.20			-2.66				7.47	6.94	-1.16	-4.16	8.83	5.15	-2.05	-3.57										
SIMS5	PS1	TB-293-A@05	Quincy Mine	1	confident	Cu	212.50	485.65	37.5	0.34	1.50	15.96	-9.30						7.06			-6.96				7.40	6.72	-5.46	-8.46	8.69	5.01	-6.35	-7.87										
SIMS6	PS1	TB-293-A@06	Quincy Mine	1	confident	Cu	212.50	485.65	37.5	0.31	1.50	15.65	-2.70						6.75			-0.36				7.06	6.45	1.14	-1.86	8.38	4.70	0.25	-1.27										
SIMS7	PS1	TB-293-A@07	Quincy Mine	1	confident	Cu	212.50	485.65	37.5	0.31	1.50	16.10							7.20			2.34				7.51	6.90	3.84	0.84	8.83	5.15	2.95	1.43										
SIMS8	PS1	TB-293-A@08	Quincy Mine	1	confident	Cu	212.50	485.65	37.5	0.31	1.50	16.29	-3.60						7.39			-1.26				7.70	7.08	0.24	-2.76	9.02	5.34	-0.65	-2.17										
SIMS9	PS1	TB-293-A@09	Quincy Mine	1	confident	Cu	212.50	485.65	37.5	0.33	1.50	16.12	-4.30						7.22			-1.96				7.56	6.89	-0.46	-3.46	8.85	5.17	-1.35	-2.87										
SIMS10	PS1	TB-293-A@10	Quincy Mine	1	confident	Cu	212.50	485.65	37.5	0.29	1.50	21.12	-3.80						12.22			-1.46				12.52	11.93	0.04	-2.96	13.85	10.17	-0.85	-2.37										
SIMS11	PS1	TB-293-A@11	Quincy Mine	1	confident	Cu	212.50	485.65	37.5	0.29	1.50	16.21	-2.90						7.31			-0.56				7.60	7.02	0.94	-2.06	8.94	5.26	0.05	-1.47										
SIMS12	PS1	TB-293-A@12	Quincy Mine	1	confident	Cu	212.50	485.65	37.5	0.29	1.50	21.64	-6.60						12.74			-4.26				13.04	12.45	-2.76	-5.76	14.37	10.69	-3.65	-5.17										
SIMS13	PS1	TB-293-A@13	Quincy Mine	1	confident	Cu	212.50	485.65	37.5	0.28	1.50	21.68	-7.40						12.78			-5.06				13.06	12.50	-3.56	-6.56	14.41	10.73	-4.45	-5.97										
SIMS14	PS1	TB-293-A@14	Quincy Mine	1	confident	Cu	212.50	485.65	37.5	0.21	1.50	20.82	-7.20						11.92			-4.86				12.13	11.71	-3.36	-6.36	13.55	9.87	-4.25	-5.77										
SIMS15	PS1	TB-293-A@15	Quincy Mine	1	confident	Cu	212.50	485.65	37.5	0.34	1.50	20.61	-6.20						11.71			-3.86				12.06	11.37	-2.36	-5.36	13.34	9.66	-3.25	-4.77										
SIMS16	PS1	TB-293-A@16	Quincy Mine	1	confident	Cu	212.50	485.65	37.5	0.41	1.50	21.07	-7.00						12.17			-4.66				12.59	11.76	-3.16	-6.16	13.80	10.12	-4.05	-5.57										
SIMS17	PS1	TB-293-A@17	Quincy Mine	1	confident	Cu	212.50	485.65	37.5	0.25	1.50	22.08	-6.20						13.18			-3.86				13.44	12.93	-2.36	-5.36	14.81	11.13	-3.25	-4.77										
SIMS18	PS1	TB-293-A@18	Quincy Mine	1	confident	Cu	212.50	485.65	37.5	0.23	1.50	20.72	-4.90						11.82			-2.56				12.05	11.59	-1.06	-4.06	13.45	9.77	-1.95	-3.47										
SIMS19	PS1	TB-293-A@19	Quincy Mine	1	confident	Cu	212.50	485.65	37.5	0.30	1.50	22.03	-6.00						13.13			-3.66				13.43	12.84	-2.16	-5.16	14.76	11.08	-3.05	-4.57										
SIMS20	PS1	TB-293-A@20	Quincy Mine	1	confident	Cu	212.50	485.65	37.5	0.26	1.50	18.51	-2.10						9.61			0.24				9.88	9.35	1.74	-1.26	11.24	7.56	0.85	-0.67										
SIMS21	PS1	TB-293-A@21	Quincy Mine	1	confident	Cu	212.50	485.65	37.5	0.41	1.50	18.11	-2.50						9.21			-0.16				9.63	8.80	1.34	-1.66	10.84	7.16	0.45	-1.07										
SIMS22	PS1	TB-293-A@22	Quincy Mine	1	confident	Cu	212.50	485.65	37.5	0.31	1.50	14.62	-2.90						5.72			-0.56				6.04	5.41	0.94	-2.06	7.35	3.67	0.05	-1.47										
SIMS23	PS1	TB-293-A@23	Quincy Mine	1	confident	Cu	212.50	485.65	37.5	0.23	1.50	17.11	-5.80						8.21			-3.46				8.44	7.98	-1.96	-4.96	9.84	6.16	-2.85	-4.37										
SIMS24	PS1	TB-293-A@24	Quincy Mine	1	confident	Cu	212.50	485.65	37.5	0.30	1.50	15.58							6.68			2.34				6.98	6.38	3.84	0.84	8.31	4.63	2.95	1.43										
SIMS25	PS1	TB-293-A@25	Quincy Mine	1	confident	Cu	212.50	485.65	37.5	0.25	1.50	16.01	-2.80						7.11			-0.46				7.37	6.86	1.04	-1.96	8.74	5.06	0.15	-1.37										
SIMS26	PS1	TB-293-A@26	Quincy Mine	1	confident	Cu	212.50	485.65	37.5	0.33	1.50	17.25	-2.10						8.35			0.24				8.69	8.02	1.74	-1.26	9.98	6.30	0.85	-0.67										
SIMS27	PS1	TB-293-A@27	Quincy Mine	1	confident	Cu	212.50	485.65	37.5	0.24	1.50	16.64	-3.40						7.74			-1.06				7.99	7.50	0.44	-2.56	9.37	5.69	-0.45	-1.97										
SIMS28	PS1	TB-293-A@28	Quincy Mine	1	confident	Cu	212.50	485.65	37.5	0.25	1.50	15.76	-3.00						6.86			-0.66				7.11	6.62	0.84	-2.16	8.49	4.81	-0.05	-1.57										
SIMS29	PS1	TB-293-A@29	Quincy Mine	1	confident	Cu	212.50	485.65	37.5	0.28	1.50	15.99	-1.90						7.09			0.44				7.37	6.81	1.94	-1.06	8.72	5.04	1.05	-0.47										
SIMS30	PS1	TB-293-A@30	Quincy Mine	1	confident	Cu	212.50	485.65	37.5	0.30	1.50	21.56	-6.20						12.66			-3.86				12.96	12.37	-2.36	-5.36	14.29	10.61	-3.25	-4.77										
SIMS31	PS1	TB-293-A@31	Quincy Mine	1	confident	Cu	212.50	485.65	37.5	0.29	1.50	22.07	-7.50						13.17			-5.16				13.46	12.89	-3.66	-6.66	14.80	11.12	-4.55	-6.07										
SIMS32	PS1	TB-293-A@32	Quincy Mine	1	confident	Cu	212.50	485.65	37.5	0.28	1.50	22.22	-7.30						13.32			-4.96				13.61	13.04	-3.46	-6.46	14.95	11.27	-4.35	-5.87										
SIMS33	PS1	TB-293-A@33	Quincy Mine	1	confident	Cu	212.50	485.65	37.5	0.33	1.50	21.72	-10.10						12.82			-7.76				13.16	12.49	-6.26	-9.26	14.45	10.77	-7.15	-8.67										
SIMS34	PS1	TB-293-A@34	Quincy Mine	1	confident	Cu	212.50	485.65	37.5	0.33	1.50	21.50	-9.00						12.60			-6.66				12.93	12.28	-5.16	-8.16	14.23	10.55	-6.05	-7.57										
SIMS35	PS1	TB-293-A@35	Quincy Mine	1	confident	Cu	212.50	485.65	37.5	0.33	1.50	21.36							12.46			2.34				12.79	12.14	3.84	0.84	14.09	10.41	2.95	1.43										
SIMS36	PS1	TB-293-A@36	Quincy Mine	1	confident	Cu	212.50	485.65	37.5	0.31	1.50	23.41	-9.30						14.51			-6.96				14.82	14.20	-5.46	-8.46	16.14	12.46	-6.35	-7.87										
SIMS37	PS1	TB-293-A@37	Quincy Mine	1	confident	Cu	212.50	485.65	37.5	0.30	1.50	22.55	-7.40						13.65			-5.06				13.96	13.35	-3.56	-6.56	15.28	11.60	-4.45	-5.97										
SIMS38	PS1	TB-293-A@38	Quincy Mine	1	confident	Cu	212.50	485.65	37.5	0.35	1.50	21.42	-5.10						12.52			-2.76				12.87	12.17	-1.26	-4.26	14.15	10.47	-2.15	-3.67										
SIMS39	PS1	TB-293-A@39	Quincy Mine	1	confident	Cu	212.50	485.65	37.5	0.24	1.50	21.94	-7.80						13.04			-5.46				13.29	12.80	-3.96	-6.96	14.67	10.99	-4.85	-6.37										
SIMS40	PS1	TB-293-A@40	Quincy Mine	1	confident	Cu	212.50	485.65	37.5	0.28	1.50	20.54	-4.00						11.64			-1.66				11.92	11.37	-0.16	-3.16	13.27	9.59	-1.05	-2.57										
SIMS41	PS1	TB-293-A@41	Quincy Mine	1	confident	Cu	212.50	485.65	37.5	0.39	1.50	21.05	-7.20						12.15			-4.86				12.54	11.77	-3.36	-6.36	13.78	10.10	-4.25	-5.77										
SIMS42	PS1	TB-293-A@42	Quincy Mine	1	confident	Cu	212.50	485.65	37.5	0.20	1.50	21.86							12.96			2.34				13.17	12.76	3.84	0.84	14.59	10.91	2.95	1.43										
SIMS43	PS1	TB-293-A@43	Quincy Mine	1	confident	Cu	212.50	485.65	37.5	0.28	1.50	23.53							14.63			2.34				14.91	14.35	3.84	0.84	16.26	12.58	2.95	1.43										
SIMS44	PS1	TB-293-A@44	Quincy Mine	1	confident	Cu	212.50	485.65	37.5	0.26	1.50	21.10	-4.10						12.20			-1.76				12.47	11.94	-0.26	-3.26	13.83	10.15	-1.15	-2.67										
SIMS45	PS1	TB-293-A@45	Quincy Mine	1	confident	Cu	212.50	485.65	37.5	0.26	1.50	22.75	-6.30						13.85			-3.96				14.11	13.59	-2.46	-5.46	15.48	11.80	-3.35	-4.87										
SIMS46	PS1	WAS121-A@1	Seneca Mine (Kearsarge D	2	confident	lm, nat	125.00	398.15	25	0.28	1.50	14.12	-4.60						-0.53			-5.09				-0.25	-0.80	-3.59	-6.59	1.48	-2.96	-4.00	-6.50										
SIMS47	PS1	WAS121-A@2	Seneca Mine (Kearsarge D	2	confident	lm, nat	125.00	398.15	25	0.32	1.50	16.07	-9.70						1.42			-10.19				1.74	1.10	-8.69	-11.69	3.43	-1.01	-9.10	-11.60										
SIMS48	PS1	WAS121-A@3	Seneca Mine (Kearsarge D	2	confident	lm, nat	125.00	398.15	25	0.24	1.50	15.62	-7.60						0.97			-8.09				1.21	0.73	-6.59	-9.59	2.98	-1.46	-7.00	-9.50										
SIMS49	PS1	WAS121-A@4	Seneca Mine (Kearsarge D	2	confident	lm, nat	125.00	398.15	25	0.28	1.50	15.66	-6.40						1.01			-6.89				1.29	0.74	-5.39	-8.39	3.02	-1.42	-5.80	-8.30										
SIMS50	PS1	WAS121-A@5	Seneca Mine (Kearsarge D	2	confident	lm, nat	125.00	398.15	25	0.23	1.50	16.03	-8.30						1.38			-8.79				1.61	1.15	-7.29	-10.29	3.39	-1.05	-7.70	-10.20										
SIMS51	PS1	WAS121-A@6	Seneca Mine (Kearsarge D	2	confident	lm, nat	125.00	398.15	25	0.36	1.50	14.54	-7.40						-0.11			-7.89				0.25	-0.47	-6.39	-9.39	1.90	-2.54	-6.80	-9.30										
SIMS52	PS1	WAS121-A@7	Seneca Mine (Kearsarge D	2	confident	lm, nat	125.00	398.15	25	0.30	1.50	14.38	-5.90						-0.27			-6.39				0.03	-0.56	-4.89	-7.89	1.74	-2.70	-5.30	-7.80										
SIMS53	PS1	WAS121-A@8	Seneca Mine (Kearsarge D	2	confident	lm, nat	125.00	398.15	25	0.29	1.50	14.82	-9.70						0.17			-10.19				0.47	-0.12	-8.69	-11.69	2.18	-2.26	-9.10	-11.60										
SIMS54	PS1	WAS121-A@9	Seneca Mine (Kearsarge D	2	confident	lm, nat	125.00	398.15	25	0.25	1.50	18.98	-4.60						4.33			-5.09				4.58	4.08	-3.59	-6.59	6.34	1.90	-4.00	-6.50										
SIMS55	PS1	WAS121-A@10	Seneca Mine (Kearsarge D	2	confident	lm, nat	125.00	398.15	25	0.27	1.50	20.22	-3.60						5.57			-4.09				5.85	5.30	-2.59	-5.59	7.58	3.14	-3.00	-5.50										
SIMS56	PS1	WAS121-A@11	Seneca Mine (Kearsarge D	2	confident	lm, nat	125.00	398.15	25	0.29	1.50	19.12	-3.40						4.47			-3.89				4.76	4.19	-2.39	-5.39	6.48	2.04	-2.80	-5.30										
SIMS57	PS1	WAS121-A@12	Seneca Mine (Kearsarge D	2	confident	lm, nat	125.00	398.15	25	0.23	1.50	19.16	-1.40						4.51			-1.89				4.74	4.28	-0.39	-3.39	6.52	2.08	-0.80	-3.30										
SIMS58	PS1	WAS121-A@13	Seneca Mine (Kearsarge D	2	confident	lm, nat	125.00	398.15	25	0.31	1.50	18.97	-2.90						4.32			-3.39				4.63	4.01	-1.89	-4.89	6.33	1.89	-2.30	-4.80										
SIMS59	PS1	WAS121-A@14	Seneca Mine (Kearsarge D	2	confident	lm, nat	125.00	398.15	25	0.36	1.50	18.83	-1.40						4.18			-1.89				4.55	3.82	-0.39	-3.39	6.19	1.75	-0.80	-3.30										
SIMS60	PS1	WAS121-A@15	Seneca Mine (Kearsarge D	2	confident	lm, nat	125.00	398.15	25	0.35	1.50	18.30	-2.10						3.65			-2.59				4.01	3.30	-1.09	-4.09	5.66	1.22	-1.50	-4.00										
SIMS61	PS1	WAS121-A@16	Seneca Mine (Kearsarge D	2	confident	lm, nat	125.00	398.15	25	0.25	1.50	19.63	-2.40						4.98			-2.89				5.23	4.74	-1.39	-4.39	6.99	2.55	-1.80	-4.30										
SIMS62	PS1	WAS121-A@17	Seneca Mine (Kearsarge D	2	confident	lm, nat	125.00	398.15	25	0.26	1.50	19.10	-2.00						4.45			-2.49				4.71	4.19	-0.99	-3.99	6.46	2.02	-1.40	-3.90										
SIMS63	PS1	WAS121-A@18	Seneca Mine (Kearsarge D	2	confident	lm, nat	125.00	398.15	25	0.30	1.50	18.66	-1.70						4.01			-2.19				4.31	3.71	-0.69	-3.69	6.02	1.58	-1.10	-3.60										
SIMS64	PS1	WAS121-A@19	Seneca Mine (Kearsarge D	2	confident	lm, nat	125.00	398.15	25	0.31	1.50	17.64	-2.90						2.99			-3.39				3.31	2.68	-1.89	-4.89	5.00	0.56	-2.30	-4.80										
SIMS65	PS1	WAS121-A@20	Seneca Mine (Kearsarge D	2	confident	lm, nat	125.00	398.15	25	0.28	1.50	18.16	-2.30						3.51			-2.79				3.79	3.23	-1.29	-4.29	5.52	1.08	-1.70	-4.20										
SIMS66	PS1	WAS121-A@21	Seneca Mine (Kearsarge D	2	confident	lm, nat	125.00	398.15	25	0.31	1.50	19.41	-0.50						4.76			-0.99				5.07	4.45	0.51	-2.49	6.77	2.33	0.10	-2.40										
SIMS67	PS1	WAS121-A@22	Seneca Mine (Kearsarge D	2	confident	lm, nat	125.00	398.15	25	0.25	1.50	18.02	-2.30						3.37			-2.79				3.63	3.12	-1.29	-4.29	5.38	0.94	-1.70	-4.20										
SIMS68	PS1	WAS121-A@23	Seneca Mine (Kearsarge D	2	confident	lm, nat	125.00	398.15	25	0.29	1.50	17.87	-3.70						3.22			-4.19				3.51	2.93	-2.69	-5.69	5.23	0.79	-3.10	-5.60										
SIMS69	PS1	WAS121-A@24	Seneca Mine (Kearsarge D	2	confident	lm, nat	125.00	398.15	25	0.26	1.50	18.55	-2.10						3.90			-2.59				4.17	3.64	-1.09	-4.09	5.91	1.47	-1.50	-4.00										
SIMS70	PS1	WAS121-A@25	Seneca Mine (Kearsarge D	2	confident	lm, nat	125.00	398.15	25	0.34	1.50	18.55	-3.20						3.90			-3.69				4.24	3.56	-2.19	-5.19	5.91	1.47	-2.60	-5.10										
SIMS71	PS1	WAS121-A@26	Seneca Mine (Kearsarge D	2	confident	lm, nat	125.00	398.15	25	0.23	1.50	18.63	-3.40						3.98			-3.89				4.21	3.75	-2.39	-5.39	5.99	1.55	-2.80	-5.30										
SIMS72	PS1	WAS121-A@27	Seneca Mine (Kearsarge D	2	confident	lm, nat	125.00	398.15	25	0.32	1.50	18.28	-4.40						3.63			-4.89				3.95	3.31	-3.39	-6.39	5.64	1.20	-3.80	-6.30										
SIMS73	PS1	WAS121-A@28	Seneca Mine (Kearsarge D	2	confident	lm, nat	125.00	398.15	25	0.34	1.50	17.57	-3.70						2.92			-4.19				3.26	2.59	-2.69	-5.69	4.93	0.49	-3.10	-5.60										
SIMS74	PS1	WAS121-A@29	Seneca Mine (Kearsarge D	2	confident	lm, nat	125.00	398.15	25	0.26	1.50	12.65	-5.20						-2.00			-5.69				-1.74	-2.26	-4.19	-7.19	0.01	-4.43	-4.60	-7.10										
SIMS75	PS1	WAS121-A@30	Seneca Mine (Kearsarge D	2	confident	lm, nat	125.00	398.15	25	0.28	1.50	14.34	-5.50						-0.31			-5.99				-0.03	-0.59	-4.49	-7.49	1.70	-2.74	-4.90	-7.40										
SIMS76	PS1	WAS752-A@1	Wolverine Mine (Kearsarg	1	confident	Cu, pr, ep	250.00	523.15	25	0.29	1.50	13.74	-6.00						6.47			-3.05				6.76	6.19	-1.55	-4.55	7.38	5.43	-2.76	-3.43										
SIMS77	PS1	WAS752-A@2	Wolverine Mine (Kearsarg	1	confident	Cu, pr, ep	250.00	523.15	25	0.31	1.50	13.94	-2.70						6.67			0.25				6.98	6.37	1.75	-1.25	7.58	5.63	0.54	-0.13										
SIMS78	PS1	WAS752-A@3	Wolverine Mine (Kearsarg	1	confident	Cu, pr, ep	250.00	523.15	25	0.31	1.50	13.92	-8.70						6.65			-5.75				6.96	6.35	-4.25	-7.25	7.56	5.61	-5.46	-6.13										
SIMS79	PS1	WAS752-A@4	Wolverine Mine (Kearsarg	1	confident	Cu, pr, ep	250.00	523.15	25	0.25	1.50	14.04	-2.40						6.77			0.55				7.03	6.52	2.05	-0.95	7.68	5.73	0.84	0.17										
SIMS80	PS1	WAS752-A@5	Wolverine Mine (Kearsarg	1	confident	Cu, pr, ep	250.00	523.15	25	0.29	1.50	13.12	-2.20						5.85			0.75				6.14	5.56	2.25	-0.75	6.76	4.81	1.04	0.37										
SIMS81	PS1	WAS752-A@6	Wolverine Mine (Kearsarg	1	confident	Cu, pr, ep	250.00	523.15	25	0.32	1.50	13.91	-4.60						6.64			-1.65				6.96	6.32	-0.15	-3.15	7.55	5.60	-1.36	-2.03										
SIMS82	PS1	WAS752-A@7	Wolverine Mine (Kearsarg	1	confident	Cu, pr, ep	250.00	523.15	25	0.30	1.50	14.24	-6.10						6.97			-3.15				7.27	6.67	-1.65	-4.65	7.88	5.93	-2.86	-3.53										
SIMS83	PS1	WAS752-A@8	Wolverine Mine (Kearsarg	1	confident	Cu, pr, ep	250.00	523.15	25	0.28	1.50	13.67	-0.20						6.40			2.75				6.69	6.12	4.25	1.25	7.31	5.36	3.04	2.37										
SIMS84	PS1	WAS752-C@1	Wolverine Mine (Kearsarg	1	confident	Cu, pr, ep	250.00	523.15	25	0.20	1.50	13.18	-7.30						5.91			-4.35				6.11	5.72	-2.85	-5.85	6.82	4.87	-4.06	-4.73										
SIMS85	PS1	WAS752-C@2	Wolverine Mine (Kearsarg	1	confident	Cu, pr, ep	250.00	523.15	25	0.33	1.50	14.10	-2.10						6.83			0.85				7.16	6.50	2.35	-0.65	7.74	5.79	1.14	0.47										
SIMS86	PS1	WAS752-C@3	Wolverine Mine (Kearsarg	1	confident	Cu, pr, ep	250.00	523.15	25	0.30	1.50	13.62	-2.20						6.35			0.75				6.65	6.06	2.25	-0.75	7.26	5.31	1.04	0.37										
SIMS87	PS1	WAS752-C@4	Wolverine Mine (Kearsarg	1	confident	Cu, pr, ep	250.00	523.15	25	0.30	1.50	14.34	-1.00						7.07			1.95				7.37	6.77	3.45	0.45	7.98	6.03	2.24	1.57										
SIMS88	PS1	WAS752-C@5	Wolverine Mine (Kearsarg	1	confident	Cu, pr, ep	250.00	523.15	25	0.30	1.50	14.11	-2.00						6.84			0.95				7.14	6.54	2.45	-0.55	7.75	5.80	1.24	0.57										
SIMS89	PS1	WAS752-C@6	Wolverine Mine (Kearsarg	1	confident	Cu, pr, ep	250.00	523.15	25	0.34	1.50	13.94	-1.30						6.67			1.65				7.01	6.33	3.15	0.15	7.58	5.63	1.94	1.27										
SIMS90	PS1	WAS752-C@7	Wolverine Mine (Kearsarg	1	confident	Cu, pr, ep	250.00	523.15	25	0.29	1.50	13.82	-5.90						6.55			-2.95				6.84	6.27	-1.45	-4.45	7.46	5.51	-2.66	-3.33										
SIMS91	PS1	WAS752-C@8	Wolverine Mine (Kearsarg	1	confident	Cu, pr, ep	250.00	523.15	25	0.28	1.50	14.02	-2.30						6.75			0.65				7.03	6.47	2.15	-0.85	7.66	5.71	0.94	0.27										
SIMS92	PS1	WAS752-C@9	Wolverine Mine (Kearsarg	1	confident	Cu, pr, ep	250.00	523.15	25	0.25	1.50	13.33	-1.60						6.06			1.35				6.31	5.82	2.85	-0.15	6.97	5.02	1.64	0.97										
SIMS93	PS1	WAS752-C@10	Wolverine Mine (Kearsarg	1	confident	Cu, pr, ep	250.00	523.15	25	0.32	1.50	13.57	-3.40						6.30			-0.45				6.62	5.98	1.05	-1.95	7.21	5.26	-0.16	-0.83										
SIMS94	PS1	WAS752-C@11	Wolverine Mine (Kearsarg	1	confident	Cu, pr, ep	250.00	523.15	25	0.33	1.50	13.81	-1.30						6.54			1.65				6.87	6.22	3.15	0.15	7.45	5.50	1.94	1.27										
SIMS95	PS1	WAS752-C@12	Wolverine Mine (Kearsarg	1	confident	Cu, pr, ep	250.00	523.15	25	0.28	1.50	13.74	-1.80						6.47			1.15				6.75	6.19	2.65	-0.35	7.38	5.43	1.44	0.77										
SIMS96	PS1	WAS752-C@13	Wolverine Mine (Kearsarg	1	confident	Cu, pr, ep	250.00	523.15	25	0.26	1.50	13.59	-3.20						6.32			-0.25				6.58	6.06	1.25	-1.75	7.23	5.28	0.04	-0.63										
SIMS97	PS1	WAS752-C@14	Wolverine Mine (Kearsarg	1	confident	Cu, pr, ep	250.00	523.15	25	0.29	1.50	13.56	-4.30						6.29			-1.35				6.59	6.00	0.15	-2.85	7.20	5.25	-1.06	-1.73										
SIMS98	PS1	WAS752-C@15	Wolverine Mine (Kearsarg	1	confident	Cu, pr, ep	250.00	523.15	25	0.34	1.50	13.61	-1.80						6.34			1.15				6.68	6.00	2.65	-0.35	7.25	5.30	1.44	0.77										
SIMS99	PS1	WAS752-C@16	Wolverine Mine (Kearsarg	1	confident	Cu, pr, ep	250.00	523.15	25	0.26	1.50	13.56	-1.70						6.29			1.25				6.56	6.03	2.75	-0.25	7.20	5.25	1.54	0.87										
SIMS100	PS1	WAS752-C@17	Wolverine Mine (Kearsarg	1	confident	Cu, pr, ep	250.00	523.15	25	0.28	1.50	13.72	-2.80						6.45			0.15				6.73	6.17	1.65	-1.35	7.36	5.41	0.44	-0.23										
SIMS101	PS1	WAS752-C@18	Wolverine Mine (Kearsarg	1	confident	Cu, pr, ep	250.00	523.15	25	0.26	1.50	13.40	-1.60						6.13			1.35				6.39	5.88	2.85	-0.15	7.04	5.09	1.64	0.97										
SIMS102	PS1	WAS752-C@19	Wolverine Mine (Kearsarg	1	confident	Cu, pr, ep	250.00	523.15	25	0.29	1.50	13.97	-1.50						6.70			1.45				6.99	6.41	2.95	-0.05	7.61	5.66	1.74	1.07										
SIMS103	PS1	WAS752-C@20	Wolverine Mine (Kearsarg	1	confident	Cu, pr, ep	250.00	523.15	25	0.32	1.50	13.96							6.69			2.95				7.01	6.37	4.45	1.45	7.60	5.65	3.24	2.57										